NUMERICAL SOLUTIONS OF ONE DIMENSIONAL WAVE EQUATION IN FUNCTIONALLY GRADED CYLINDRICAL MEDIA

BY

ÖMER F. POLAT

AUGUST 2005

NUMERICAL SOLUTIONS OF ONE DIMENSIONAL WAVE EQUATION IN FUNCTIONALLY GRADED CYLINDRICAL MEDIA

by

Ömer F. POLAT

A thesis submitted to
the Graduate Institute of Sciences and Engineering
of

Fatih University

In partial fulfillment of the requirements for the degree of
Master of Science
in

Mathematics

August 2005
Istanbul, Turkey

APPROVAL PAGE

I certify that this thesis satisfies all the requirements as a thesis for the degree of Master of Science.

Assist. Prof. Dr. Ali SAHIN
Head of Department

This is to certify that I have read this thesis and that in my opinion it is fully adequate, in scope and quality, as a thesis for the degree of Master of Science.

Assist. Prof. Dr. Ibrahim ABU-ALSHAIKH
Supervisor

Examining Committee
Assist. Prof. Dr. Erdal KORKMAZ
Assist. Prof. Dr. Ali SAHIN
Assist. Prof. Dr. Ibrahim ABU-ALSHAIKH

It is approved that this thesis has been written in compliance with the formatting rules laid down by the Graduate Institute of Sciences and Engineering.

Assist. Prof. Dr. Metin TULU
Deputy Director

August 2005

NUMERICAL SOLUTIONS OF ONE DIMENSIONAL WAVE EQUATION IN FUNCTIONALLY GRADED CYLINDRICAL MEDIA

Ömer F. POLAT
M. S. Thesis – Mathematics
August 2005

Supervisor: Ibrahim ABU-ALSHAIKH

ABSTRACT

In this thesis, numerical solution of one-dimensional wave equation in multilayered cylindrical functionally graded media is investigated. The multilayered medium consists of N different layers of Functionally Graded Materials (FGMs), i.e., it is assumed that the stiffness and the density of each layer are varying continuously in the radius direction which is perpendicular to the layering direction but isotropic and homogeneous in the circumferential and axial directions. The inner surface of the layered medium is subjected to a uniform dynamic in-plane time-dependent normal stress; whereas, the outer surface of the layered medium is assumed free of surface traction or fixed. Moreover, the multilayered medium is assumed to be initially at rest and its layers are assumed to be perfectly bonded to each other. The method of characteristics is employed to obtain the numerical solutions of this initial-boundary value problem. The numerical results are obtained and displayed in curves denoting the variation of normal stress component with time. These curves reveal clearly the scattering effects caused by the reflections and refractions of waves at the boundaries and at the interfaces of the layers. The curves also display the effects of non-homogenity in the wave profiles. The curves further show that the numerical technique applied in this study is capable of predicting the sharp variations in the field variables in the neighborhood of the wave fronts.

Keywords: Wave equation, functionally graded material, method of characteristics, cylindrical layered media.

BİRİNCİ DERECEDEN DALGA DENKLEMİNİN FONKSİYONEL DERECELENDİRİLMİŞ SİLİNDİRİK TABAKADA Kİ NÜMERİK ÇÖZÜMÜ

Ömer F. POLAT
Yüksek Lisans Tezi – Matematik
Ağustus 2005

Tez Yöneticisi: Ibrahim ABU-ALSHAIKH

ÖZ

Bu tezde, birinci dereceden dalga denklemlerinin, çok katmanlı fonksiyonel derecelendirilmiş silindirik tabakadaki nümerik çözümleri araştırılmıştır. Bu çok katmanlı tabaka N farklı fonksiyonel derecelendirilmiş material katmanından oluşmaktadır. Burada her katmanın sertliğinin ve de yoğunluğunun devamlı olarak katman yönüne dik olan yarıçap yönünde değiştiği varsayılır; fakat izotropik ve homojen, çevrel ve de aksis yönlerinde. Katmanlı tabakanın iç yüzeyi normal basıncı zamana bağlı tek biçimli dinamik düzleme maruz bırakılır, halbuki katmanlı tabakanın dış yüzeyi yüzey çekmesi açısından serbest ya da bağlı veya iç yüzeydeki gerilmelerine maruz olabilir. Bundan başka, çok katmanlı tabaka başlangıçta sabit ve her katmanının kendi aralarında mükemmel bir bağlılık gösterdiği kabul edilir. Karakteristikler metodu bu başlangıç-sınır değer probleminin çözümlerini elde etmek için kullanılır. Sayısal sonuçlar elde edilir ve normal basıncın zamanla değişimini belirten eğrilerle gösterilir. Bu eğriler, sınırlarda ve katmanların arayüzlerinde ki yansımalar ve de dalga kırılmalarının etkilerini açık bir şekilde gösterir. Ayrıca bu eğriler, dalga profillerinde ki homojen olmayan etkileri de gösterir. Ve de bu eğriler gösterdi ki, bu çalışmada kullanılan sayısal teknik, dalga civarındaki keskin değişimleri tahmin etmede oldukça başarılı.

Anahtar Kelimeler: Dalga denklemi, fonksiyonel derecelendirilmiş materyaller, karakteristikler metodu, silindirik katmanlı tabaka.

DEDICATION

To my parents

ACKNOWLEDGEMENT

I am glad to take this opportunity to thank my supervisor Assist. Prof. Dr. Ibrahim ABU-ALSHAIKH for his genuine help, patience and special encouragement throughout the research.

I would like to thank my parents for their support and help.

TABLE OF CONTENTS

LIST OF FIGURES

FIGURE

LIST OF TABLES

TABLE

CHAPTER 1

INTRODUCTION

Functionally graded materials are a new generation of engineering materials which are continuously or discretely changing their thermal and mechanical properties at the macroscopic or continuum scale [1]. Functionally graded materials are increasingly expected to be used in structural applications where high strength-to-weight and stiffness-to-weight ratios are required. These applications involving severe thermal gradients, ranging from thermal structures in advanced aircraft and aerospace engines to microelectronics. Example applications include pressure vessels and pipes in nuclear reactors can be found in the review papers [2] and [3]. In such applications a metallic-rich region of a functionally graded material is exposed to low temperature with a gradual micro structural transition in the direction of the temperature gradient, while a ceramic-rich region is exposed to high temperature. Among a few recent books including a comprehensive treatment of the science and technology of functionally graded materials, one can mention [4] and [5].

Several models for the case where a dynamic load is applied to the outer boundaries of a functionally graded composite body have been studied in literature. Five models, for example, are presented in [6]; two of which simulate fiber phases in which the material is modeled as layers of different volume fractions and three simulate particle phases whereas the material properties are considered to change continuously in the thickness direction. Accordingly, two models may be used to deal with transient dynamic response in the inhomogeneous bodies; they are the homogeneous layered model and the inhomogeneous continuous model. In the first type, the FGM layer is subdivided into a large number of homogeneous thin layers each of which has its own constant volume fraction [7]. In the second kind, the FGM plate is subdivided into inhomogeneous layers whose material properties are varying continuously in the direction perpendicular to the layering [8, 9]. In these papers Ohyoshi has developed an

analytical method using linearly inhomogeneous layer elements approach to investigate waves through inhomogeneous structures.

Due to the fact that the material properties of functionally graded materials are functions of one or more space variable, wave propagation problems related to functionally graded materials are generally difficult to analyze without employing some numerical approaches. Numerical solutions of one-dimensional stress wave propagation in an FGM plate subjected to shear or normal tractions are discussed in [10-13]. In these studies, the material properties are assumed to be vary in the thickness direction and the FGM plate is divided into; linearly inhomogeneous elements [10] or quadratic inhomogeneous layer elements [11,12], whereas in [13], the material properties of the FGM plate throughout the thickness direction are assumed to be functions with arbitrary powers. Two-dimensional transient wave propagation problems in an FGM plate are, recently, discussed applying a composite wave-propagation algorithm in [14,15], and using finite elements with graded properties in [16] to simulate elastic wave propagation in continuously non-homogeneous materials. However, to the authors' the best knowledge, the transient dynamic response of a multilayered FGM body subjected to a uniform pressure wavelet has not been investigated in literature.

In this thesis, the method of characteristics is employed to obtain the solutions. This method has been employed effectively in investigating one and two-dimensional transient wave propagation problems in multilayered plane, cylindrical and spherical homogeneous layered media [17-19]. In these references, the multilayered medium consists of N layers of isotropic, homogeneous and linearly elastic or viscoelastic material with one or two relaxation times. A brief review on combining the method of characteristics with Fourier transform to investigate two-dimensional transient wave propagation in viscoelastic homogeneous layered media can be found in [20-21]. It is well known that, for one-dimensional homogeneous case the characteristic manifold consists of straight lines in the zt-plane (here, t: time; z: space variable) and the canonical equations holding on them are ordinary differential equations which can be integrated accurately using a numerical method, such as, implicit trapezoidal rule formula [17-21]. However, in functionally graded material the characteristic manifold consists of nonlinear curves in the zt-plane and the canonical equations can be integrated approximately along the characteristic curves by employing a small time discretization. This step-by-step numerical technique is capable of describing the sharp

variation of disturbance in the neighborhood of the wave front without showing any sign of instability. Hence, and as will be shown in this study, the method of characteristics can be used conveniently for one-dimensional transient wave propagation through functionally graded materials, and we guess that it can be combined with a transformation technique to handle two-dimensional transient wave propagation in multilayered functionally graded materials, as well.

In this study, in cylindrical coordinate system, the following one-dimensional wave equation (hyperbolic differential equation) is required to be solved numerically by the method of characteristics;

$$c\frac{\partial^2 u_r}{\partial r^2}+\left(\frac{dc}{dr}+\frac{c}{r}\right)\frac{\partial u_r}{\partial r}+\left(\frac{d\lambda}{dr}-\frac{c}{r}\right)\frac{u_r}{r}=\rho\frac{\partial^2 u_r}{\partial t^2}\ ,\ 0\le t,\ R_i\le r\le R_o \qquad (1.1)$$

where $u_r = u_r(r,t)$ is the only dependent variable and r (radial-direction in cylindrical coordinate) and t (time) are the independent variables. $c = c(r)$, $\lambda = \lambda(r)$ and $\rho = \rho(r)$ are the data of the problem (material properties).

The above equation is a second order hyperbolic partial differential equation subjected to the following conditions:

Initial conditions; at $t = 0$:

$u_r(r,0) = 0$ and $\frac{\partial u_r}{\partial r}(r,0) = 0$.

Boundary conditions; at $r = R_i$ and $r = R_o$

$$c\frac{\partial u_r}{\partial r}+\lambda\frac{u_r}{r}=P_o f(t),$$

$$u_r(R_o,t)=0 \quad \text{or} \quad c\frac{\partial u_r}{\partial r}+\lambda\frac{u_r}{r}=0$$

where R_i is the inner boundary, R_o is the outer boundary, P_o is the intensity of the applied load and $f(t)$ is a prescribed function of t.

It will be shown in the next chapter that the domain of the problem is assumed to be consists of perfectly bonded different layers. By other mean Eq. (1.1), with the specified boundary and initial conditions prescribes above, represents the one-dimensional wave equation of a hollow cylinder that is made of functionally graded material. Functionally graded means that the material properties within the cylinder's domain are functions of the radial direction (r). Thus, the field variables and solutions of the problem under consideration are functions of t (time) and r, this means that, at

every plane parallel to the inner surface $(r = R_i)$ the wave velocity will be a function of r.

To this end, we can conclude from the above discussion that, there have been many works done on wave propagation problems related to, elastic, viscoelastic and plane FGM materials. However, studies on transient responses (wave propagation problems) of cylindrical FGM shells have not been found in literature, [22], which will be the subject of the thesis. In the recent work of Abu-Alshaikh and Kokluce, [23], similar problem have been solved but the domain of the problem in that paper is assumed to be plane not cylindrical. Let us now briefly describe the contents of the thesis. It consists of four chapters:

The second chapter; we present the derivation of Eq. (1.1), that is the mathematical model of the problem under consideration which is derived from the basic governing equations of theory of elasticity in cylindrical coordinate system. The solution of the problem using the method of characteristics. The third chapter contains numerical examples and discussion of the results. The last chapter contains the computer program used within the thesis.

CHAPTER 2

2.1 THE FUNDAMENTAL EQUATIONS OF THE LINEAR THEORY OF ELASTICITY IN CYLINDRICAL COORDINATE SYSTEM

We start our study by reviewing the basic equations of the linear theory of elasticity in curvilinear coordinates and then derive them in cylindrical coordinate. In this thesis, the material is modeled as elastic, isotropic and non-homogeneous, that is, functionally graded material. The plane-strain problem considered in this thesis is referred to the cylindrical coordinates $(r,\ \theta, z)$, respectively. For the derivation of the basic governing equations presented in this chapter, see Refs. [24, 25, 26].

2.1.1 Curvilinear Coordinates

If a set of curvilinear coordinates x^k is used to express the basic equations of the theory of elasticity in place of rectangular coordinates, then all we need is to make some simple interpretations to find the forms of the basic governing equations related to the problem under consideration.

Let $z^1, z^2, z^3,$ or $z^k\ (k=1,2,3)$ be rectangular coordinates of a geometrical point, and $x^1, x^2, x^3,$ or $x^i\ (i=1,2,3)$ be three variables. If we can establish a correspondence between z^k and x^i, then we ay that there exists a coordinate transformation between z^k and x^i. This can be expressed in the form of three functions

$$z^k = z^k\left(x^1, x^2, x^3\right), \quad (k=1,2,3). \tag{2.1}$$

If this correspondence is one-to-one, then there exists a unique inverse of (2.1) in the form

$$x^k = x^k\left(z^1, z^2, z^3\right), \quad (k=1,2,3). \tag{2.2}$$

It can be shown that such a unique inverse exists in some neighborhood of z^k if the Jacobean

$$J = \det\left(\frac{\partial z^k}{\partial x^l}\right) = \begin{vmatrix} \partial z^1/\partial x^1 & \partial z^1/\partial x^2 & \partial z^1/\partial x^3 \\ \partial z^2/\partial x^1 & \partial z^2/\partial x^2 & \partial z^2/\partial x^3 \\ \partial z^3/\partial x^1 & \partial z^3/\partial x^2 & \partial z^3/\partial x^3 \end{vmatrix} \neq 0 . \tag{2.3}$$

For a fixed set of values of z^1, z^2, z^3 the transformation (2.1) gives three non-coincident surfaces, called **curvilinear surfaces**, which intersect each other at a single point P with a fixed x^1, x^2, x^3. This point can therefore be marked with the values of x^k called **curvilinear coordinates** of P, Fig. 2.1. The intersection of any two of the surfaces (2.1) gives a line, through P, called a **curvilinear coordinate line**.

For example, in cylindrical coordinates; the cylindrical coordinates x^k are defined by their relations to rectangular coordinates z^i:

$$z^1 = x^1 \cos x^2, \quad z^2 = x^1 \sin x^2, \quad z^3 = x^3 \tag{2.4}$$

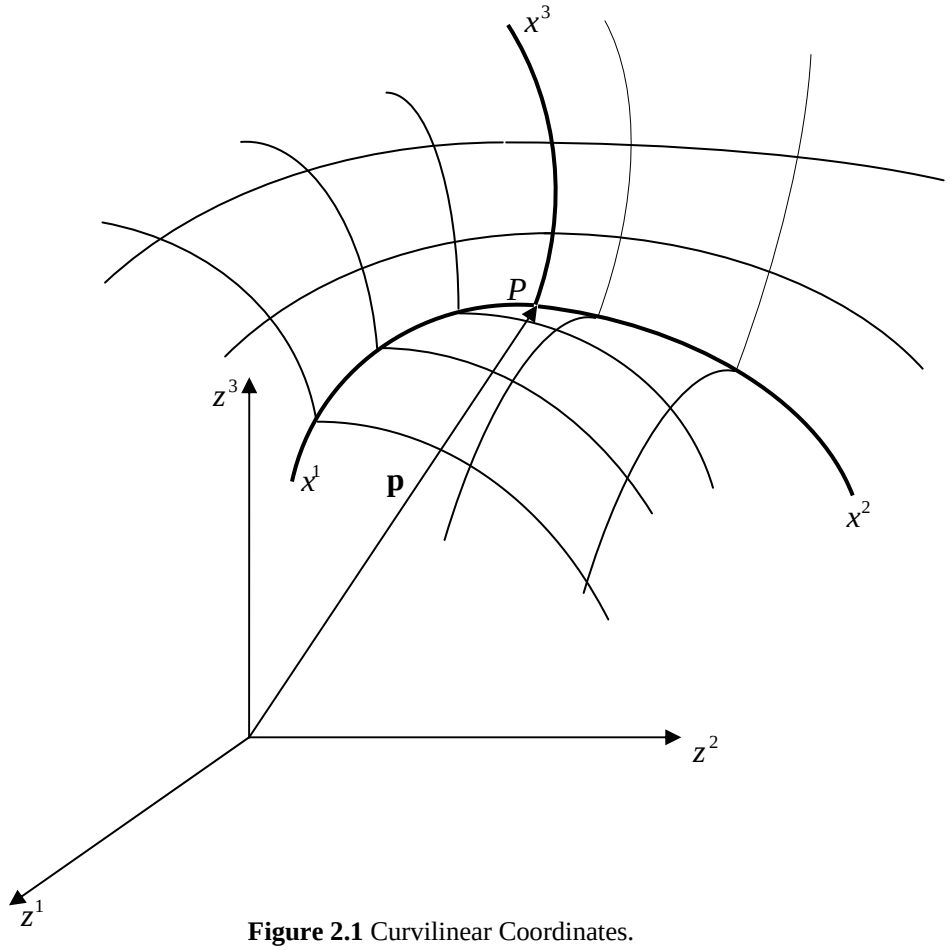

Figure 2.1 Curvilinear Coordinates.

The Jacobean J in this case is

$$J=\begin{vmatrix}\cos x^2 & -x^1\sin x^2 & 0\\ \sin x^2 & x^1\cos x^2 & 0\\ 0 & 0 & 1\end{vmatrix}=x^1,\ \left(\cos^2 x^2+\sin^2 x^2\right)=1.$$

Hence a unique inverse to (2.4) exists everywhere except at $x^1=0,$ and this

$$x^1=\sqrt{\left(z^1\right)^2+\left(z^2\right)^2},\quad x^2=\arctan\left(z^2/z^1\right),\quad x^3=z^3. \tag{2.5}$$

The coordinate surfaces are circular cylinders having the x^3-axis, as their axis, vertical planes through the x^3-axis, and planes perpendicular to the x^3-axis, Fig. 2.2.

The position vector **p** of a point P has the rectangular coordinates z^k, that is,

$$\mathbf{p}=z^k\,\mathbf{i}_k \tag{2.6}$$

where $\mathbf{i}_k$ $\left(k=1,2,3\right)$ are the unit rectangular base vectors. The repeated indices in diagonal positions (one as superscript and one as subscript) represent summation over the range $\left(k=1,2,3\right)$ of the indices. When coordinates are rectangular, however, no need arises for the use of the summation convention in this form, and we may revert superscripts back to subscript positions if we wish.

Base vectors $\mathbf{g}_k$ $\left(x^1,x^2,x^3\right)$ are defined by [25].

$$\mathbf{g}_k=\frac{\partial\mathbf{p}}{\partial x^k}=\frac{\partial z^m}{\partial x^k}\mathbf{i}_m=\frac{\partial z^1}{\partial x^k}\,\mathbf{i}_1+\frac{\partial z^2}{\partial x^k}\,\mathbf{i}_2+\frac{\partial z^3}{\partial x^k}\,\mathbf{i}_3. \tag{2.7}$$

By multiplying both sides of (2.7) by $\dfrac{\partial x^k}{\partial z^n}$ we also obtain

$$\mathbf{i}_n=\frac{\partial x^k}{\partial z^n}\mathbf{g}_k. \tag{2.8}$$

Just as with the rectangular base vectors $\mathbf{i}_k$, the curvilinear base vectors $\mathbf{g}_k$ are tangent to the curvilinear coordinate lines. This is clear from (2.7) and Fig. 2.2. For cylindrical coordinates through (2.4) and (2.7) we find that

$$\begin{aligned}\mathbf{g}_1&=\left(\cos x^2\right)\mathbf{i}_1+\left(\sin x^2\right)\mathbf{i}_2,\\ \mathbf{g}_2&=-\left(x^1\sin x^2\right)\mathbf{i}_1+\left(x^1\cos x^2\right)\mathbf{i}_2,\\ \mathbf{g}_3&=\mathbf{i}_3.\end{aligned} \tag{2.9}$$

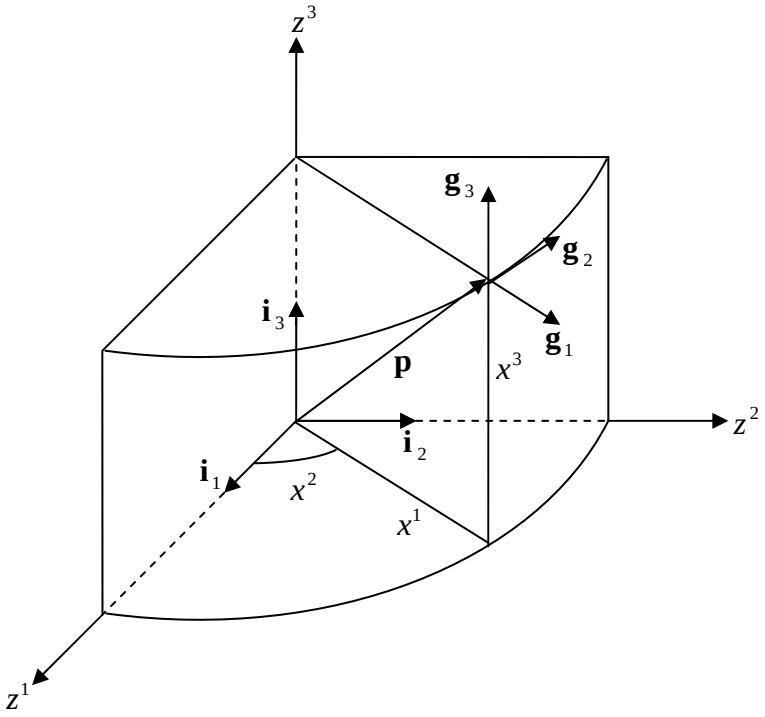

Figure 2.2 Cylindrical coordinates.

An *infinitesimal* vector $d\mathbf{p}$ can be expressed as

$$d\mathbf{p} = \frac{\partial \mathbf{p}}{\partial x^k} dx^k = \mathbf{g}_k dx^k . \tag{2.10}$$

We may use (2.10) to calculate the length of such vectors and the angle between any two of them. For example, the square of the arc length, ds^2, of $d\mathbf{p}$ is obtained through

$$ds^2 = d\mathbf{p} \cdot d\mathbf{p} = \left(\mathbf{g}_k dx^k\right) \cdot \left(\mathbf{g}_l dx^l\right) = v_{kl}(\mathbf{x}) dx^k dx^l \tag{2.11}$$

where

$$v_{kl} \equiv \mathbf{g}_k \cdot \mathbf{g}_l = \frac{\partial z^m}{\partial x^k} \frac{\partial z^n}{\partial x^l} \delta_{mn} \tag{2.12}$$

is called the **metric tensor**. This name is justified through the fact that when v_{kl} is known we can calculate the length of any vector and the angle between two vectors.

In general, the curvilinear coordinates may not be orthogonal, that is,

$$\mathbf{g}_k \cdot \mathbf{g}_l = v_{kl} \neq 0 \ \textbf{for} \ k \neq 1. \tag{2.13}$$

Note that vanishing $v_{kl}\,(k \neq 1)$ is necessary and sufficient for orthogonality of the curvilinear coordinates.

The reciprocal base vectors $\mathbf{g}^k(\mathbf{x})$ may be constructed by finding the solution of the nine equations.

$$\mathbf{g}^k \cdot \mathbf{g}_l = \delta^k{}_l \tag{2.14}$$

where $\delta^k{}_l$ is the Kronecker delta. It can be verified that the unique solution of (2.14) is

$$\mathbf{g}^k = v^{kl}(\mathbf{x})\,\mathbf{g}_l \tag{2.15}$$

where v^{kl} is the reduced cofactor in the determinant of v_{kl}, that is,

$$v^{kl}(\mathrm{x}) = \frac{\text{cofactor } v_{kl}}{v}, \qquad v \equiv \det v_{kl}\,. \tag{2.16}$$

From (2.15), by taking the scalar products with $\mathbf{g}^m$ and $\mathbf{g}_\mathrm{m}$, we obtain

$$v^{km} = \mathbf{g}^k \cdot \mathbf{g}^m, \qquad \delta^k{}_m = v^{kl} v_{lm}\,. \tag{2.17}$$

For cylindrical coordinates using (2.9) in (2.12) and (2.16), we find that

$$\begin{aligned} \left\| v_{kl} \right\| &= \begin{bmatrix} 1 & 0 & 0 \\ 0 & \left(x^1\right)^2 & 0 \\ 0 & 0 & 1 \end{bmatrix}, \\ \left\| v^{kl} \right\| &= \begin{bmatrix} 1 & 0 & 0 \\ 0 & 1/\left(x^1\right)^2 & 0 \\ 0 & 0 & 1 \end{bmatrix}. \end{aligned} \tag{2.18}$$

The magnitudes of the base vectors $\mathbf{g}_k$ and $\mathbf{g}^k$, respectively, are

$$\left|\mathbf{g}_k\right| = \sqrt{v_{\underline{k}\,\underline{k}}}, \qquad \left|\mathbf{g}^k\right| = \sqrt{v^{\underline{k}\,\underline{k}}} \tag{2.19}$$

where underscores are placed under the indices to suspend the summation.

The passage from rectangular coordinates to curvilinear coordinates may be made by observing the following two simple rules: (a) The partial differentiation symbol (,) must be replaced by the covariant differentiation symbol (;), (b) The repeated indices must be on diagonal positions.

Thus, for example, the Cauchy equations of motion:

$$\tau_{kl,l} + \rho\left(f_l - \dot{v}_l\right) = 0 \tag{2.20}$$

in curvilinear coordinates will have the form

$$\tau^{k}{}_{l;l} + \rho\left(f_l - \dot{v}_l \right) = 0 \tag{2.21}$$

where $\tau^{k}{}_{l}$ are the mixed components of the stress tensor and an index following a semi-colon indicates the covariant partial differentiation, that is, according to [25],

$$\tau^{k}{}_{l;r} \equiv \tau^{k}{}_{l,r} + \left\{ \begin{matrix} k \\ mr \end{matrix} \right\} \tau^{m}{}_{l} - \left\{ \begin{matrix} m \\ rl \end{matrix} \right\} \tau^{k}{}_{m} \tag{2.22}$$

where $\left\{ \begin{matrix} k \\ mr \end{matrix} \right\}$ are the Christoffel symbols of the second kind that can be found as follows:

The partial derivative of a vector in rectangular coordinates is obtained by

$$\frac{\partial \mathbf{u}}{\partial z^l} = \frac{\partial\left(u^k \mathbf{i}_k \right)}{\partial z^l} = \frac{\partial u^k}{\partial z^l} \mathbf{i}_k$$

since the rectangular base vectors are constant vectors. However, the same for curvilinear coordinates requires the calculation of the partial derivatives of $\mathbf{g}_k$ for

$$\frac{\partial \mathbf{u}}{\partial x^l} = \frac{\partial\left(u^k \mathbf{g}_k \right)}{\partial x^l} = \frac{\partial u^k}{\partial x^l} \mathbf{g}_k + u^k \frac{\partial \mathbf{g}_k}{\partial x^l} \ .$$

Through (2.7) we can calculate

$$\frac{\partial \mathbf{g}_k}{\partial x^l} = \frac{\partial}{\partial x_l}\left(\frac{\partial z^n}{\partial x_k} \mathbf{i}_n \right) = \frac{\partial^2 z^n}{\partial x^k \partial x^l} \mathbf{i}_n \, .$$

Upon replacing $\mathbf{i}_n$ by (2.8) we find

$$\frac{\partial \mathbf{g}_k}{\partial x^l} = \left\{ \begin{matrix} m \\ kl \end{matrix} \right\} \mathbf{g}_m \tag{2.23}$$

where

$$\left\{ \begin{matrix} m \\ kl \end{matrix} \right\} \equiv \frac{\partial^2 z^n}{\partial x^k \partial x^l} \frac{\partial x^m}{\partial z^n} \tag{2.24}$$

are known as the Christoffel symbols of the second kind. The Christoffel symbols of the first kind are also of frequent occurrence; they are defined by [25],

$$\left[kl, m \right] \equiv v_{mn} \left\{ \begin{matrix} n \\ kl \end{matrix} \right\} \quad \text{or} \quad \left\{ \begin{matrix} m \\ kl \end{matrix} \right\} \equiv v^{mn} \left[kl, n \right]. \tag{2.25}$$

Using (2.12), we can show that

$$\left[kl, m \right] = \frac{1}{2}\left(\frac{\partial v_{km}}{\partial x^l} + \frac{\partial v_{lm}}{\partial x^k} - \frac{\partial v_{kl}}{\partial x^m} \right). \tag{2.26}$$

Both symbols are symmetric in two indices, that is

$$\begin{Bmatrix} m \\ kl \end{Bmatrix} = \begin{Bmatrix} m \\ lk \end{Bmatrix},\ [kl,m] = [lk,m]. \tag{2.27}$$

We should note that the Christoffel symbols are not tensors.

By use of $\mathbf{g}^k = v^{kl}(\mathbf{x})\mathbf{g}_l$ we also find [25].

$$\frac{\partial \mathbf{g}^{\mathbf{m}}}{\partial x^l} = -\begin{Bmatrix} m \\ lk \end{Bmatrix} \mathbf{g}^k. \tag{2.28}$$

By use of (2.23) it is now possible to find an expression for the partial derivative of a vector. Hence,

$$\frac{\partial \mathbf{u}}{\partial x_k} = \frac{\partial}{\partial x_k}\left(u^m \mathbf{g}_m\right) = \frac{\partial u^m}{\partial x^k}\mathbf{g}_m + u^m \frac{\partial \mathbf{g}_m}{\partial x^k} = \left(\frac{\partial u^m}{\partial x^k} + \begin{Bmatrix} m \\ kl \end{Bmatrix} u^l\right)\mathbf{g}_m .$$

This may be written, in short,

$$\frac{\partial \mathbf{u}}{\partial x_k} = u^m{}_{;k}\,\mathbf{g}_m \tag{2.29}$$

thus, defining the covariant partial derivative of a contravariant vector

$$u^m{}_{;k} \equiv \frac{\partial u^m}{\partial x^k} + \begin{Bmatrix} m \\ kl \end{Bmatrix} u^l . \tag{2.30}$$

Similarly, by differentiating $\mathbf{u} = u_m \mathbf{g}^m$ and using (2.28), we obtain the covariant partial derivative of a covariant vector

$$u_{m;k} \equiv \frac{\partial u_m}{\partial x^k} - \begin{Bmatrix} l \\ mk \end{Bmatrix} u_l \tag{2.31}$$

so that

$$\frac{\partial \mathbf{u}}{\partial x^k} = u_{m;k}\,\mathbf{g}^m . \tag{2.32}$$

In rectangular coordinates, the Christoffel symbols vanish, thus reducing covariant partial differentiation to the usual partial differentiation.

The covariant derivative of a contravariant vector is a mixed second-order tensor, and that of a covariant vector is a covariant second-order tensor.

Christoffel symbols and the covariant derivative of a contravariant vector u^k in cylindrical coordinates are calculated through (2.25) and (2.30)

$$[12,2] = [21,2] = x^1,\ [22,1] = -x^1,\ \text{all other } [kl,m] = 0,$$

$$\begin{Bmatrix} 2 \\ 12 \end{Bmatrix} = \begin{Bmatrix} 2 \\ 21 \end{Bmatrix} = \frac{1}{x^1},\quad \begin{Bmatrix} 1 \\ 22 \end{Bmatrix} = -x^1,\ \text{all other } \begin{Bmatrix} m \\ kl \end{Bmatrix} = 0\ , \tag{2.33}$$

$$\left\{\begin{array}{l} u^1{}_{;1}=\dfrac{\partial u^1}{\partial x^1},\quad u^1{}_{;2}=\dfrac{\partial u^1}{\partial x^2}-x^1u^2,\quad u^1{}_{;3}=\dfrac{\partial u^1}{\partial x^3} \\ u^2{}_{;1}=\dfrac{\partial u^2}{\partial x^1}+\dfrac{1}{x^1}u^2,\quad u^2{}_{;2}=\dfrac{\partial u^2}{\partial x^2}+\dfrac{1}{x^1}u^1,\quad u^2{}_{;3}=\dfrac{\partial u^2}{\partial x^3} \\ u^3{}_{;k}=\dfrac{\partial u^3}{\partial x^k}\quad (k=1,2,3) \end{array}\right\}. \tag{2.34}$$

The covariant partial derivatives of higher-order tensors are defined in a similar fashion, for example,

$$\begin{aligned} A^{kl}{}_{;m} &\equiv \frac{\partial A^{kl}}{\partial x^m}+\left\{\begin{matrix} k \\ mn \end{matrix}\right\}A^{nl}+\left\{\begin{matrix} l \\ mn \end{matrix}\right\}A^{kn}, \\ A^k{}_{l;m} &\equiv \frac{\partial A^k{}_l}{\partial x^m}-\left\{\begin{matrix} n \\ lm \end{matrix}\right\}A^k{}_n+\left\{\begin{matrix} k \\ mn \end{matrix}\right\}A^{nl}, \\ A_{kl;m} &\equiv \frac{\partial A_{kl}}{\partial x^m}-\left\{\begin{matrix} n \\ km \end{matrix}\right\}A_{nl}-\left\{\begin{matrix} n \\ lm \end{matrix}\right\}A_{kn}. \end{aligned} \tag{2.35}$$

These covariant partial derivatives are third-order tensors.

For a relative scalar ϕ, a vector u^k and a tensor $A^k{}_l$ of weight N, the covariant derivatives include an extra term, for example,

$$\phi_{;k} \equiv \frac{\partial \phi}{\partial x^k}-N\left\{\begin{matrix} r \\ kr \end{matrix}\right\}\phi \text{ (relative scalar),} \tag{2.36a}$$

$$u^m{}_{;k} \equiv \frac{\partial u^m}{\partial x^k}+\left\{\begin{matrix} m \\ kl \end{matrix}\right\}u^l-N\left\{\begin{matrix} r \\ kr \end{matrix}\right\}u^m \text{ (relative vector),} \tag{2.36b}$$

$$A^k{}_{l;m} \equiv \frac{\partial A^k{}_l}{\partial x^m}-\left\{\begin{matrix} n \\ lm \end{matrix}\right\}A^k{}_n+\left\{\begin{matrix} k \\ mn \end{matrix}\right\}A^n{}_l-N\left\{\begin{matrix} r \\ mr \end{matrix}\right\}A^k{}_l \text{ (relative mixed tensor).} \tag{2.36c}$$

Applying covariant partial differentiation to v^{kl} and $\delta^k{}_l$ we find that

$$v_{kl;m}=v^{kl}{}_{;m}=\delta^k{}_{l;m}=0. \tag{2.37}$$

This theorem is known as **Ricci's theorem**. Therefore, in the process of covariant differentiation, v_{kl}, v^{kl} and $\delta^k{}_l$ are not affected, that is,

$$\begin{aligned} A^k{}_{;l} &= \left(v^{km}A_m\right)_{;l}=v^{km}A_{m;l}, \\ A_{k;l} &= \left(v_{km}A^m\right)_{;l}=v_{km}A^m{}_{;l}. \end{aligned} \tag{2.38}$$

We can easily see that

$$\left(A^kB_{lm}\right)_{;r}=A^k{}_{;r}B_{lm}+A^kB_{lm;r}.$$

A useful result that can be proved by differentiation is

$$\frac{\partial}{\partial x^k}\left(\log\sqrt{v}\right)=\begin{Bmatrix} m \\ mk \end{Bmatrix};\quad v\equiv \det v_{kl}\,. \tag{2.39}$$

This result can also be obtained through Ricci's theorem in the form $\left(\sqrt{v}\right)_{;k}=0$ and by using (2.29a) and noting that $\sqrt{v}$ is a relative scalar of weight one.

The differential operators **gradient**, of an absolute scalar ϕ and the divergence and curl of an absolute vector **A** are defined as [25]

$$\begin{aligned} &\text{grad}\,\phi\equiv\frac{\partial\phi}{\partial x^k}\mathbf{g}_k\,,\\ &\text{div}\,\mathbf{A}=A^k{}_{;k}\,,\\ &\text{curl}\,\mathbf{A}=\varepsilon^{klm}A_{m;l}\mathbf{g}_k \end{aligned} \tag{2.40}$$

where

$$\varepsilon^{klm}\equiv\frac{\varepsilon^{klm}}{\sqrt{v}} \tag{2.41}$$

is a third-order absolute tensor known as the $\varepsilon-symbol$, and e^{klm} is the usual permutation symbol. Also used is the covariant $\varepsilon-symbol$

$$\varepsilon_{klm}\equiv e_{klm}\sqrt{v}\,, \tag{2.42}$$

Sometimes it is convenient to use the operator ∇ defined by

$$\nabla\equiv\mathbf{g}^k\frac{\partial}{\partial x^k}\,. \tag{2.43}$$

By use of this, we can show that

$$\begin{aligned} &\text{grad}\,\phi\equiv\nabla\phi=\mathbf{g}_k\frac{\partial\phi}{\partial x^k}\\ &\text{div}\,\mathbf{A}=\nabla\cdot\mathbf{A}=\mathbf{g}^k\frac{\partial}{\partial x^k}(A^l\mathbf{g}_l)=\mathbf{g}^k\cdot\mathbf{g}_l A^l{}_{;k}\,,\\ &\qquad\qquad=A^k{}_{;k}=\frac{1}{\sqrt{v}}\frac{\partial}{\partial x^k}\left(\sqrt{v}A^k\right),\\ &\text{curl}\,\mathbf{A}\equiv\nabla\times\mathbf{A}=\mathbf{g}^k\frac{\partial}{\partial x^k}\times(A_l\mathbf{g}^l)=\mathbf{g}^k\times\mathbf{g}^l A_{l;k}\,,\\ &\qquad\equiv e^{klm}A_{m;l}\mathbf{g}^k\,. \end{aligned} \tag{2.44}$$

The last expression of div **A** is obtained as follows:

$$A^k{}_{;k}=\frac{\partial A^k}{\partial x^k}+\begin{Bmatrix} k \\ km \end{Bmatrix}A^m=\frac{\partial A^k}{\partial x^k}+A^k\frac{\partial}{\partial x^k}\left(\log\sqrt{v}\right)=\frac{1}{\sqrt{v}}\frac{\partial}{\partial x^k}\left(\sqrt{v}A^k\right)$$

where we used (2.32). For the Laplacian ∇^2 in curvilinear coordinates, we have

$$\nabla^2\phi \equiv \text{div grad}\,\phi = \left(v^{kl}\frac{\partial\phi}{\partial x^l}\right)_{;k} = v^{kl}\left(\frac{\partial\phi}{\partial x^l}\right)_{;k} = \frac{1}{\sqrt{v}}\frac{\partial}{\partial x^k}\left(\sqrt{v}v^{kl}\frac{\partial\phi}{\partial x^l}\right). \tag{2.45}$$

In orthogonal curvilinear coordinates the expressions of these operators are:

$$\begin{aligned} &ds^2 = v_{11}\left(dx^1\right)^2 + v_{22}\left(dx^2\right)^2 + v_{33}\left(dx^3\right)^2, \\ &\overset{kk}{v} = \frac{1}{v_{kk}}, \quad \mathbf{g}^k = \overset{kk}{v}\mathbf{g}_k, \quad v = v_{11}v_{22}v_{33}, \end{aligned} \tag{2.46}$$

$$\begin{aligned} &\left\{\begin{matrix} l \\ k\,k \end{matrix}\right\} = -\frac{1}{2v_{ll}}\frac{\partial v_{kk}}{\partial x^l}, \quad \left\{\begin{matrix} k \\ kl \end{matrix}\right\} = \frac{\partial}{\partial x^l}\left(\log\sqrt{v_{kk}}\right), \\ &\left\{\begin{matrix} k \\ k\,k \end{matrix}\right\} = \frac{\partial}{\partial x^k}\left(\log\sqrt{v_{kk}}\right), \quad \left\{\begin{matrix} k \\ lm \end{matrix}\right\} = 0 \quad (k \neq l \neq m), \end{aligned} \tag{2.47}$$

$$\text{grad}\,\phi = \frac{1}{\sqrt{v_{11}}}\frac{\partial\phi}{\partial x^1}\mathbf{e}_1 + \frac{1}{\sqrt{v_{22}}}\frac{\partial\phi}{\partial x^2}\mathbf{e}_2 + \frac{1}{\sqrt{v_{33}}}\frac{\partial\phi}{\partial x^3}\mathbf{e}_3,$$

$$\text{div}\,\mathbf{A} = \left(v_{11}v_{22}v_{33}\right)^{-1/2}\left[\frac{\partial}{\partial x^1}\left(\sqrt{v_{22}v_{33}}A^{(1)}\right) + \frac{\partial}{\partial x^2}\left(\sqrt{v_{33}v_{11}}A^{(2)}\right) + \frac{\partial}{\partial x^3}\left(\sqrt{v_{11}v_{22}}A^{(3)}\right)\right],$$

$$\begin{aligned} \text{curl}\,\mathbf{A} = {} & \left(v_{22}v_{33}\right)^{-1/2}\left[\frac{\partial}{\partial x^2}\sqrt{v_{33}}A^{(3)} - \frac{\partial}{\partial x^3}\sqrt{v_{22}}A^{(2)}\right]\mathbf{e}_1 \\ & + \left(v_{33}v_{11}\right)^{-1/2}\left[\frac{\partial}{\partial x^3}\sqrt{v_{11}}A^{(1)} - \frac{\partial}{\partial x^1}\sqrt{v_{33}}A^{(3)}\right]\mathbf{e}_2 \\ & + \left(v_{11}v_{22}\right)^{-1/2}\left[\frac{\partial}{\partial x^1}\sqrt{v_{22}}A^{(2)} - \frac{\partial}{\partial x^2}\sqrt{v_{11}}A^{(1)}\right]\mathbf{e}_3, \end{aligned}$$

$$\nabla^2\,\phi = \left(v_{11}v_{22}v_{33}\right)^{-1/2}\left[\frac{\partial}{\partial x^1}\left(\frac{\sqrt{v_{22}v_{33}}}{\sqrt{v_{11}}}\frac{\partial\phi}{\partial x^1}\right) + \frac{\partial}{\partial x^2}\left(\frac{\sqrt{v_{33}v_{11}}}{\sqrt{v_{22}}}\frac{\partial\phi}{\partial x^2}\right) + \frac{\partial}{\partial x^3}\left(\frac{\sqrt{v_{11}v_{22}}}{\sqrt{v_{33}}}\frac{\partial\phi}{\partial x^3}\right)\right].$$

Cylindrical coordinates (r, θ, z) are defined in terms of rectangular coordinates z^k [we use $x^1 \equiv r$, $x^2 \equiv \theta$, $x^3 \equiv z$, $A^{(1)} \equiv A_r$, $A^{(2)} \equiv A_\theta$, $A^{(3)} \equiv A_z$].

$$\begin{aligned} &z^1 = r\cos\theta, \quad z^2 = r\sin\theta, \quad z^3 = z, \\ &ds^2 = dr^2 + r^2 d\theta^2 + dz^2, \\ &v_{11} = v^{11} = v_{33} = v^{33} = 1 \quad v_{22} = \frac{1}{v^{22}} = r^2, \\ &\left\{\begin{matrix} 2 \\ 12 \end{matrix}\right\} = \left\{\begin{matrix} 2 \\ 21 \end{matrix}\right\} = \frac{1}{r}, \quad \left\{\begin{matrix} 1 \\ 22 \end{matrix}\right\} = -r \quad \text{all other}\ \left\{\begin{matrix} k \\ lm \end{matrix}\right\} = 0, \end{aligned}$$

$$
\begin{aligned}
&\text{grad}\,\phi = \frac{\partial \phi}{\partial \mathrm{r}}\mathbf{e}_r + \frac{1}{r}\frac{\partial \phi}{\partial \theta}\mathbf{e}_\theta + \frac{\partial \phi}{\partial \mathrm{z}}\mathbf{e}_\mathbf{z}\,,\\
&\text{div}\,\mathbf{A} = \frac{1}{r}\frac{\partial}{\partial r}\left(rA_r\right) + \frac{1}{r}\frac{\partial A_\theta}{\partial \theta} + \frac{\partial A_\mathrm{z}}{\partial \mathrm{z}},\\
&\text{curl}\,\mathbf{A} = \left(\frac{1}{r}\frac{\partial A_\mathrm{z}}{\partial \theta} - \frac{\partial A_\theta}{\partial \mathrm{z}}\right)\mathbf{e}_r + \left(\frac{\partial A_r}{\partial \mathrm{z}} - \frac{\partial A_\mathrm{z}}{\partial r}\right)\mathbf{e}_\theta + \left(\frac{1}{r}\frac{\partial}{\partial r}\left(rA_\theta\right) - \frac{1}{r}\frac{\partial A_r}{\partial \theta}\right)\mathbf{e}_z\,,\\
&\nabla^2\phi = \frac{\partial^2 \phi}{\partial r^2} + \frac{1}{r}\frac{\partial \phi}{\partial r} + \frac{1}{r^2}\frac{\partial^2 \phi}{\partial \theta^2} + \frac{\partial^2 \phi}{\partial \mathrm{z}^2}.
\end{aligned}
\tag{2.48}
$$

The infinitesimal strains are given by

$$\varepsilon_{kl} = \frac{1}{2}\left(u_{k;l} + u_{l;k}\right) \tag{2.49}$$

where

$$u_{k;l} \equiv u_{k,l} - \begin{Bmatrix} m \\ kl \end{Bmatrix} u_m\,. \tag{2.50}$$

Often these equations are expressed in terms of the physical components of the vectors and tensors involved. The physical components $\tau^{(k)}{}_{(l)}$ and $u^{(k)}$ of $\tau^k{}_l$ and u^k are related to each other by physical components:

A vector $\mathbf{u}$ referred to bases $\mathbf{g}_k$ (and $\mathbf{g}^k$) is expressible in terms of its contravariant (covariant) components by

$$\mathbf{u} = u^k\mathbf{g}_k\,, \quad \mathbf{u} = u_k\mathbf{g}^k\,. \tag{2.51}$$

Since all members of $\mathbf{g}_k$ and $\mathbf{g}^k$ are not, in general, of unit magnitude we see that all members u^k and u_k will not have the same physical dimensions.

For example, if $\mathbf{u}$ is a displacement vector then it has the dimension L.

Referred to cylindrical coordinates

$$\left|\mathbf{g}_1\right| = \sqrt{v_{11}} = 1, \quad \left|\mathbf{g}_2\right| = \sqrt{v_{22}} = x^1, \quad \left|\mathbf{g}_3\right| = \sqrt{v_{33}} = 1$$

so that the dimension of the components u^1 and u^3 are L, but the dimension of u^2 is $L/L = 1$. Thus, there is a need for finding the physical components of vectors and tensors. This is accomplished by taking the parallel projections of vectors on unit vectors lying along the coordinate curves. We define the physical component $u^{(k)}$ of the vector u^k by

$$\mathbf{u} \equiv u^k\mathbf{e}_k \tag{2.52}$$

where $\mathbf{e}_k$ are the unit vectors defined by

$$\mathbf{e}_k \equiv \frac{\mathbf{g}_k}{\sqrt{v_{\underline{k}\underline{k}}}}. \tag{2.53}$$

Through (2.51) and (2.53) we see that

$$\mathbf{u} = u^k \mathbf{g}_k = u^{(k)} \mathbf{e}_k \tag{2.54}$$

or comparing the components

$$u^{(k)} = u^k \sqrt{v_{\underline{k}\underline{k}}}, \quad u^k = \frac{u^{(k)}}{\sqrt{v_{\underline{k}\underline{k}}}}. \tag{2.55}$$

If we want to replace u_k by its physical component, then all we need is to lower the index of u^k, that is,

$$u_k = v_{kl} u^l = \sum_l v_{kl} \frac{u^{(l)}}{\sqrt{v_{ll}}}$$

where we inserted the summation sign again since the index l is repeated more than twice, thus bringing an ambiguity in the order of summations.

An equally consistent definition of physical components may be made by parallel projections on unit vectors lying along $\mathbf{g}^k$. To be consistent with a convention we will always select $\mathbf{e}_k$ lying on $\mathbf{g}_k$.

The physical components of second-and higher-order tensors may be found by their relations to vectors and scalars. In nonorthogonal coordinates, several different types of physical components arise. We consider here only the case of symmetric second-order mixed tensor $\tau^k{}_l$ is related to a contravariant vector τ^k through

$$\tau^k = \tau^k{}_l n^l$$

where n^l is also a contravariant vector. Now place τ^k and n^l by their physical components as given by expressions of the form (2.55)

$$\frac{\tau^{(k)}}{\sqrt{v_{\underline{k}\underline{k}}}} = \sum_l \tau^k{}_l \frac{n^{(l)}}{\sqrt{v_{ll}}}$$

or

$$\tau^{(k)} = \sum_l \tau^k{}_l \frac{\sqrt{v_{\underline{k}\underline{k}}}}{\sqrt{v_{ll}}} n^{(l)}.$$

The physical components $\tau^{(k)}{}_{(l)}$ of $\tau^k{}_l$ may then be defined by

$$\tau^{(k)}{}_{(l)} = \tau^{k}{}_{l}\frac{\sqrt{v_{\underline{k}\underline{k}}}}{\sqrt{v_{ll}}}. \tag{2.56}$$

When the coordinates are orthogonal

$$v_{\underline{k}\underline{k}} = 1/v_{\underline{k}\underline{k}}; \quad v_{kl} = 0, \quad k \neq 1$$

and $\tau^{k}{}_{l}$ symmetric we can easily show that

$$\tau^{(k)}{}_{(l)} = \frac{\tau_{kl}}{\sqrt{v_{\underline{k}\underline{k}}v_{\underline{l}\underline{l}}}} = \tau^{kl}\sqrt{v_{\underline{k}\underline{k}}v_{\underline{l}\underline{l}}} = \tau^{k}{}_{l}\frac{\sqrt{v_{\underline{k}\underline{k}}}}{\sqrt{v_{\underline{l}\underline{l}}}}\ , \tag{2.57}$$

$$\tau^{k}{}_{l} = \tau^{(k)}{}_{(l)}\frac{\sqrt{v_{\underline{l}\underline{l}}}}{\sqrt{v_{\underline{k}\underline{k}}}}, \quad u^{k} = \frac{u^{(k)}}{\sqrt{v_{\underline{k}\underline{k}}}}. \tag{2.58}$$

We now give the expressions of (2.21) and (2.49) in orthogonal curvilinear coordinates only. In this case we have $v_{kl} = 0$ when $k \neq 1$, and

$$\begin{aligned} &ds^2 = v_{11}\left(dx^1\right)^2 + v_{22}\left(dx^2\right)^2 + v_{33}\left(dx^3\right)^2, \\ &v^{\underline{k}\underline{k}} = 1/v_{\underline{k}\underline{k}}, \quad v \equiv \det v_{kl} = v_{11}v_{22}v_{33}, \end{aligned} \tag{2.59}$$

$$\left\{\begin{matrix} k \\ lm \end{matrix}\right\} = \frac{1}{2v_{\underline{k}\underline{k}}}\left(\frac{\partial v_{\underline{k}\underline{k}}}{\partial x^{m}}\delta_{kl} + \frac{\partial v_{\underline{m}\underline{m}}}{\partial x^{l}}\delta_{km} - \frac{\partial v_{\underline{l}\underline{l}}}{\partial x_{k}}\delta_{lm}\right).$$

Using (2.58) and (2.59) in (2.21), we get

$$\begin{aligned} &\sum_{k=1}^{3}\left\{\frac{1}{\sqrt{v}}\frac{\partial}{\partial x^{k}}\left[\tau^{(k)}{}_{(l)}\frac{\sqrt{v}}{\sqrt{v_{kk}}}\right] + \frac{1}{\sqrt{v_{kk}v_{\underline{l}\underline{l}}}}\frac{\partial\sqrt{v_{\underline{l}\underline{l}}}}{\partial x^{k}}\tau^{(k)}{}_{(l)} - \frac{1}{\sqrt{v_{kk}v_{\underline{l}\underline{l}}}}\frac{\partial\sqrt{v_{kk}}}{\partial x^{l}}\tau^{(k)}{}_{(k)}\right\} \\ &+ \rho\left(f^{(l)} - \ddot{V}^{(l)}\right) = 0 \end{aligned} \tag{2.60}$$

where $f^{(l)} = f^{l}/\sqrt{v_{\underline{l}\underline{l}}}$ are the physical components of the body force. To express (2.49) in physical components of the displacement vector we first express it in the form

$$\varepsilon^{k}{}_{l} = \frac{1}{2}\left(u^{k}{}_{;l} + v_{nl}v^{km}u^{n}{}_{;m}\right) \tag{2.61}$$

where $u^{k} = v^{kl}u_{l}, \quad u^{k}{}_{;l} \equiv u^{k}{}_{,l} + \left\{\begin{matrix} k \\ ml \end{matrix}\right\}u^{m}$. (2.62)

The forms (2.58) can be employed to replace $\boldsymbol{\varepsilon}$ and **u** by their physical components $\varepsilon^{(k)}{}_{(l)}$ and $u^{(k)}$. Upon using (2.59) in (2.61) we obtain

$$\varepsilon^{(k)}{}_{(l)} = \varepsilon^{k}{}_{l}\frac{\sqrt{\underset{--}{v_{kk}}}}{\sqrt{\underset{--}{v_{ll}}}} = \frac{1}{2}\left[\frac{\sqrt{\underset{--}{v_{kk}}}}{\sqrt{\underset{--}{v_{ll}}}}\frac{\partial}{\partial x^{l}}\left(\frac{u^{(k)}}{\sqrt{\underset{--}{v_{kk}}}}\right)+\frac{\sqrt{\underset{--}{v_{ll}}}}{\sqrt{\underset{--}{v_{kk}}}}\frac{\partial}{\partial x^{k}}\left(\frac{u^{(l)}}{\sqrt{\underset{--}{v_{ll}}}}\right)\right]$$
$$+\frac{1}{2}\left[\frac{1}{\sqrt{\underset{--}{v_{kk}}\underset{--}{v_{ll}}}}\sum_{m=1}^{3}\frac{\partial \underset{--}{v_{kk}}}{\partial x^{m}}\frac{u^{(m)}}{\sqrt{v_{mm}}}\delta_{kl}\right]. \tag{2.63}$$

Similarly

$$\tilde{r}{}^{(k)}{}_{(l)} = \frac{1}{2\sqrt{\underset{--}{v_{kk}}\underset{--}{v_{ll}}}}\left[\frac{\partial}{\partial x^{l}}\left(\sqrt{\underset{--}{v_{kk}}}u^{(k)}\right)-\frac{\partial}{\partial x^{k}}\left(\sqrt{\underset{--}{v_{ll}}}u^{(l)}\right)\right], \tag{2.64a}$$

$$\tilde{r}{}^{(m)} = \frac{1}{2}\sum_{k,l}\varepsilon^{mlk}\tilde{r}{}^{(k)}{}_{(l)} \quad 2\tilde{\mathbf{r}} = \nabla\times\mathbf{u}. \tag{2.64b}$$

The stress constitutive equations, as usual, are

$$\tau^{(k)}{}_{(l)} = \lambda_{\varepsilon}\varepsilon^{(m)}{}_{(m)}\delta^{k}{}_{l} + 2\mu_{\varepsilon}\varepsilon^{(k)}{}_{(l)} \tag{2.65}$$

Equations (2.60), (2.63) and (2.64) are all that are needed for the treatment of problems in any set of orthogonal curvilinear coordinates. The passage from physical components of vectors and tensors to tensor components is made through such equations as (2.58).

Navier's equations in curvilinear coordinates are obtained by combining (2.63) and (2.65) with (2.60). This is rather than cumbersome. The tensor expression of these equations is written immediately bye use of the rules stated above. In fact (2.20) in any curvilinear coordinates may be expressed as

$$\left(\lambda_{\varepsilon}+\mu_{\varepsilon}\right)u^{l}{}_{;lk} + \mu_{\varepsilon}u_{k;}{}^{l}{}_{l} + \rho\left(f_{k} - \dot{V}_{k}\right) = 0. \tag{2.66}$$

A vectorial form of this equation is found if we remember the vector identities

$$u_{k;}{}^{l}{}_{l} = -\left(\nabla\times\nabla\times\mathbf{u}\right)_{k} + \left(\nabla\nabla\cdot\mathbf{u}\right)_{k},$$
$$u^{l}{}_{;kl} = \left(\nabla\nabla\cdot\mathbf{u}\right)_{k}$$

where ∇ is the gradient operator. Upon using these identities in (2.66) we get

$$\left(\lambda_{\varepsilon}+2\mu_{\varepsilon}\right)\nabla\nabla\cdot\mathbf{u} - \mu_{\varepsilon}\nabla\times\nabla\times\mathbf{u} + \rho\left(\mathbf{f} - \ddot{\mathbf{u}}\right) = 0. \tag{2.67}$$

By substituting the expressions of the gradient, divergence, and curl operators, this equation can be expressed in any coordinate system. We now give the forms of these equations in cylindrical coordinates.

2.1.2 Cylindrical Coordinates

Cylindrical coordinates (r,θ,z) are related to rectangular coordinates (x,y,z) by $x = r\cos\theta, \quad x = r\sin\theta, \quad z = z$. (2.68)

The square of arc length, ds^2, and metric tensor, v_{kl}, are given by

$$\begin{aligned} &ds^2 = dr^2 + r^2 d\theta^2 + dz^2, \\ &v_{11} = 1, \quad v_{22} = r^2, \quad v_{33} = 1, \quad v_{kl} = 0 \quad (k \neq 1). \end{aligned} \tag{2.69}$$

Cauchy's equations of motion, strains, and rotations are obtained by substituting v_{kl}, given above, into (2.60), (2.63) and (2.64b), respectively. Thus,

$$\left.\begin{aligned} &\frac{\partial \tau_{rr}}{\partial r} + \frac{1}{r}\frac{\partial \tau_{r\theta}}{\partial \theta} + \frac{\partial \tau_{rz}}{\partial z} + \frac{\tau_{rr} - \tau_{\theta\theta}}{r} + \rho(f_r - \ddot{u}_r) = 0, \\ &\frac{\partial \tau_{r\theta}}{\partial r} + \frac{1}{r}\frac{\partial \tau_{\theta\theta}}{\partial \theta} + \frac{\partial \tau_{\theta z}}{\partial z} + \frac{2}{r}\tau_{r\theta} + \rho(f_\theta - \ddot{u}_\theta) = 0, \\ &\frac{\partial \tau_{rz}}{\partial r} + \frac{1}{r}\frac{\partial \tau_{\theta z}}{\partial \theta} + \frac{\partial \tau_{zz}}{\partial z} + \frac{1}{r}\tau_{rz} + \rho(f_z - \ddot{u}_z) = 0, \end{aligned}\right\} \tag{2.70}$$

$$\left\{\begin{aligned} &\varepsilon_{rr} = \frac{\partial u_r}{\partial r} \\ &\varepsilon_{\theta\theta} = \frac{1}{r}\frac{\partial u_\theta}{\partial \theta} + \frac{u_r}{r} \\ &\varepsilon_{zz} = \frac{\partial u_z}{\partial z} \\ &\varepsilon_{r\theta} = \frac{1}{2}\left(\frac{1}{r}\frac{\partial u_r}{\partial \theta} + \frac{\partial u_\theta}{\partial r} - \frac{u_\theta}{r}\right) \\ &\varepsilon_{rz} = \frac{1}{2}\left(\frac{\partial u_z}{\partial r} + \frac{\partial u_r}{\partial z}\right) \\ &\varepsilon_{\theta z} = \frac{1}{2}\left(\frac{\partial u_\theta}{\partial z} + \frac{1}{r}\frac{\partial u_z}{\partial \theta}\right) \end{aligned}\right\} \tag{2.71}$$

where $(\tau_{rr}, \tau_{r\theta}, ..., \tau_{zz})$, $(\varepsilon_{rr}, \varepsilon_{r\theta}, ..., \varepsilon_{zz})$ and (u_r, u_θ, u_z) denote, respectively, the physical components of stress, strain, and displacement in cylindrical coordinates, Fig. 2.3.

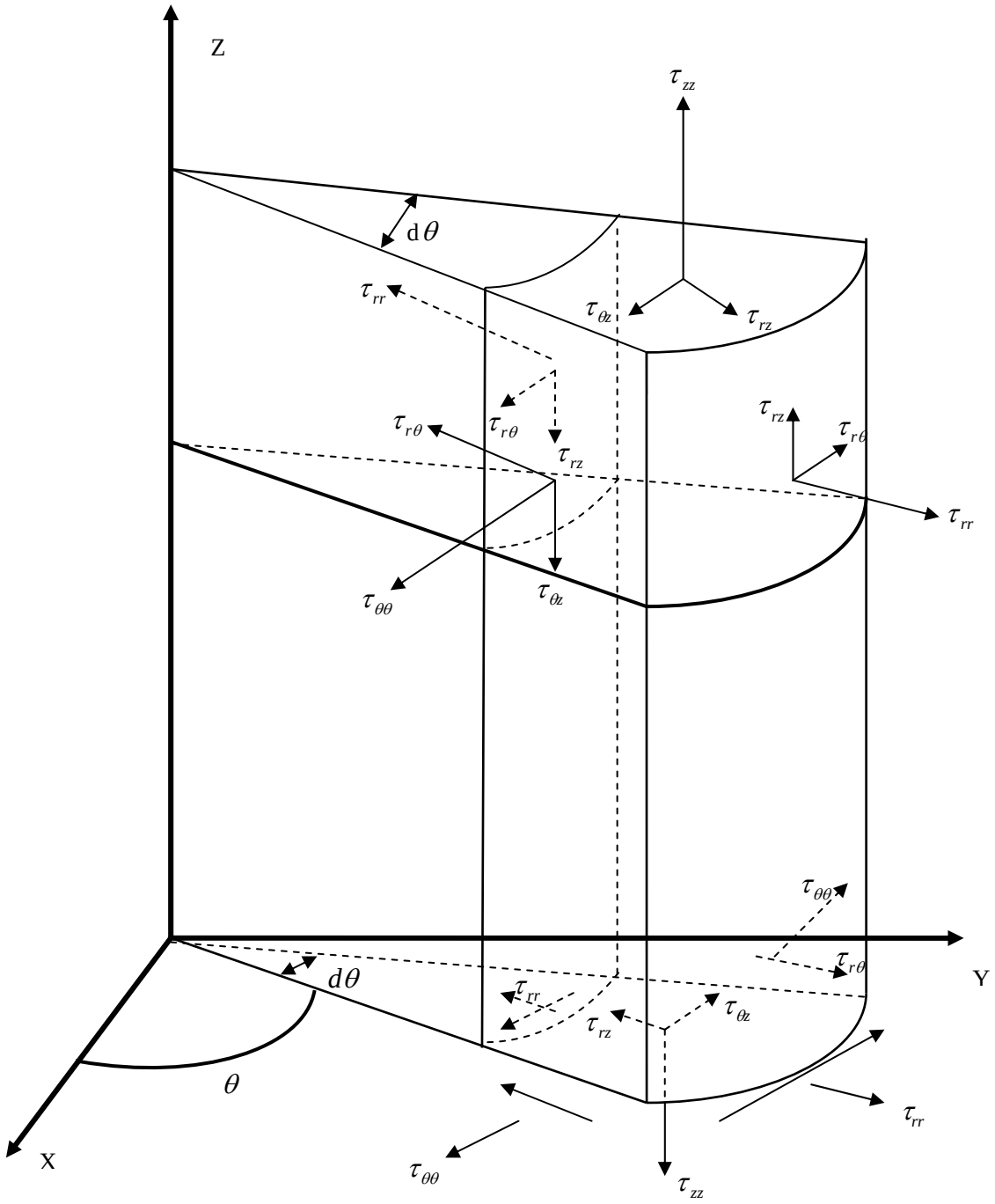

Figure 2.3 Stress components acting on an infinitesimal cylindrical volume element.

The stress-strain relations for an isotropic, homogeneous and linearly elastic material can be expressed in indicial notation as [26]

$$\tau_{ij} = 2\mu\varepsilon_{ij} + \lambda\delta_{ij}\varepsilon_{kk} \qquad \text{with}(i, j = 1, 2, 3) \tag{2.72}$$

where λ, μ are elastic constants which are known as Lame's constants. δ_{ij} is called the Kronecker's delta defined as

$$\delta_{ij} = \begin{cases} 1 & \text{if } \mathrm{i} = \mathrm{j} \\ 0 & \text{if } \mathrm{i} \neq \mathrm{j} \end{cases} . \tag{2.73}$$

In Eqs. (2.72, 2.73), indicial notation and rules pertaining to its use are employed. In indicial notation a repeated index implies summation, for example, $\varepsilon_{kk} = \varepsilon_{rr} + \varepsilon_{\theta\theta} + \varepsilon_{zz}$. Thus, the stress-strain relations, Eq. (2.72), can also be written in the use of Eq. (2.73) explicitly as [26]

$$\left.\begin{aligned} \tau_{rr} &= 2\mu\varepsilon_{rr} + \lambda\left(\varepsilon_{rr} + \varepsilon_{\theta\theta} + \varepsilon_{zz}\right), \\ \tau_{\theta\theta} &= 2\mu\varepsilon_{\theta\theta} + \lambda\left(\varepsilon_{rr} + \varepsilon_{\theta\theta} + \varepsilon_{zz}\right), \\ \tau_{zz} &= 2\mu\varepsilon_{zz} + \lambda\left(\varepsilon_{rr} + \varepsilon_{\theta\theta} + \varepsilon_{zz}\right), \\ \tau_{r\theta} &= 2\mu\varepsilon_{r\theta}, \\ \tau_{rz} &= 2\mu\varepsilon_{rz}, \\ \tau_{\theta z} &= 2\mu\varepsilon_{\theta z}, \end{aligned}\right\} \tag{2.74}$$

This completes the summary of the basic equations of the linear theory of elasticity that will be used in deriving the governing equations of the problem considered in this thesis.

2.2 FORMULATION OF THE PROBLEM

In this thesis, the dynamic response of layered composites consisting of N isotropic, elastic and functionally graded cylindrical layers (non-homogeneous) will be investigated. The composite medium consists of cylindrical layers, see Fig. (2.4). In this figure, the cylindrical composite is referred to cylindrical coordinate system where the distance normal to the layering is measured by r. The body is assumed to be subjected to uniform time-dependent uniform dynamic input at its inner boundary $\left(r = R_i\right)$. The dynamic input is normal traction in the in-plane direction for this plane-stain problem. The outer surface $(r = R_o)$ of the body is assumed to be free of surface traction or fixed. Moreover, the body is assumed to be initially at rest and the layers of

the composite body are assumed to be perfectly bonded to each other at the interfaces. Under these boundary, initial and interface conditions, the responses of the bodies are ax symmetrical, that is all the field variables are functions of r and t. Moreover, the only non vanishing displacement component is u_r, that is the displacement component in the direction normal to the layering $(r-direction)$. Thus, the displacement vector for a typical plane layer can be expressed as:

$$\begin{aligned} u_r &= u_r(r,t), \\ u_\theta &= u_z = 0. \end{aligned} \tag{2.75}$$

In view of Eq. (2.75), the stress equations of motion, the strain-displacement relations and the stress-strain relations given by Eqs. (2.70), (2.71) and (2.74), respectively, for the three-dimensional case reduce our problem to,

$$\begin{aligned} &\frac{\partial \tau_{rr}}{\partial r} + \frac{\tau_{rr} - \tau_{\theta\theta}}{r} = \rho \frac{\partial^2 u_r}{\partial t^2}, \\ &\frac{\partial u_r}{\partial r} - \varepsilon_{rr} = 0 \\ &\frac{u_r}{r} - \varepsilon_{\theta\theta} = 0 \\ &\tau_{rr} = (2\mu + \lambda)\varepsilon_{rr} + \lambda\varepsilon_{\theta\theta} \\ &\tau_{\theta\theta} = (2\mu + \lambda)\varepsilon_{\theta\theta} + \lambda\varepsilon_{rr} \\ &\tau_{zz} = \lambda\varepsilon_{\theta\theta} + \lambda\varepsilon_{rr} \end{aligned} \tag{2.76}$$

Where all other stress and strain components are zero and v_r is the particle velocity in the $r-direction$, i.e.,

$$\frac{\partial u_r}{\partial t} - v_r = 0 \tag{2.77}$$

In Eq. (2.76) the stiffness $c = 2\mu + \lambda$ and the mass density ρ of the medium are assumed to be vary continuously in $r-$direction, but homogeneous and isotropic in θ and $z-$directions, that is

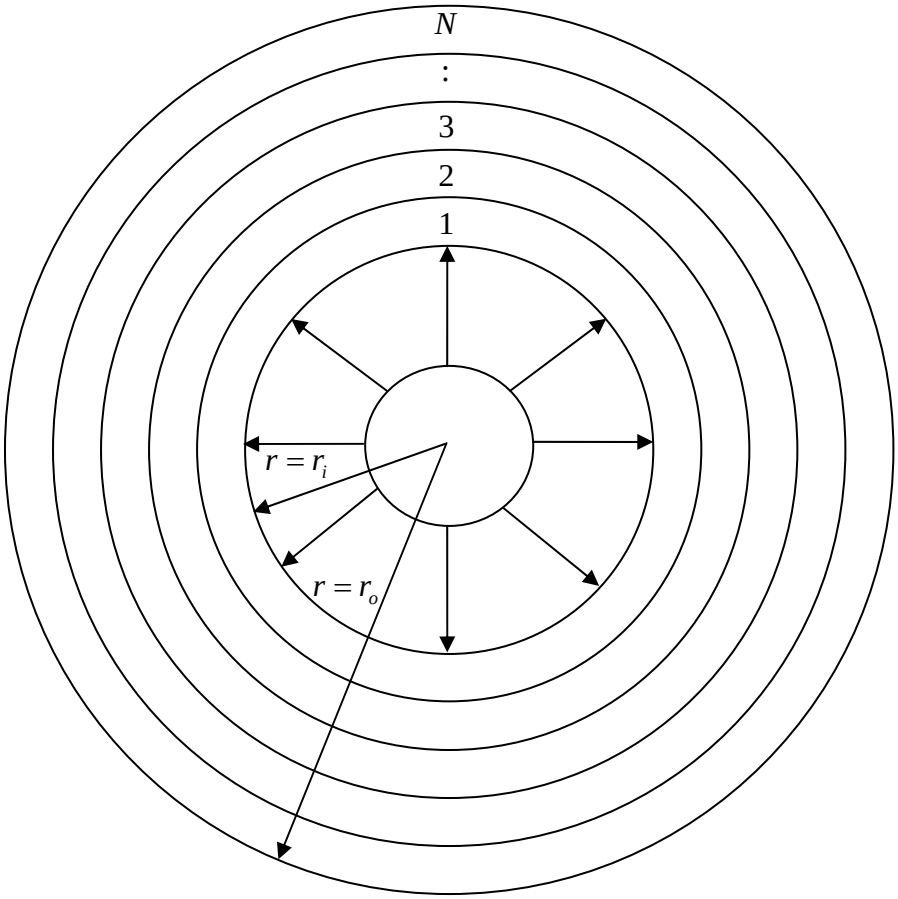

Figure 2.4 A cylindrical layered medium consists of N different FGM layers subjected to uniform pressure.

$$c = c_0(a+br)^m = (2\mu_0 + \lambda_0)(a+br)^m,$$

$$\rho = \rho_0 (a+b\,r)^n, \tag{2.78}$$

$$\mu = \mu_0(a+br)^m$$

$$\lambda = \lambda_0(a+br)^m$$

where a and b are dimensionless constants representing the gradients of the typical FGM layer. $c_0 = 2\mu_0 + \lambda_0$ and ρ_0 are the reference stiffness and mass density of the typical layer, respectively. Similar forms of Eq. (2.78) with $a = 1$ and $m = n = 1$ were used by Liu *et al*. [12], with $a = 1$ and $m = n = 2$ by Han *et al*. [10] and with $a = 1$ by Chiu and Erdogan [13], in investigating one-dimensional transient wave propagation in an FGM plate subjected to a uniform pressure wavelet at one of its outer boundaries. This general form of Eq. (2.78) is selected because it is suitable for a multilayered medium that consists of more than one FGM layer. The advantage of selecting equation (2.78) in this form will be discussed later in Chapter 4.

In view of Eq. (2.78), the constitutive equations, Eq. (2.75), can be combined in one equivalent equation (wave equation), in terms of the displacement component u_r, as

$$\frac{\partial}{\partial r}\left(c\frac{\partial u_r}{\partial r}+\lambda\frac{u_r}{r}\right)+\frac{1}{r}\left(c\frac{\partial u_r}{\partial r}+\lambda\frac{u_r}{r}-c\frac{u_r}{r}-\lambda\frac{\partial u_r}{\partial r}\right)=\rho\frac{\partial^2 u_r}{\partial t^2}$$

Since $(c=2\mu+\lambda)$ and λ are functions of r, only, and $u_r=u_r(r,t)$ then the last equation can be written as:

$$\frac{dc}{dr}\frac{\partial u_r}{\partial r}+c\frac{\partial^2 u_r}{\partial r^2}+\frac{d\lambda}{dr}\frac{u_r}{r}+\frac{\lambda}{r}\frac{\partial u_r}{\partial r}-\frac{\lambda u_r}{r^2}+\frac{2\mu}{r}\frac{\partial u_r}{\partial r}-\frac{2\mu}{r^2}u_r=\rho\frac{\partial^2 u_r}{\partial t^2}$$

$$\frac{\partial u_r}{\partial r}\left(\frac{dc}{dr}+\frac{\lambda}{r}+\frac{2\mu}{r}\right)+\frac{u_r}{r}\left(\frac{d\lambda}{dr}-\frac{\lambda}{r}-\frac{2\mu}{r}\right)+c\frac{\partial^2 u_r}{\partial r^2}=\rho\frac{\partial^2 u_r}{\partial t^2}$$

$$\frac{\partial u_r}{\partial r}\left(\frac{dc}{dr}+\frac{c}{r}\right)+\frac{u_r}{r}\left(\frac{d\lambda}{dr}-\frac{c}{r}\right)+c\frac{\partial^2 u_r}{\partial r^2}=\rho\frac{\partial^2 u_r}{\partial t^2}$$

which can be rearranged as

$$c\frac{\partial^2 u_r}{\partial r^2}+\left(\frac{dc}{dr}+\frac{c}{r}\right)\frac{\partial u_r}{\partial r}+\left(\frac{d\lambda}{dr}-\frac{c}{r}\right)\frac{u_r}{r}=\rho\frac{\partial^2 u_r}{\partial t^2}, \tag{2.79}$$

where $0\le t,\ R_i\le r\le R_o$. The last equation that is the same as Eq. (1.1), is one-dimensional wave equation which is required to be solved, in this thesis, satisfying boundary, initial and interface conditions. The boundary condition at the inner surface $(r=R_i)$ of the multilayered medium is a time-dependent pressure pulse defined as

$$\tau_{rr}(R_i,t)=c\frac{\partial u_r}{\partial r}+\lambda\frac{u_r}{r}=-p_0 f(t), \tag{2.80}$$

where p_0 is the intensity of the applied load and $f(t)$ is a prescribed function of t. The outer surface $(r=R_o)$ is assumed to be either free of surface traction, fixed or it can be assumed to be subjected to the same load applied at the inner surface, Eq. (2.80). Hence, the free or fixed boundary conditions can be written, respectively, as

$$\tau_{rr}(R_o,t)=0 \quad \text{or} \quad u_r(R_o,t)=0. \tag{2.81}$$

In the method employed in this study, we note that other alternatives for boundary conditions, such as mixed-mixed boundary conditions on both surfaces, i.e., one component of displacement and the other component of the surface traction can be handled with equal ease on both surfaces. Furthermore, Eq. (2.80) can be replaced by Eq. (2.81) at the inner boundary and Eq. (2.81) can be replaced by Eq. (2.80) at the outer boundary. The layers of the multilayered medium are assumed to be perfectly

bonded to each other; hence, the interface conditions imply that the normal stress (τ_{rr}) and the displacement (u_r) are continuous across the interfaces of the layers. The multilayered medium is assumed to be initially at rest; hence, all the field variables are zero at $(t \le 0)$. The formulation of the problem is thus now complete.

In view of Eq. (2.78), the governing field equations, Eq. (2.77), are to be applied to each layer and the solutions will be required to satisfy the interface conditions at the interfaces, the boundary conditions at inner and outer surfaces, Eqs. (2.80-2.81), and quiescent initial condition.

2.3 SOLUTION OF THE PROBLEM

The solution is obtained by employing the method of characteristics. This numerical technique involves first rewriting the constitutive hyperbolic differential equation, Eq. (2.79), in view of Eqs. (2.77-2.78) as a system of first order partial differential equations as:

$$
\begin{aligned}
&\frac{\partial \tau_{rr}}{\partial t} - (2\mu + \lambda)\frac{\partial v_r}{\partial r} - \frac{\lambda}{r} v_r = 0 \\
&\frac{\partial \tau_{\theta\theta}}{\partial t} - (2\mu + \lambda)\frac{v_r}{r} - \lambda \frac{\partial v_r}{\partial r} = 0 \\
&\frac{\partial \varepsilon_{rr}}{\partial t} - \frac{\partial v_r}{\partial r} = 0 \\
&\frac{\partial u_r}{\partial t} - v_r = 0 \\
&\frac{\partial v_r}{\partial t} - \frac{1}{\rho}\frac{d(2\mu + \lambda)}{dr}\varepsilon_{rr} - \frac{(2\mu + \lambda)}{\rho}\frac{\partial \varepsilon_{rr}}{\partial r} - \\
&\quad \frac{1}{\rho r}\frac{d\lambda}{dr}u_r - \frac{\lambda}{\rho r}\frac{\partial u_r}{\partial r} + \frac{\lambda}{r^2 \rho}u_r - \frac{1}{\rho r}\tau_{rr} + \frac{1}{\rho r}\tau_{\theta\theta} = 0
\end{aligned}
\qquad (2.82a)
$$

Thus, solving this system is equivalent to solving the second order partial differential equation given in (2.79). For simplicity, Eq. (2.82a) can also be written in matrix form as:

$$\underline{A}\,\underline{U}_{,t} + \underline{B}\,\underline{U}_{,r} + \underline{F} = \underline{0} \qquad (2.82b)$$

where

$$\underline{A} = \underline{I} = \begin{bmatrix} 1 & 0 & 0 & 0 & 0 \\ 0 & 1 & 0 & 0 & 0 \\ 0 & 0 & 1 & 0 & 0 \\ 0 & 0 & 0 & 1 & 0 \\ 0 & 0 & 0 & 0 & 1 \end{bmatrix}, \tag{2.83}$$

with $\underline{I}$ being a (5x5) identity matrix. Recalling that $c = 2\mu + \lambda$ in Eq. (2.82b), $\underline{B}$ is (5x5) square matrix that can be expressed as:

$$\underline{B} = \begin{bmatrix} 0 & 0 & 0 & 0 & -c \\ 0 & 0 & 0 & 0 & -\lambda \\ 0 & 0 & 0 & 0 & -1 \\ 0 & 0 & 0 & 0 & 0 \\ 0 & 0 & \dfrac{-c}{\rho} & \dfrac{-\lambda}{\rho r} & 0 \end{bmatrix}, \tag{2.84}$$

$\underline{F}$ is a five-dimensional column vector with the elements

$$\underline{F} = \begin{bmatrix} -\dfrac{\lambda}{r} v_r \\ \dfrac{-c}{r} v_r \\ 0 \\ -v_r \\ -\dfrac{1}{\rho}\left(\dfrac{dc}{dr}\right)\varepsilon_{rr} - \dfrac{1}{\rho r}\dfrac{d\lambda}{dr} u_r + \dfrac{\lambda}{r^2 \rho} u_r - \dfrac{1}{\rho r}\tau_{rr} + \dfrac{1}{\rho r}\tau_{\theta\theta} \end{bmatrix} \tag{2.85}$$

and $\underline{U}$ is a five-dimensional column vector containing the unknown field variables:

$$\underline{U} = \begin{bmatrix} \tau_{rr} \\ \tau_{\theta\theta} \\ \varepsilon_{rr} \\ u_r \\ v_r \end{bmatrix}, \tag{2.86}$$

In Eq. (2.82b), comma denotes partial differentiation with respect to the corresponding variable, i.e.,

$$\underline{U}_{,t} = \frac{\partial \underline{U}}{\partial t}, \qquad \underline{U}_{,r} = \frac{\partial \underline{U}}{\partial r}. \tag{2.87}$$

Before establishing the canonical form of the governing equations, we will establish the characteristic lines along which these equations are valid. These lines are governed by the characteristic equation, which can be written as, see Ref. [27]

$$\det(\underline{B} - V\,\underline{A}) = 0 \tag{2.88}$$

where $V = \dfrac{dr}{dt}$ defines the characteristic lines on the $(r-t)$ plane.

Substituting Eqs. (2.83, 2.84) into Eq. (2.88), the characteristic equation can be expressed as

$$\left\| \begin{bmatrix} 0 & 0 & 0 & 0 & -c \\ 0 & 0 & 0 & 0 & -\lambda \\ 0 & 0 & 0 & 0 & -1 \\ 0 & 0 & 0 & 0 & 0 \\ 0 & 0 & \dfrac{-c}{\rho} & \dfrac{-\lambda}{\rho r} & 0 \end{bmatrix} + \begin{bmatrix} -V & 0 & 0 & 0 & 0 \\ 0 & -V & 0 & 0 & 0 \\ 0 & 0 & -V & 0 & 0 \\ 0 & 0 & 0 & -V & 0 \\ 0 & 0 & 0 & 0 & -V \end{bmatrix} \right\|$$

$$= \begin{vmatrix} -V & 0 & 0 & 0 & -c \\ 0 & -V & 0 & 0 & -\lambda \\ 0 & 0 & -V & 0 & -1 \\ 0 & 0 & 0 & -V & 0 \\ 0 & 0 & \dfrac{-c}{\rho} & \dfrac{-\lambda}{\rho r} & -V \end{vmatrix} =$$

$$= -V^5 + \frac{\lambda V^3}{\rho} + \frac{2\mu V^3}{\rho} = -V^3\left(V^2 - \frac{c}{\rho}\right) = 0\,. \tag{2.89}$$

The roots of the above equation are

$$V_1 = c_p, V_2 = -c_p, V_3 = 0, V_4 = 0, V_5 = 0 \tag{2.90}$$

where

$$c_p = \sqrt{\frac{c}{\rho}} = \sqrt{\frac{\lambda + 2\mu}{\rho}} = \sqrt{\frac{(2\mu_0 + \lambda_0)(a+br)^m}{\rho_0 (a+br)^n}}, \tag{2.91}$$

where c_p is the dilatational wave velocity. In some references c_p is called pressure or longitudinal wave. The waves generated by c_p propagation in the direction perpendicular to the layering direction. Thus, for the problem under consideration, since the inner surface of the cylindrical domain is subjected to uniform radial pressure, dilatational wave is the only wave generated in the domain.

The characteristic lines are defined by:

$$\frac{dr}{dt} = V_1 = c_p \quad \text{along} \quad C^{(1)},$$

$$\frac{dr}{dt} = V_2 = -c_p \quad \text{along} \quad C^{(2)},$$

$$\frac{dr}{dt} = V_3 = 0 \quad \text{along} \quad C^{(3)}, \tag{2.92}$$

$$\frac{dr}{dt} = V_4 = 0 \quad \text{along} \quad C^{(4)},$$

$$\frac{dr}{dt} = V_5 = 0 \quad \text{along} \quad C^{(5)}.$$

Integration of Eq. (2.92), gives the families of the characteristic lines $C^{(i)}$ $(i = 1, 2, 3, 4, 5)$ as

$$C^{(1)}: t = \int \frac{dr}{\sqrt{\dfrac{(2\mu_0 + \lambda_0)(a+br)^m}{\rho_0 (a+br)^n}}},$$

$$C^{(2)}: t = \int \frac{dr}{-\sqrt{\dfrac{(2\mu_0 + \lambda_0)(a+br)^m}{\rho_0 (a+br)^n}}}, \tag{2.93}$$

$C^{(3)}: r$ = constant,

$C^{(4)}: r$ = constant,

$C^{(5)}: r$ = constant.

We note that $C^{(i)}$ $(i = 1,2)$ describe two families of curves with slopes c_p and $-c_p$ respectively, whereas $C^{(3)}$, $C^{(4)}$ and $C^{(5)}$ describes a family of straight lines parallel to the t-axis in the $(r - t)$ plane, see Fig. (2.5). We further, note that for specific values of m and n the integrations presented in Eq. (2.93) can be found easily using Mathematica.

The next step in establishing the canonical form of the governing equations is finding the left-hand eigenvectors $\underline{l}_i$ $(i = 1, 2, 3, 4,5)$ defined as

$$\underline{l}_i^{\,T} (\underline{B} - V_i \underline{A}) = \underline{0} \tag{2.94a}$$

where the letter T over a matrix quantity denotes its transpose. Alternately, we can write

$$(\underline{B}^T - V_i \underline{A}^T) \underline{l}_i^{\,T} = \underline{0}. \tag{2.94b}$$

In view of Eqs. (2.83), (2.84) and Eq. (2.91), Eq. (2.94b) can be written explicitly as:

$$\left[\begin{bmatrix} 0 & 0 & 0 & 0 & -c \\ 0 & 0 & 0 & 0 & -\lambda \\ 0 & 0 & 0 & 0 & -1 \\ 0 & 0 & 0 & 0 & 0 \\ 0 & 0 & \frac{-c}{\rho} & \frac{-\lambda}{\rho r} & 0 \end{bmatrix}^T + \begin{bmatrix} -V & 0 & 0 & 0 & 0 \\ 0 & -V & 0 & 0 & 0 \\ 0 & 0 & -V & 0 & 0 \\ 0 & 0 & 0 & -V & 0 \\ 0 & 0 & 0 & 0 & -V \end{bmatrix}^T\right] \begin{bmatrix} l_1^{(1)} \\ l_2^{(1)} \\ l_3^{(1)} \\ l_4^{(1)} \\ l_5^{(1)} \end{bmatrix} = \begin{bmatrix} 0 \\ 0 \\ 0 \\ 0 \\ 0 \end{bmatrix}$$

$$\begin{bmatrix} -V_i & 0 & 0 & 0 & -c \\ 0 & -V_i & 0 & 0 & -\lambda \\ 0 & 0 & -V_i & 0 & -1 \\ 0 & 0 & 0 & -V_i & 0 \\ 0 & 0 & \frac{-c}{\rho} & \frac{-\lambda}{\rho r} & -V_i \end{bmatrix}^T \begin{bmatrix} l_1^{(i)} \\ l_2^{(i)} \\ l_3^{(i)} \\ l_4^{(i)} \\ l_5^{(i)} \end{bmatrix} = \begin{bmatrix} 0 \\ 0 \\ 0 \\ 0 \\ 0 \end{bmatrix}$$

$$\begin{bmatrix} -V_i & 0 & 0 & 0 & 0 \\ 0 & -V_i & 0 & 0 & 0 \\ 0 & 0 & -V_i & 0 & \frac{-c}{\rho} \\ 0 & 0 & 0 & -V_i & \frac{-\lambda}{\rho r} \\ -c & -\lambda & -1 & 0 & -V_i \end{bmatrix} \begin{bmatrix} l_1^{(i)} \\ l_2^{(i)} \\ l_3^{(i)} \\ l_4^{(i)} \\ l_5^{(i)} \end{bmatrix} = 0$$

$$\begin{aligned} &-V_i l_1^{(i)} = 0, \quad -V_i l_2^{(i)} = 0, \\ &-V_i l_3^{(i)} - \frac{c}{\rho} l_5^{(i)} = 0, \\ &-V_i l_4^{(i)} - \frac{\lambda}{\rho r} l_5^{(i)} = 0, \\ &-c\, l_1^{(i)} - \lambda\, l_2^{(i)} - l_3^{(i)} - V_i l_5^{(i)} = 0. \end{aligned} \tag{2.95}$$

The solution of this matrix equation for $(i = 1, 2, 3, 4, 5)$ gives:

The first eigenvector that can be determined as follows:

for $i = 1$ and $V_1 = c_p$

$$\begin{bmatrix} l_1^{(1)} \\ l_2^{(1)} \\ l_3^{(1)} \\ l_4^{(1)} \\ l_5^{(1)} \end{bmatrix} = \begin{bmatrix} 0 \\ 0 \\ -c_p \\ \left(\frac{-\lambda}{\rho\, r c_p}\right) \\ 1 \end{bmatrix} * \text{constant} \tag{2.96}$$

The second eigenvector that can be written as:

for $i = 2$ and $V_2 = -c_p$

$$\begin{bmatrix} l_1^{(2)} \\ l_2^{(2)} \\ l_3^{(2)} \\ l_4^{(2)} \\ l_5^{(2)} \end{bmatrix} = \begin{bmatrix} 0 \\ 0 \\ c_p \\ \left(\dfrac{\lambda}{\rho\, rc_p} \right) \\ 1 \end{bmatrix} * \text{constant} \tag{2.97}$$

Similarly, for $i = 3$ where $V_3 = 0$ we can find the third eigenvector:

$$\begin{bmatrix} l_1^{(3)} \\ l_2^{(3)} \\ l_3^{(3)} \\ l_4^{(3)} \\ l_5^{(3)} \end{bmatrix} = \begin{bmatrix} 1 \\ 0 \\ -c \\ 0 \\ 0 \end{bmatrix} * \text{constant} \tag{2.98}$$

for $i = 4$ where $V_4 = 0$:

$$\begin{bmatrix} l_1^{(4)} \\ l_2^{(4)} \\ l_3^{(4)} \\ l_4^{(4)} \\ l_5^{(4)} \end{bmatrix} = \begin{bmatrix} 1 \\ \dfrac{-c}{\lambda} \\ 0 \\ 0 \\ 0 \end{bmatrix} * \text{constant.} \tag{2.99}$$

for $i = 5$ where $V_5 = 0$:

$$\begin{bmatrix} l_1^{(5)} \\ l_2^{(5)} \\ l_3^{(5)} \\ l_4^{(5)} \\ l_5^{(5)} \end{bmatrix} = \begin{bmatrix} 0 \\ 0 \\ 0 \\ 1 \\ 0 \end{bmatrix} * \text{constant.} \tag{2.100}$$

We note here that this set of eigenvectors (2.96 – 2.100), should be linearly independent in order to get non-trivial solution for Eq. (2.82b).

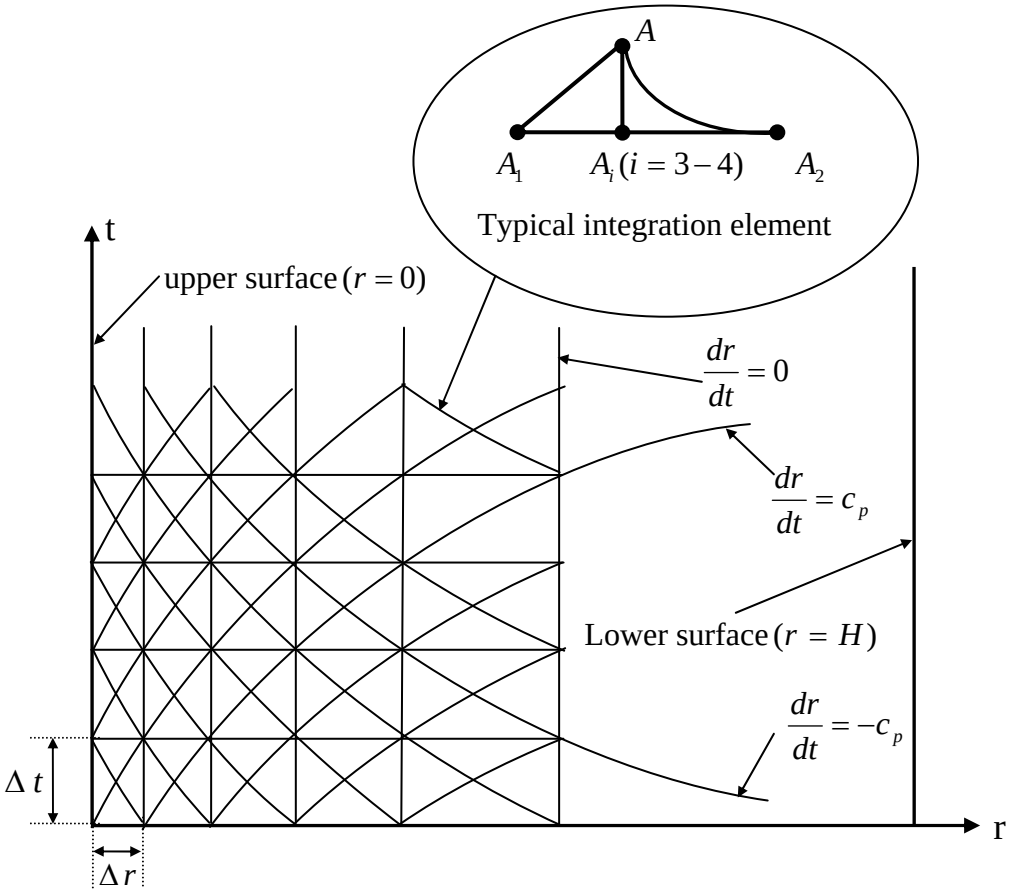

Figure 2.5 Network of characteristic curves on the $(r-t)$ plane.

We now want to obtain the canonical equations. For this purpose, we premultiply Eq. (2.82b) by l_i^T to get

$$\underline{l}_i^T \underline{A}\underline{U}_{,t} + \underline{l}_i^T \underline{B}\underline{U}_{,r} + \underline{l}_i^T \underline{F} = 0 \tag{2.101}$$

Using Eq. (2.94a), the last equation can be expressed as:

$$\underline{l}_i^T \underline{A}\left(\underline{U}_{,t} + V_i \underline{U}_{,r}\right) + \underline{l}_i^T \underline{F} = 0 \tag{2.102}$$

Noting that, $V_i = \dfrac{dr}{dt}$ and the total derivative of $\underline{U}$ with respect to is:

$$\frac{d\underset{\sim}{U}}{dt} = \underset{\sim}{U}_{,t} + \frac{dr}{dt}\underset{\sim}{U}_{,r}$$

the above equation, (2.102), can be expressed as

$$\underset{\sim}{l}_i^T \underset{\sim}{A}\frac{d\underset{\sim}{U}}{dt} + \underset{\sim}{l}_i^T \underset{\sim}{F} = 0 \quad \text{along} \quad \frac{dr}{dt} = V_i\,(i=1-5) \tag{2.103}$$

These equations are called the canonical equations which are valid along the characteristic lines defined by $V_i = \frac{dx}{dt}$ $(i = 1-5)$. In view of Eqs. (2.83, 2.85) and Eqs. (2.96-2.100), the canonical equations can be written explicitly as:

for $i = 1$,

$$\begin{bmatrix} 0 & 0 & -c_p & \frac{-\lambda}{\rho r c_p} & 1 \end{bmatrix} \begin{bmatrix} 1 & 0 & 0 & 0 & 0 \\ 0 & 1 & 0 & 0 & 0 \\ 0 & 0 & 1 & 0 & 0 \\ 0 & 0 & 0 & 1 & 0 \\ 0 & 0 & 0 & 0 & 1 \end{bmatrix} \begin{bmatrix} \frac{d\tau_{rr}}{dt} \\ \frac{d\tau_{\theta\theta}}{dt} \\ \frac{d\varepsilon_{rr}}{dt} \\ \frac{du_r}{dt} \\ \frac{dv_r}{dt} \end{bmatrix} +$$

$$\begin{bmatrix} 0 & 0 & -c_p & \frac{-\lambda}{\rho r c_p} & 1 \end{bmatrix} \begin{bmatrix} -\frac{\lambda}{r} v_r \\ \frac{-c}{r} v_r \\ 0 \\ -v_r \\ -\frac{1}{\rho}\left(\frac{dc}{dr}\right)\varepsilon_{rr} - \frac{1}{\rho r}\frac{d\lambda}{dr} u_r + \frac{\lambda}{r^2 \rho} u_r - \frac{1}{\rho r}\tau_{rr} + \frac{1}{\rho r}\tau_{\theta\theta} \end{bmatrix} = \begin{bmatrix} 0 \\ 0 \\ 0 \\ 0 \\ 0 \end{bmatrix},$$

or simply as:

$$\begin{aligned} & -c_p \frac{d\varepsilon_{rr}}{dt} - \frac{\lambda}{\rho r c_p}\frac{du_r}{dt} + \frac{dv_r}{dt} + \frac{\lambda}{\rho\, r c_p} v_r - \frac{1}{\rho}\frac{dc}{dr}\varepsilon_{rr} \\ & u_r\left(\frac{\lambda}{r^2 \rho} - \frac{1}{\rho r}\frac{d\lambda}{dr}\right) - \frac{1}{\rho r}\tau_{rr} + \frac{1}{\rho r}\tau_{\theta\theta} = 0, \end{aligned} \tag{2.104}$$

which is valid along the family curves $V = c_p$

for $i = 2$,

$$\begin{bmatrix} 0 & 0 & c_p & \dfrac{\lambda}{\rho r c_p} & 1 \end{bmatrix} \begin{bmatrix} 1 & 0 & 0 & 0 & 0 \\ 0 & 1 & 0 & 0 & 0 \\ 0 & 0 & 1 & 0 & 0 \\ 0 & 0 & 0 & 1 & 0 \\ 0 & 0 & 0 & 0 & 1 \end{bmatrix} \begin{bmatrix} \dfrac{d\tau_{rr}}{dt} \\ \dfrac{d\tau_{\theta\theta}}{dt} \\ \dfrac{d\varepsilon_{rr}}{dt} \\ \dfrac{du_r}{dt} \\ \dfrac{dv_r}{dt} \end{bmatrix} +$$

$$\begin{bmatrix} 0 & 0 & c_p & \dfrac{\lambda}{\rho r c_p} & 1 \end{bmatrix} \begin{bmatrix} -\dfrac{\lambda}{r} v_r \\ \dfrac{-c}{r} v_r \\ 0 \\ -v_r \\ -\dfrac{1}{\rho}\left(\dfrac{dc}{dr}\right)\varepsilon_{rr} - \dfrac{1}{\rho r}\dfrac{d\lambda}{dr} u_r + \dfrac{\lambda}{r^2 \rho} u_r - \dfrac{1}{\rho r}\tau_{rr} + \dfrac{1}{\rho r}\tau_{\theta\theta} \end{bmatrix} = \begin{bmatrix} 0 \\ 0 \\ 0 \\ 0 \\ 0 \end{bmatrix},$$

or simply as:

$$\begin{aligned} & c_p \frac{d\varepsilon_{rr}}{dt} + \frac{\lambda}{\rho r c_p}\frac{du_r}{dr} + \frac{dv_r}{dr} + \frac{-\lambda}{\rho r c_p} v_r - \frac{1}{\rho}\frac{dc}{dr}\varepsilon_{rr} \\ & + u_r\left(\frac{\lambda}{r^2\rho} - \frac{1}{\rho r}\frac{d\lambda}{dr}\right) - \frac{1}{\rho r}\tau_{rr} + \frac{1}{\rho r}\tau_{\theta\theta} = 0, \end{aligned} \tag{2.105}$$

for $i = 3$,

$$\begin{bmatrix} 0 & 0 & -c & 0 & 0 \end{bmatrix} \begin{bmatrix} 1 & 0 & 0 & 0 & 0 \\ 0 & 1 & 0 & 0 & 0 \\ 0 & 0 & 1 & 0 & 0 \\ 0 & 0 & 0 & 1 & 0 \\ 0 & 0 & 0 & 0 & 1 \end{bmatrix} \begin{bmatrix} \dfrac{d\tau_{rr}}{dt} \\ \dfrac{d\tau_{\theta\theta}}{dt} \\ \dfrac{d\varepsilon_{rr}}{dt} \\ \dfrac{du_r}{dt} \\ \dfrac{dv_r}{dt} \end{bmatrix} +$$

$$\begin{bmatrix}0 & 0 & -c & 0 & 0\end{bmatrix}\begin{bmatrix} -\frac{\lambda}{r}v_r \\ \frac{-c}{r}v_r \\ 0 \\ -v_r \\ -\frac{1}{\rho}\left(\frac{dc}{dr}\right)\varepsilon_{rr} - \frac{1}{\rho r}\frac{d\lambda}{dr}u_r + \frac{\lambda}{r^2\rho}u_r - \frac{1}{\rho r}\tau_{rr} + \frac{1}{\rho r}\tau_{\theta\theta} \end{bmatrix} = \begin{bmatrix}0\\0\\0\\0\\0\end{bmatrix},$$

or simply as:

$$\frac{d\tau_{rr}}{dt} - c\frac{d\varepsilon_{rr}}{dt} - \frac{\lambda}{r}v_r = 0 \tag{2.106}$$

for $i = 4$,

$$\begin{bmatrix}1 & \frac{-c}{\lambda} & 0 & 0 & 0\end{bmatrix}\begin{bmatrix}1&0&0&0&0\\0&1&0&0&0\\0&0&1&0&0\\0&0&0&1&0\\0&0&0&0&1\end{bmatrix}\begin{bmatrix}\frac{d\tau_{rr}}{dt}\\ \frac{d\tau_{\theta\theta}}{dt}\\ \frac{d\varepsilon_{rr}}{dt}\\ \frac{du_r}{dt}\\ \frac{dv_r}{dt}\end{bmatrix} +$$

$$\begin{bmatrix}1 & \frac{-c}{\lambda} & 0 & 0 & 0\end{bmatrix}\begin{bmatrix} -\frac{\lambda}{r}v_r \\ \frac{-c}{r}v_r \\ 0 \\ -v_r \\ -\frac{1}{\rho}\left(\frac{dc}{dr}\right)\varepsilon_{rr} - \frac{1}{\rho r}\frac{d\lambda}{dr}u_r + \frac{\lambda}{r^2\rho}u_r - \frac{1}{\rho r}\tau_{rr} + \frac{1}{\rho r}\tau_{\theta\theta} \end{bmatrix} = \begin{bmatrix}0\\0\\0\\0\\0\end{bmatrix},$$

or simply as:

$$\frac{d\tau_{rr}}{dt} - \frac{c}{\lambda}\frac{d\tau_{\theta\theta}}{dt} - \frac{\lambda}{r}v_r + \frac{c^2}{r\lambda}v_r = 0 \tag{2.107}$$

and finally,

for $i = 5$,

$$\begin{bmatrix} 0 & 0 & 0 & 1 & 0 \end{bmatrix} \begin{bmatrix} 1 & 0 & 0 & 0 & 0 \\ 0 & 1 & 0 & 0 & 0 \\ 0 & 0 & 1 & 0 & 0 \\ 0 & 0 & 0 & 1 & 0 \\ 0 & 0 & 0 & 0 & 1 \end{bmatrix} \begin{bmatrix} \dfrac{d\tau_{rr}}{dt} \\ \dfrac{d\tau_{\theta\theta}}{dt} \\ \dfrac{d\varepsilon_{rr}}{dt} \\ \dfrac{du_r}{dt} \\ \dfrac{dv_r}{dt} \end{bmatrix} +$$

$$\begin{bmatrix} 0 & 0 & 0 & 1 & 0 \end{bmatrix} \begin{bmatrix} -\dfrac{\lambda}{r} v_r \\ \dfrac{-c}{r} v_r \\ 0 \\ -v_r \\ -\dfrac{1}{\rho}\left(\dfrac{dc}{dr}\right)\varepsilon_{rr} - \dfrac{1}{\rho r}\dfrac{d\lambda}{dr} u_r + \dfrac{\lambda}{r^2 \rho} u_r - \dfrac{1}{\rho r}\tau_{rr} + \dfrac{1}{\rho r}\tau_{\theta\theta} \end{bmatrix} = \begin{bmatrix} 0 \\ 0 \\ 0 \\ 0 \\ 0 \end{bmatrix},$$

or simply as:

$$\frac{du_r}{dr} - v_r = 0 \tag{2.108}$$

Thus, the system of governing partial differential equations, (2.82b), is transformed into a set of ordinary differential equations, (2.104–2.108) which are valid along the characteristic lines.

A through description of the method of characteristics is given by Courant and Hilbert, see Ref [27]. For more details of the derivations of the basic equations used in the method of characteristics, see Appendix A.

Our aim now, is to solve the canonical equations, (2.104–2.108), by integrating them numerically along the characteristic lines. For this purpose, the trapezoidal technique will be used in the following subsection.

2.4 INTEGRATION OF THE CANONICAL EQUATIONS

The canonical forms of the governing equations valid along the characteristic lines are given by Eqs. (2.104–2.108). These equations which are valid along the characteristic curves, $\frac{dz}{dt}=V_i \quad (i=1-5)$, can be written in a more compact form in indicial notation as:

$$G_{ij}\frac{dU_j}{dt}=H_{ij}U_j,\,(i,j=1-5) \tag{2.109}$$

where the repeated index j implies summation, U_j are the components of the unknown vector defined in Eq. (2.86) and K_{ij} and F_{ij} can be expressed explicitly as:

$$G_{ij}=\begin{bmatrix} 0 & 0 & -c_p & \frac{-\lambda}{\rho r c_p} & 1 \\ 0 & 0 & c_p & \frac{\lambda}{\rho r c_p} & 1 \\ 1 & 0 & -c & 0 & 0 \\ 1 & \frac{-c}{\lambda} & 0 & 0 & 0 \\ 0 & 0 & 0 & 1 & 0 \end{bmatrix} \tag{2.110}$$

$$H_{ij}=\begin{bmatrix} \frac{1}{\rho r} & \frac{-1}{\rho r} & \frac{1}{\rho}\frac{dc}{dr} & \left(\frac{-\lambda}{r^2\rho}+\frac{1}{\rho r}\frac{d\lambda}{dr}\right) & \frac{-\lambda}{\rho r c_p} \\ \frac{1}{\rho r} & \frac{-1}{\rho r} & \frac{1}{\rho}\frac{dc}{dr} & \left(\frac{-\lambda}{r^2\rho}-\frac{1}{\rho r}\frac{d\lambda}{dr}\right) & \frac{\lambda}{\rho r c_p} \\ 0 & 0 & 0 & 0 & \frac{\lambda}{r} \\ 0 & 0 & 0 & 0 & \left(\frac{\lambda}{r}-\frac{c^2}{r\lambda}\right) \\ 0 & 0 & 0 & 0 & 1 \end{bmatrix} \tag{2.111}$$

Before proceeding further, we note an important comment about the wave fronts. A wave front separates the undisturbed region from the disturbed region, or the already disturbed region from the region having additional disturbance. This means that the field variables or their derivatives should have finite jumps across the wave fronts. Therefore, from the definition of characteristic, it follows that the wave fronts should be members of the characteristic families. Due to zero initial conditions, we have one wave front in our problems, which is a member of the characteristic family

$V_1 = \dfrac{dr}{dt} = c_p$, and emanate from the origin ($r = R_i$, $t = 0$). Using the typical integration element shown in Fig. 2.6, we now integrate the canonical equations, i.e., Eq. (2.109), along the characteristic lines as:

$$\int_{A_i}^{A} G_{ij} \frac{dU_j}{dt} dt = \int_{A_i}^{A} H_{ij} U_j dt, \tag{2.112}$$

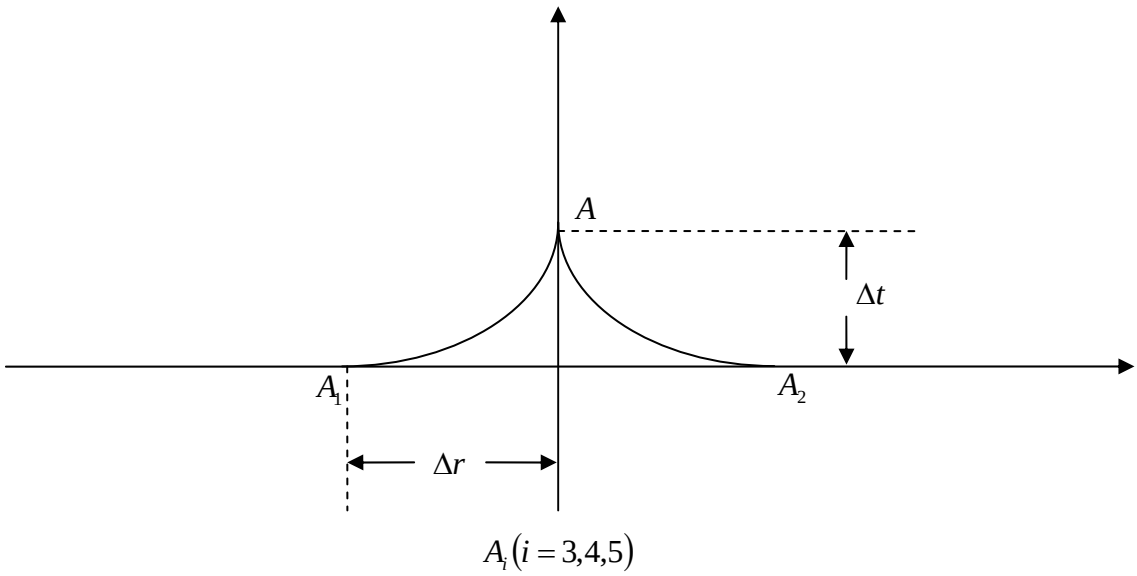

Fig.2.6 The typical integration element used in the numerical analysis.

$$G = \begin{bmatrix} 0 & 0 & -c_p & \dfrac{-\lambda}{\rho r c_p} & 1 \\ 0 & 0 & c_p & \dfrac{\lambda}{\rho r c_p} & 1 \\ 1 & 0 & -(2\mu+\lambda) & 0 & 0 \\ 1 & \dfrac{-(2\mu+\lambda)}{\lambda} & 0 & 0 & 0 \\ 0 & 0 & 0 & 1 & 0 \end{bmatrix} \tag{2.113}$$

$$H=\begin{bmatrix} \frac{-1}{\rho r} & \frac{1}{\rho r} & \frac{-1}{\rho}\frac{d(2\mu+\lambda)}{dr} & \left(\frac{\lambda}{r^2\rho}-\frac{1}{\rho r}\frac{d\lambda}{dr}\right) & \frac{\lambda}{\rho r c_p} \\ \frac{-1}{\rho r} & \frac{1}{\rho r} & \frac{-1}{\rho}\frac{d(2\mu+\lambda)}{dr} & \left(\frac{\lambda}{r^2\rho}-\frac{1}{\rho r}\frac{d\lambda}{dr}\right) & \frac{-\lambda}{\rho r c_p} \\ 0 & 0 & 0 & 0 & \left(\frac{-\lambda}{r}+\frac{(2\mu+\lambda)^2}{\lambda r}\right) \\ 0 & 0 & 0 & 0 & \left(\frac{-\lambda}{r}\right) \\ 0 & 0 & 0 & 0 & -1 \end{bmatrix} \tag{2.114}$$

where A and A_i are consecutive points along the characteristic lines defined, respectively, at current and previous time steps as shown in the typical integration element shown inside Fig. (2.6). Taking into consideration that the coefficients K_{ij} are constants and the coefficients F_{ij} are functions of r only, the above integration can be performed easily by using the trapezoidal rule as [29]

$$G_{ij}U_j(A)-G_{ij}U_j(\underline{A_i})-(\frac{\Delta t}{2})\{H_{ij}(A)U_j(A)+H_{ij}(\underline{A_i})U_j(\underline{A_i})\}=0. \tag{2.115}$$

Alternately, this equation can be rewritten as:

$$W_{\underline{ij}}U_j(A)=M_{\underline{ij}}U_j(\underline{A_i}) \quad (i,j=1-5), \tag{2.116}$$

$$\text{where, } W_{ij}=G_{ij}-(\frac{\Delta t}{2})H_{ij}(A) \quad \text{and} \quad M_{\underline{ij}}=G_{\underline{ij}}+(\frac{\Delta t}{2})H_{ij}(\underline{A_i}). \tag{2.117}$$

or in matrix form as

$$W=\begin{bmatrix} \frac{-\Delta t}{2\rho r} & \frac{\Delta t}{2\rho r} & -c_p-\frac{\Delta t}{2\rho}\frac{dc}{dr} & \frac{-\lambda}{\rho c_p}+\frac{\Delta t}{2}\left(\frac{\lambda}{r^2\rho}-\frac{1}{\rho r}\frac{d\lambda}{dr}\right) & 1+\frac{\Delta t\lambda}{2\rho r c_p} \\ \frac{-\Delta t}{2\rho r} & \frac{\Delta t}{2\rho r} & c_p-\frac{\Delta t}{2\rho}\frac{dc}{dr} & \frac{\lambda}{\rho c_p}+\frac{\Delta t}{2}\left(\frac{\lambda}{r^2\rho}-\frac{1}{\rho r}\frac{d\lambda}{dr}\right) & 1-\frac{\Delta t\lambda}{2\rho r c_p} \\ 1 & 0 & -c & 0 & \frac{-\Delta t}{2}\left(\frac{\lambda}{r}\right) \\ 1 & \frac{-c}{\lambda} & 0 & 0 & \frac{\Delta t}{2}\left(\frac{-\lambda}{r}+\frac{c^2}{\lambda r}\right) \\ 0 & 0 & 0 & 1 & \frac{-\Delta t}{2} \end{bmatrix} \tag{2.118}$$

$$M=\begin{bmatrix} \frac{\Delta t}{2\rho r} & \frac{-\Delta t}{2\rho r} & -c_p+\frac{\Delta t}{2\rho}\frac{dc}{dr} & \frac{-\lambda}{\rho r c_p}-\frac{\Delta t}{2}\left(\frac{\lambda}{r^2\rho}-\frac{1}{\rho r}\frac{d\lambda}{dr}\right) & 1-\frac{\Delta t\lambda}{2\rho r c_p} \\ \frac{\Delta t}{2\rho r} & \frac{-\Delta t}{2\rho r} & c_p+\frac{\Delta t}{2\rho}\frac{dc}{dr} & \frac{\lambda}{\rho r c_p}-\frac{\Delta t}{2}\left(\frac{\lambda}{r^2\rho}-\frac{1}{\rho r}\frac{d\lambda}{dr}\right) & 1+\frac{\Delta t\lambda}{2\rho r c_p} \\ 1 & 0 & -c & 0 & \frac{\Delta t}{2}\left(\frac{\lambda}{r}\right) \\ 1 & \frac{-c}{\lambda} & 0 & 0 & \frac{-\Delta t}{2}\left(\frac{-\lambda}{r}+\frac{c^2}{\lambda r}\right) \\ 0 & 0 & 0 & 1 & \frac{\Delta t}{2} \end{bmatrix} \tag{2.119}$$

The elements of K_{ij} and F_{ij} are given in Eqs. (2.113-2.114). In Eqs. (2.115-2.117) there is no summation over the underlined index $(\underline{i})$, therefore, Eq. (2.115) represents five equations defined by $i=1-5$ and for each value of the index i, there is a summation over j which takes the values $j=1-5$. The composite body considered in this thesis consists of $N-$different, non-homogeneous and linearly elastic layers. In the numerical procedure each layer $(1, 2, 3,..., N)$ is subdivided into $p-$homogeneous layers, so that the equations derived at the beginning of this chapter will be valid to each layer. Eqs. (2.116) were derived for a typical layer which will be considered as the p^{th} layer and all quantities pertaining to it will be denoted by the subscripts or superscripts p in between parenthesis, i.e. , $c^{(P)(L)}$, $\mu^{(P)}$, $\lambda^{(P)(L)}$, $\rho^{(P)(L)}$ and so on...

For the composite domain consistency of $N-$layers $(L=1, 2, ..., N)$ each is subdivided into p layers where p depends on the gradient material properties of each layer from 1 to N, Eq. (2.116) can be written as:

$$W_{\underline{i}j}^{(P)(L)}U_j^{(P)(L)}(A)=M_{\underline{i}j}^{(P)(L)}U_j^{(P)(L)}(A_{\underline{i}}) \tag{2.120}$$

$(i, j=1, 2, 3, 4, 5),\quad (L=1, 2,..., N),\quad (P=1, 2,...)$

Where $W_{\underline{i}j}^{(P)(L)}$ and $M_{\underline{i}j}^{(P)(L)}$ can be obtained simply by denoting all quantities appearing in the matrices of Eqs. (2.118-2.119) with the subscript or superscript $(P)(L)$ in parenthesis.

Thus, when the values of $U_j^{(p)}$ are known at points $A_{\underline{i}}$ $(i=1-5)$, the unknown vector at point A, $\{U_j^{(p)}(A)\quad j=1-5)\}$, can be determined form Eq. (2.116) easily by

a step-by-step numerical procedure discussed below. In other words, using the triangle element shown inside Fig. 2.6, the field variables at a specific point along any line parallel to the x_r - axis in the solution region can be found in terms of the known field variables defined on the previous line. For this purpose, we refer to the network of the characteristic lines, Fig. 2.6. To compute the components of the unknown vector $\{U_j^{(p)}(\ j=1-5)\}$ presented in Eq. (2.119) at every intersection point between the characteristic lines on the $r-t$ plane: we start our solution on the network from the r - axis, where the values of all field variables are zero due to zero initial conditions, and advance into the solution region by computing U_j at the intersection points of the network between the top and the outer boundary along the lines $t=\Delta t,\ t=2\Delta t,\ t=3\Delta t,.....,\ t=J_{\max}\Delta t.....$ etc. In this computational process, the inner layer is considered to be layer 1, while the lower layer is considered to be layer N. To explain this numerical procedure we refer to four different locations of the typical integration element;

(a) When the typical integration element is located at the inner boundary then the first equation of Eqs. (2.120), which is valid along the curve $A-A_1$ is replaced by the boundary condition applied at the inner boundary, that is, when the point A of the typical element is located at the boundary $(r=R_i)$; Eqs. (2.120) can be written as:

$$W_{\underline{ij}}^{(P)(L)}U_j^{(P)(L)}(A)=M_{\underline{ij}}^{(P)(L)}U_j^{(P)(L)}(A_{\underline{i}}) \qquad (2.121)$$

$(i=2,3,4,5),\quad (j=1-5),$

The equation for $i=1$ is given by the boundary condition of the inner surface $(r=R_o)$, that is by Eq. (2.80). The superscript (P) in equation (2.121) represents the properties of the first sublayer of the FGM layer, that is $P=1$.

(b) Second, if the integration element is an interior element, then the procedure involves the determination of the values of the unknown vector at a point A in terms of their values at A_1, A_2 and A_i, $(i=3-4)$ using Eqs. (2.120).

(c) Third, if a point A of an integration element is located at an interface between two different FGM layers then the first two equations are replaced by the interface continuity conditions, whereas, in this case the number of field variables becomes double at that point.

For example, Eq. (2.120) can be written for the interface between layer L and $(L+1)$ as:

$$W_{ij}^{(P)(L)} U_j^{(P)(L)}(A) = M_{\underline{i}\,j}^{(P)(L)} U_j^{(P)(L)}(A_{\underline{i}}) \qquad (2.122)$$

$$(i = 1, 3, 4, 5), \quad (j = 1-5),$$

$$W_{ij}^{(P)(L+1)} U_j^{(P)(L+1)}(A) = M_{\underline{i}\,j}^{(P)(L+1)} U_j^{(P)(L+1)}(A_{\underline{i}})$$

$$(i = 2, 3, 4, 5), \quad (j = 1,-5)$$

Where the superscript L donates the layer that precedes the interface and $(L+1)$ defines the layer that follows it. Eqs. (2.122) for $i = 2$ for the L^{th} layer and for $i = 1$ for the $(L+1)^{th}$ layer are replaced by the interface conditions imposing that u_r and τ_{rr} are conditions across the interface, which are:

$$\begin{aligned} u_1^{(P)(L)}(A) &= u_1^{(P)(L+1)}(A) \\ u_4^{(P)(L)}(A) &= u_4^{(P)(L+1)}(A) \end{aligned} \qquad (2.123)$$

In the first equation of Eqs. (2.122) P denote the last sublayer of the L^{th} layer and in the second equation it denotes the first sublayer of the $(N+1)^{th}$ layer. Furthermore, we should note that for N layers ($L = 1,2,...,N$) we have $(N-1)$ interfaces.

(d) Finally, the second equation of Eqs. (2.115) is replaced by the boundary condition applied at the outer boundary, if the typical integration element lies at that boundary.

That is for $L = N$ Eqs. (2.120) becomes

$$W_{ij}^{(P)(N)} U_j^{(P)(N)}(A) = M_{\underline{i}\,j}^{(P)(N)} U_j^{(P)(N)}(A_{\underline{i}}) \qquad (2.124)$$

$$(i = 1, 3, 4, 5), \quad (j = 1, 2, 3, 4, 5)$$

which is valid for the last sublayer of the N^{th} layer that is at $(r = R_o)$. Thus, Eq. (2.124) for $i = 2$ is replaced by the one of the outer boundary conditions given in Eq. (2.81)

The procedure discussed above is repeated as we proceed along the $t-$axis, for example along the line $t = 2\Delta t$ instead of using the initial conditions along the line $t = 0$, we use the field variable which is already evaluated in the previous step along the line $t = \Delta t$. This process is repeated until getting results for a sufficient value of t, for example $t = J_{\max}\Delta t$ where $J_{\max}$ is the maximum number of intervals considered in the t-direction. The code of the numerical procedure is written in Fortran 90, see Appendix B.

CHAPTER 3

NUMERICAL RESULTS AND DISCUSSION

In this chapter, we would like to give some numerical examples related to the formulation presented in chapter 2.

In the following examples, the numerical computations have been carried out and 1the results are displayed in terms of non-dimensional quantities. These dimensionless quantities are taken in terms of the thickness of the first layer ($h_{(1)}$), density of the first layer ($\rho_0^{(1)}$) and dilatational wave velocity ($c_p^{(1)}$) of the first layer. Thus these dimensionless quantities are defined as follows:

$$\bar{\rho}_0^{(1)} = \frac{\rho_0^{(1)}}{\rho_0^{(1)}} = 1, \quad \bar{\rho}_0^{(2)} = \frac{\rho_0^{(2)}}{\rho_0^{(1)}}, \quad \bar{\mu}_0^{(1)} = \frac{\mu_0^{(1)}}{\lambda_0^{(1)} + 2\mu_0^{(1)}}, \quad \bar{\lambda}_0^{(1)} = \frac{\lambda_0^{(1)}}{\lambda_0^{(1)} + 2\mu_0^{(1)}},$$

$$\bar{\mu}_0^{(2)} = \frac{\mu_0^{(2)}}{\lambda_0^{(1)} + 2\mu_0^{(1)}}, \quad \bar{\lambda}_0^{(2)} = \frac{\lambda_0^{(2)}}{\lambda_0^{(1)} + 2\mu_0^{(1)}}, \quad \bar{t} = \frac{t c_p^{(1)}}{h_{(1)}}, \quad \bar{h}_{(1)} = \frac{h_{(1)}}{h_{(1)}} = 1$$

$$\bar{h}_{(2)} = \frac{h_{(2)}}{h_{(1)}}, \quad \bar{r}_i = \frac{r_i}{h_{(1)}}, \bar{v}_r^{(1)} = \frac{v_r^{(1)}}{c_p^{(1)}}, \quad \bar{v}_r^{(2)} = \frac{v_r^{(2)}}{c_p^{(1)}}, \quad \bar{\tau}_{rr}^{(1)} = \frac{\tau_{rr}^{(1)}}{\rho_0^{(1)}\left(c_p^{(1)}\right)^2},$$

$$\bar{\tau}_{rr}^{(2)} = \frac{\tau_{rr}^{(2)}}{\rho_0^{(1)}\left(c_p^{(1)}\right)^2}, \quad \bar{\tau}_{\theta\theta}^{(1)} = \frac{\tau_{\theta\theta}^{(1)}}{\rho_0^{(1)}\left(c_p^{(1)}\right)^2}, \quad \bar{\tau}_{\theta\theta}^{(2)} = \frac{\tau_{\theta\theta}^{(2)}}{\rho_0^{(1)}\left(c_p^{(1)}\right)^2} \tag{3.1}$$

In Eqs. (3.1), the non-dimensional quantities are shown by putting bars over them. We recall that the quantities pertaining to layers 1 and 2 are denoted by putting subscripts 1 and 2 or superscripts 1 and 2 in parenthesis, respectively. For example $\bar{\rho}_0^{(1)}$ and $\bar{\rho}_0^{(2)}$ denote the mass densities, whereas $\bar{v}_r^{(1)}$ and $\bar{v}_r^{(2)}$ denote the dimensionless particle velocities in layers 1 and 2, respectively. Furthermore, $h_{(1)}$ and $h_{(2)}$ represent the thicknesses of layers 1 and 2, respectively. All the other quantities appearing in Eqs. (3.1) are defined in Chapter 2.

3.1 Example 1; Verification problem

We consider the solution of Eq. (1.1) for which λ and c are assumed to constant functions through the thickness of the cylindrical layer. That is, in Eq. (2.71) $a=1$ and b is assumed to be zero. In the numerical examples investigated in this study, the following values for the non-dimensional material and geometrical properties are assumed:

$$\begin{aligned} &\bar{\mu}_0^{(1)}=0.254, \quad \bar{\mu}_0^{(2)}=0.964, \quad \bar{\lambda}_0^{(1)}=0.492, \quad \bar{\lambda}_0^{(2)}=0.972 \\ &\bar{\rho}_0^{(1)}=1, \quad \bar{\rho}_0^{(2)}=2.9, \quad \bar{h}_1=1, \quad \bar{r}_i=1, \quad \bar{h}_2=1, \quad \bar{r}_o=6 \end{aligned} \tag{3.2}$$

3.2 Example 2:

In this example we consider similar properties presented in Eqs. (3.2), but λ and c are assumed to be linear functions in $r-$direction and uniform in the other two directions. That is, in Eq. (2.71) a, b, m and n are assumed to be as follows:

$$a=\frac{5}{6}, \quad b=\frac{1}{6}, \quad m=1, \quad n=1, \tag{3.3}$$

In this case as we noted from the above non-dimensional quantities the cylindrical layered media is assumed to be made of functionally graded material whereas the properties are assumed to be vary linearly through thickness direction.

In these examples (1 & 2), the inner surface ($\bar{r}=1$) is assumed to be subjected to uniform pressure with an initial ramp, see Fig. (3.1), where $\bar{t}_0=0.2$ and $\bar{P}_0=1$, that is

$$f(t)=\begin{cases} 5t & \text{if } t\le 0.2 \\ 1 & \text{if } t>0.2 \end{cases} \tag{3.4}$$

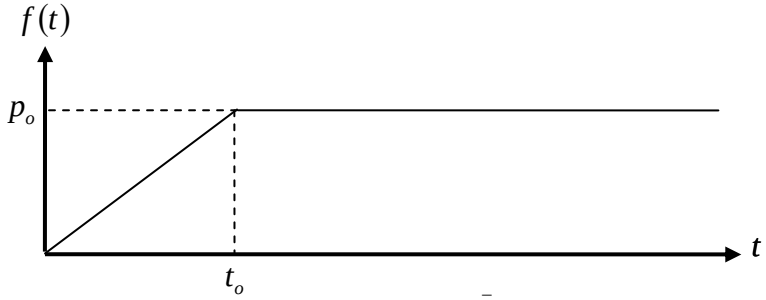

Fig. 3.1 Time variation of the load applied at the inner boundary ($\bar{r}=1$).

on the hand, the outer surface ($\bar{r}=7$) is assumed to be fixed, that is $u_r=0$.

The numerical results presented in these examples have been obtained for three pairs of alternating layers. The innermost layer is taken as layer 1, whereas the outermost layer is taken as layer 2. In Figs. (3.2-3.7) the variations of the dimensionless normal stresses $\frac{\tau_{rr}}{\rho_0}$ and $\frac{\tau_{\theta\theta}}{\rho_0}$ with non-dimensional time at $\bar{r} = 1.5, \bar{r} = 2.5$ and $\bar{r} = 3.5$ are shown for the layered composite with cylindrical layers. In these figures, solid curves are given for the cases where the homogeneous effects are neglected. These solutions in the absence of the homogenity effects, that is for $a = 1$ and $b = 0$ have been investigated in detail in [30]. Our solutions presented in Figs. (3.4-3.5) at $\bar{r} = 2.5$ for the homogeneous case fit exactly those solutions presented in [29]. These results give us more confidence of the method applied in this thesis. On the other hand, solutions presented by dashed curves are devoted for FGM composites with properties given in Eqs. (3.3). From Figs. (3.2-3.7) one can see clearly that the stress level for the homogeneous material are greater than those correspond to FGM composite; this is due to the fact that the outer boundary of the FGM composite is stiffer than the inner boundary. The curves of Figs. (3.2-3.7), further show the effects of reflections and refractions from the inner and outer boundaries and from the interfaces. These effects can be noticed from the sudden changes of stress levels. We note that large changes are due to the reflections and refractions from the outer and inner boundaries, whereas small changes in stress levels are due to reflections and refractions from the interfaces between layers.

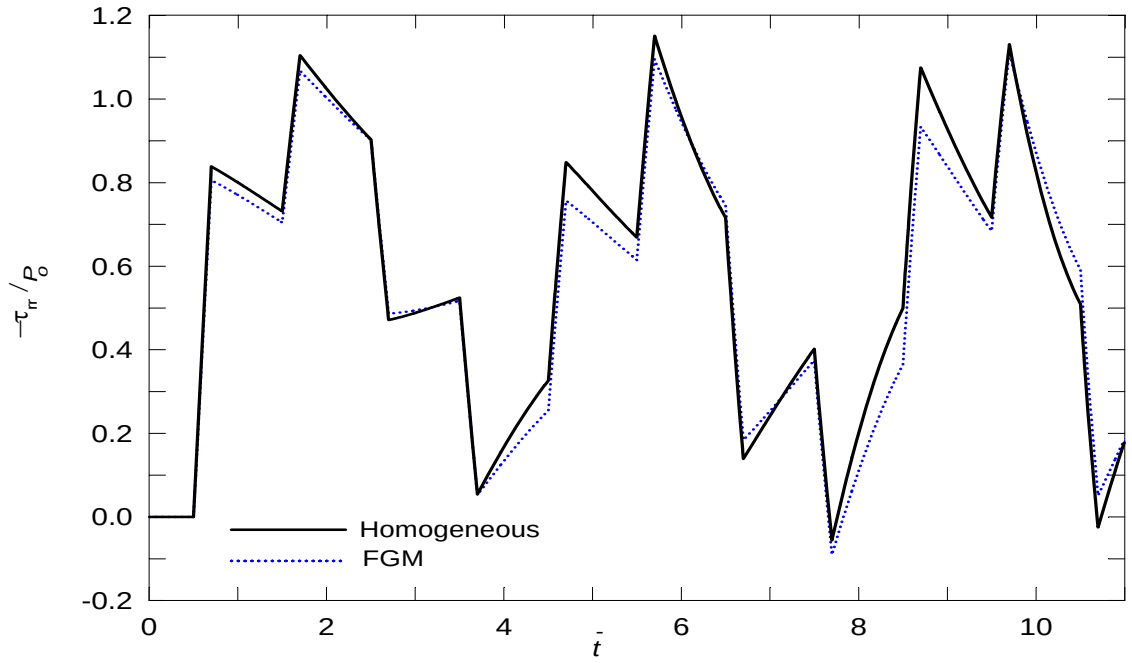

Fig. 3.2 Time variation of the normal stress $\frac{\tau_{rr}}{\rho_0}$ at $\bar{r} = 1.5$ for three pairs of alternating layered cylindrical domain.

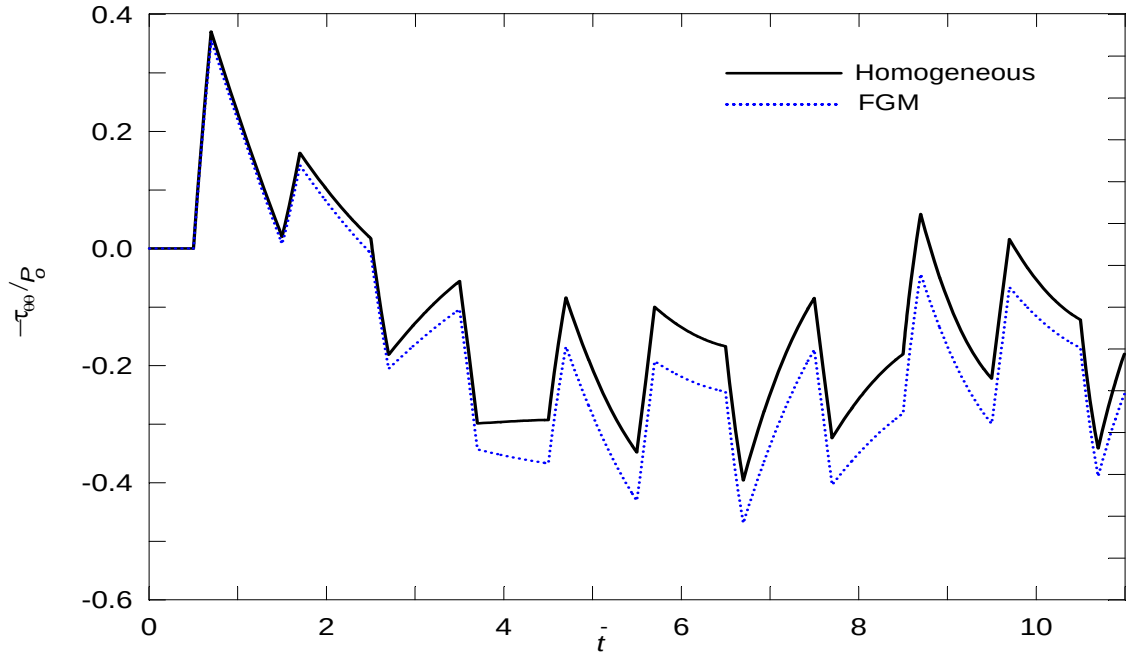

Fig. 3.3 Time variation of the normal stress $\frac{\tau_{\theta\theta}}{\rho_0}$ at $\bar{r} = 1.5$ for three pairs of alternating layered cylindrical domain.

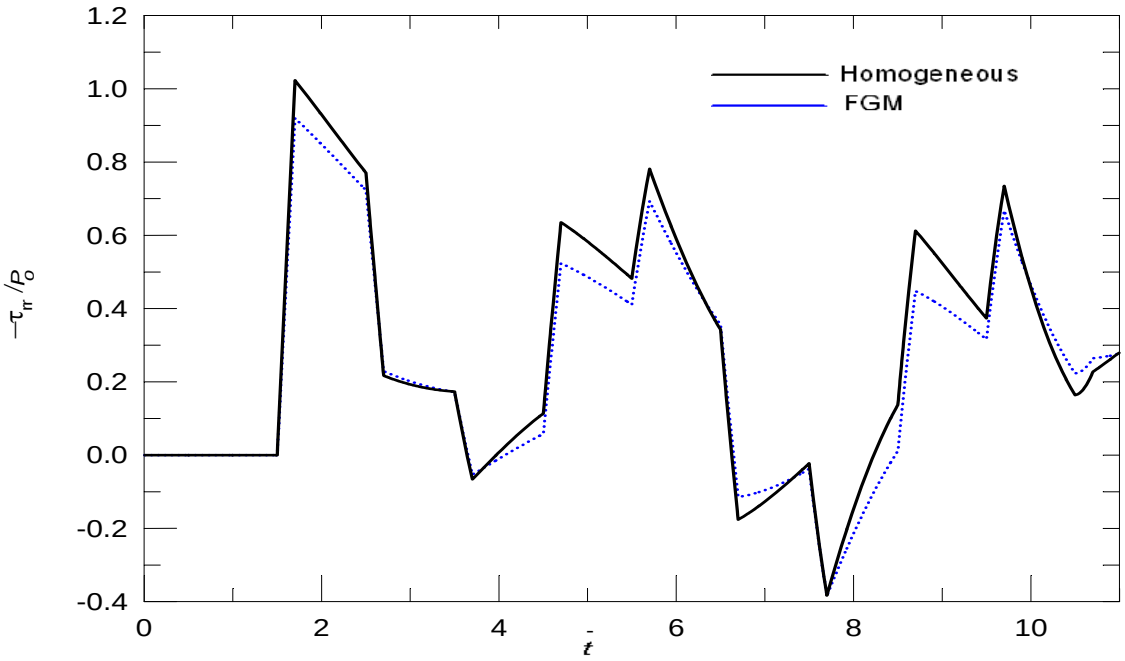

Fig. 3.4 Time variation of the normal stress $\frac{\tau_{rr}}{\rho_0}$ at $\bar{r} = 2.5$ for three pairs of alternating layered cylindrical domain

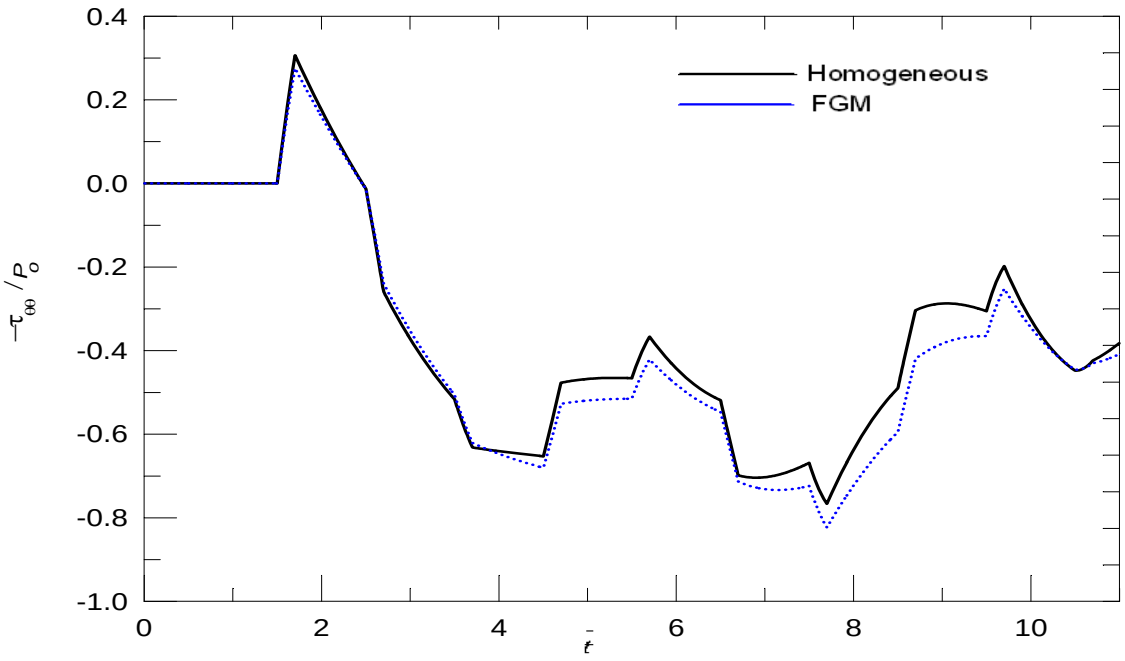

Fig. 3.5 Time variation of the normal stress $\frac{\tau_{\theta\theta}}{\rho_0}$ at $\bar{r} = 2.5$ for three pairs of alternating layered cylindrical domain.

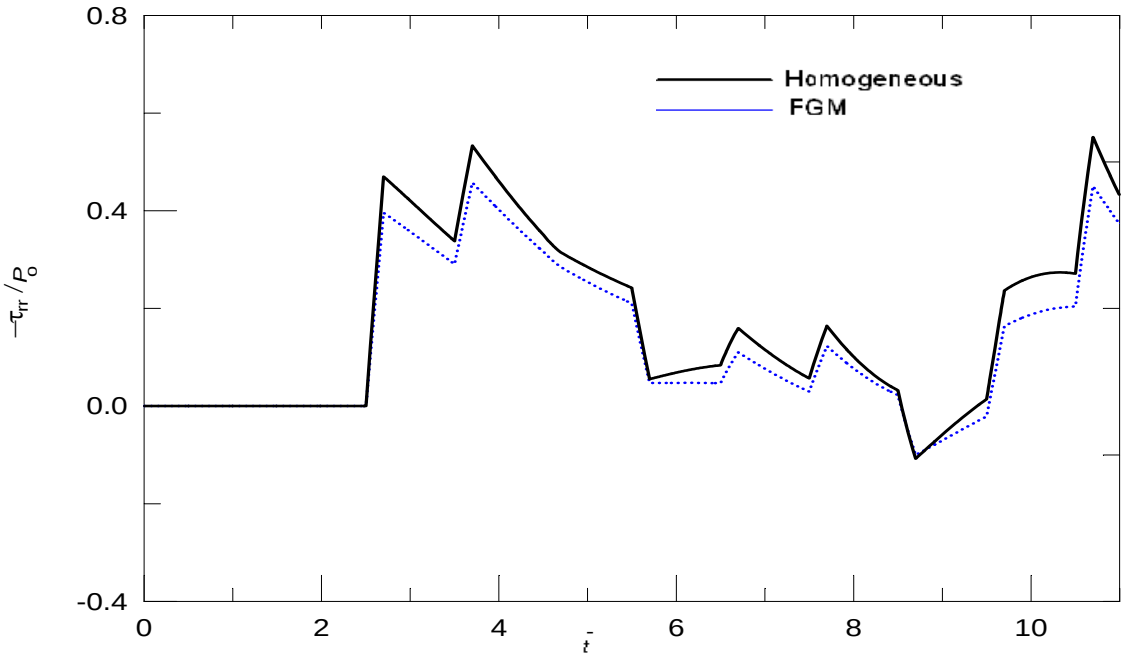

Fig. 3.6 Time variation of the normal stress $\frac{\tau_{rr}}{\rho_0}$ at $\bar{r} = 3.5$ for three pairs of alternating layered cylindrical domain

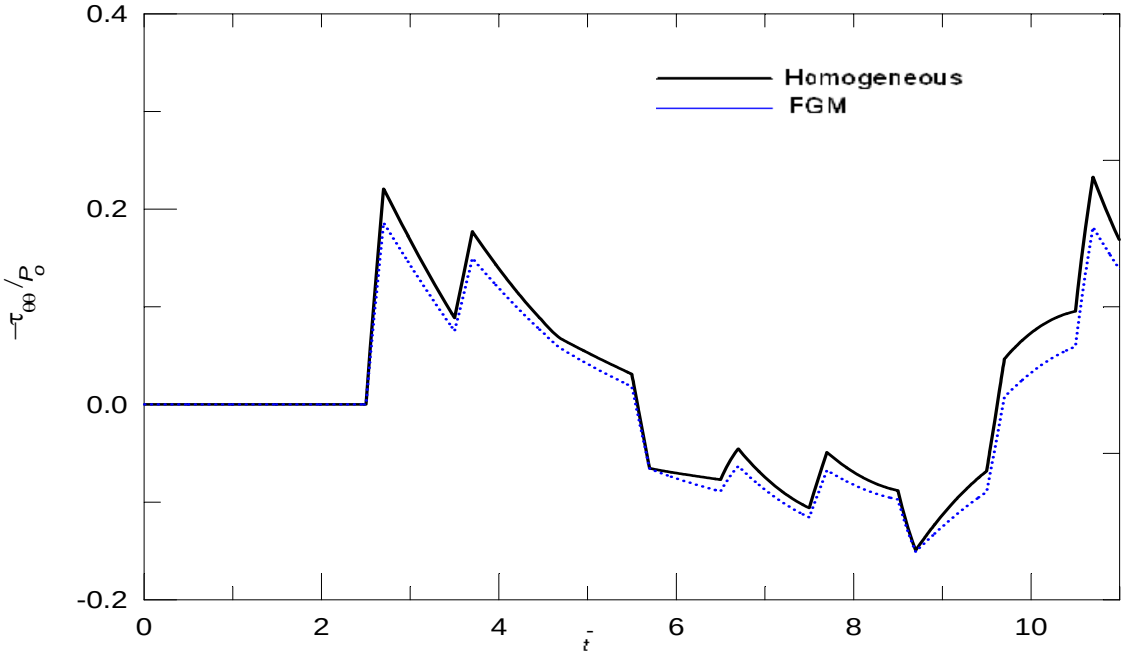

Fig. 3.7 Time variation of the normal stress $\frac{\tau_{\theta\theta}}{\rho_0}$ at $\bar{r} = 3.5$ for three pairs of alternating layered cylindrical domain.

3.3 Example 3:

The numerical results presented in Figs. (3.8-3.13) show the time variation of normally stresses at different locations for six similar layers. The geometrical and mechanical properties of the six layers are taken similar to Eqs. (3.2) with subscript or superscript 1. Whereas the inner boundary is subjected to time pulse given in Eq. (3.4) and the outer boundary is assumed to be fixed. In Figs. (3.8-3.13), the geometric and homogeneity effects are seen clearly from the discrepancy between the homogeneous and non-homogeneous (FGM) solutions. Furthermore, the reflections from the outer and inner boundaries are seen through the high jumps of stress levels, while the effects of reflections and refractions from the interfaces are not seen (as in Examples 1 & 2) because the six layers have the same properties.

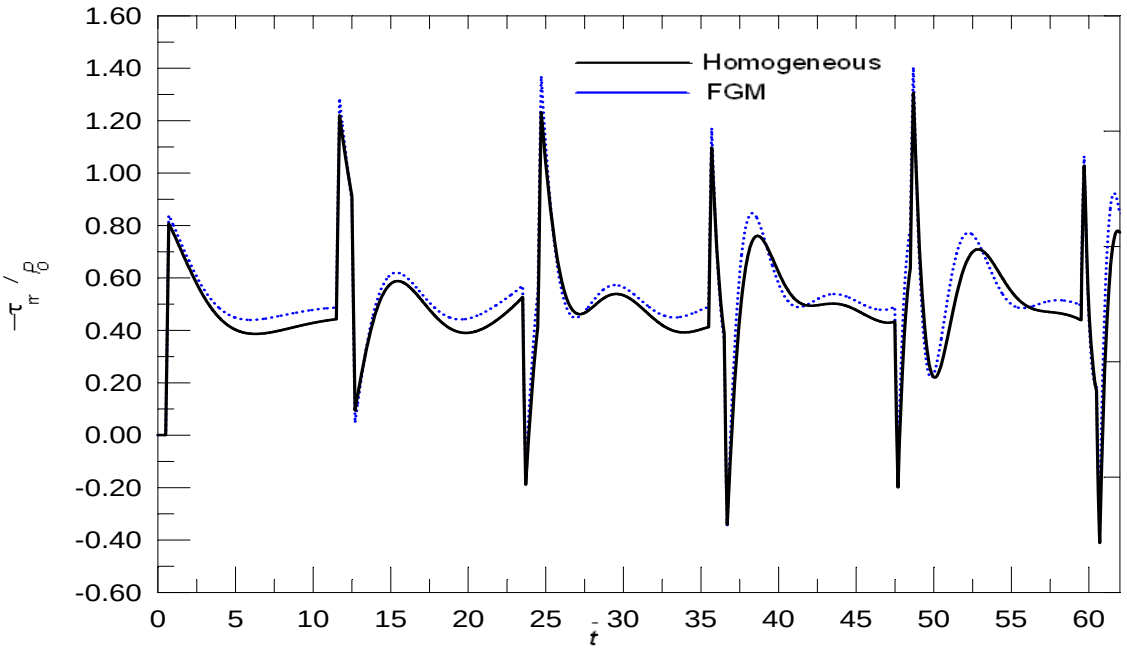

Fig. 3.8 Time variation of the normal stress $\frac{\tau_{rr}}{\rho_0}$ at $\bar{r} = 1.5$ for six similar cylindrical layers.

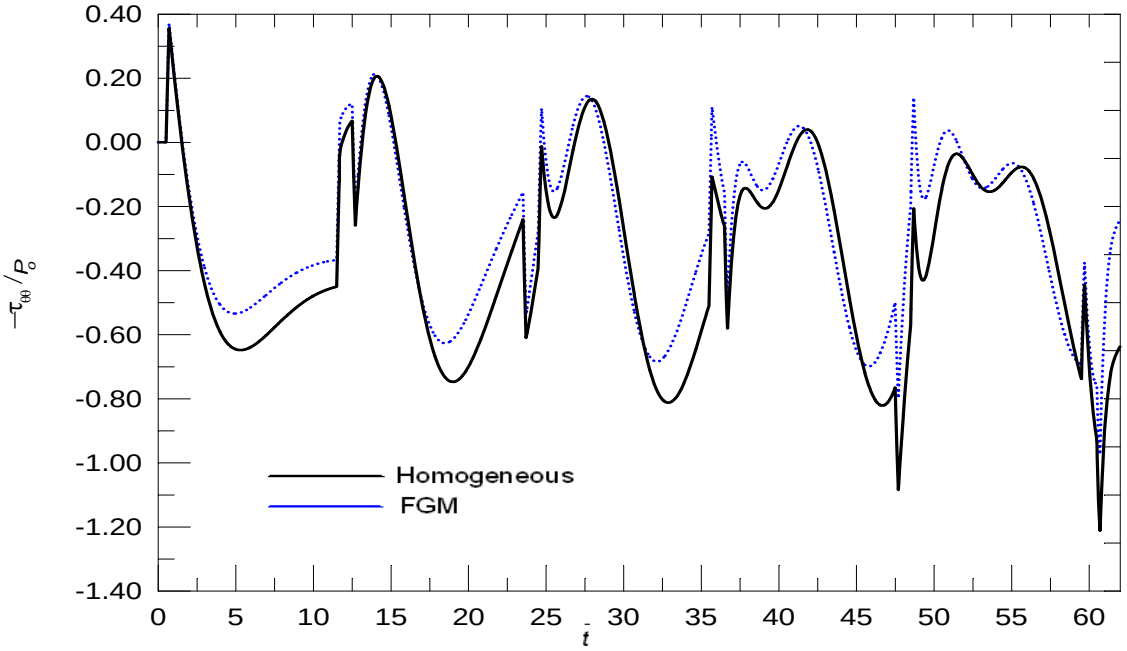

Fig. 3.9 Time variation of the normal stress $\frac{\tau_{\theta\theta}}{\rho_0}$ at $\bar{r} = 1.5$ for three pairs of layered cylindrical domain

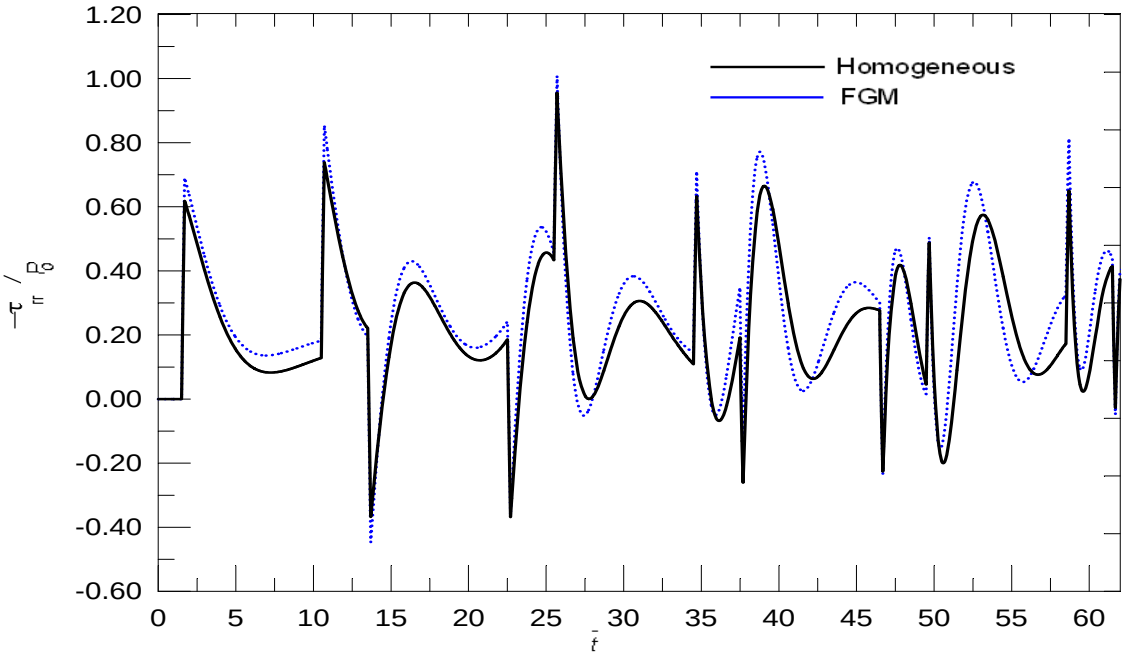

Fig. 3.10 Time variation of the normal stress $\frac{\tau_{rr}}{\rho_0}$ at $\bar{r} = 2.5$ for three pairs of layered cylindrical domain

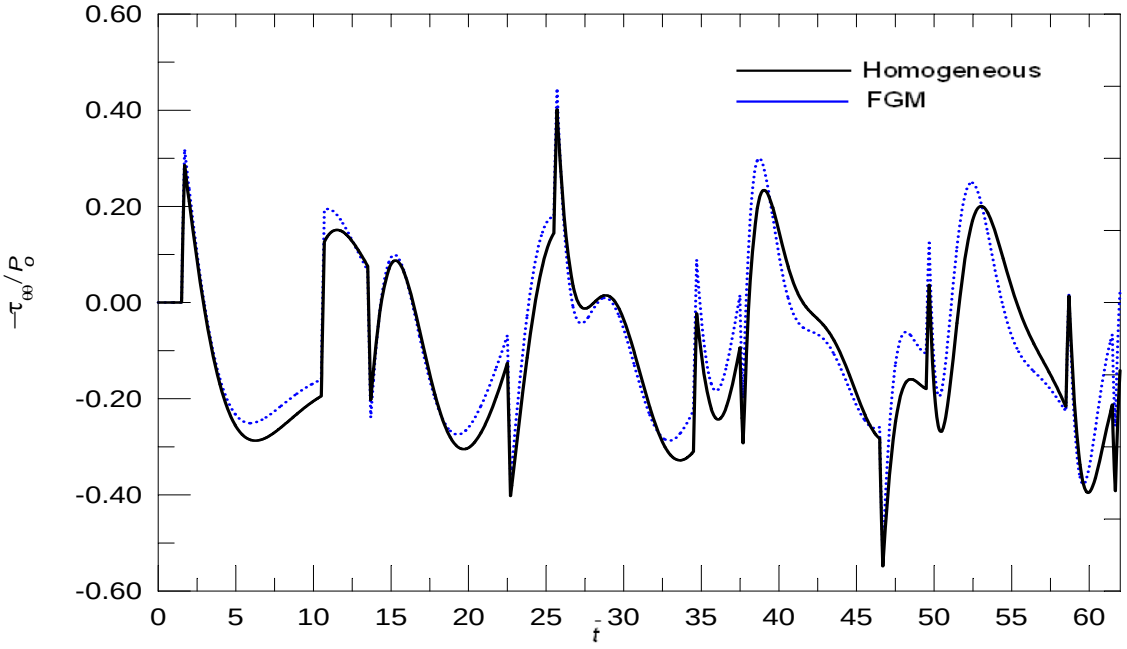

Fig. 3.11 Time variation of the normal stress $\frac{\tau_{\theta\theta}}{\rho_0}$ at $\bar{r} = 2.5$ for three pairs of layered cylindrical domain.

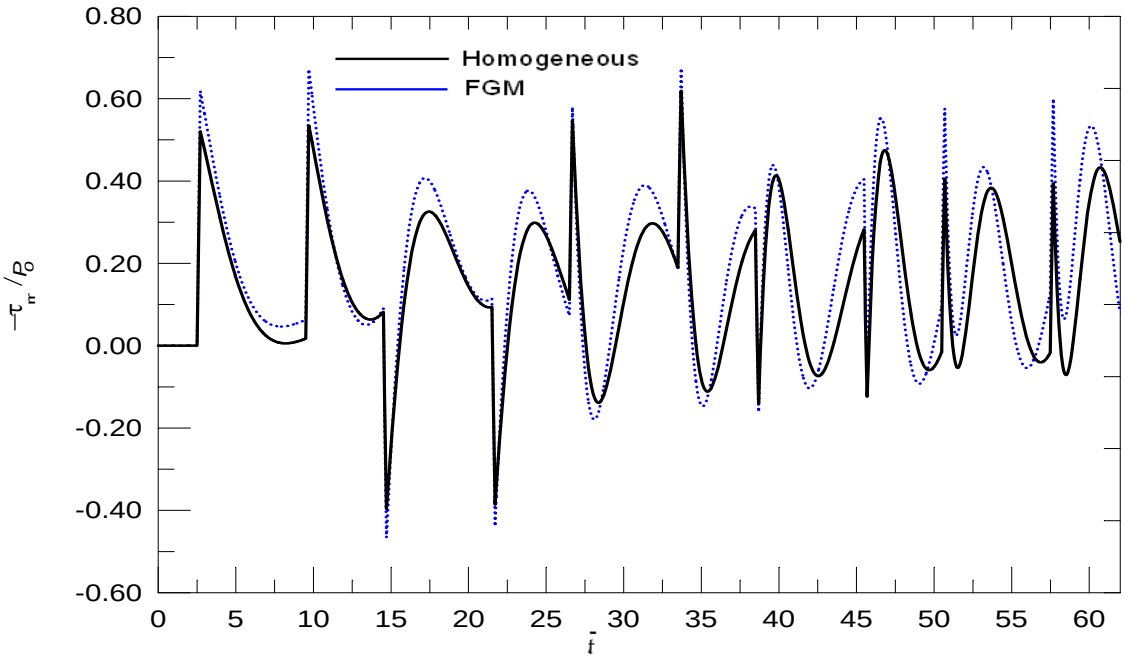

Fig. 3.12 Time variation of the normal stress $\frac{\tau_{rr}}{\rho_0}$ at $\bar{r} = 3.5$ for three pairs of layered cylindrical domain

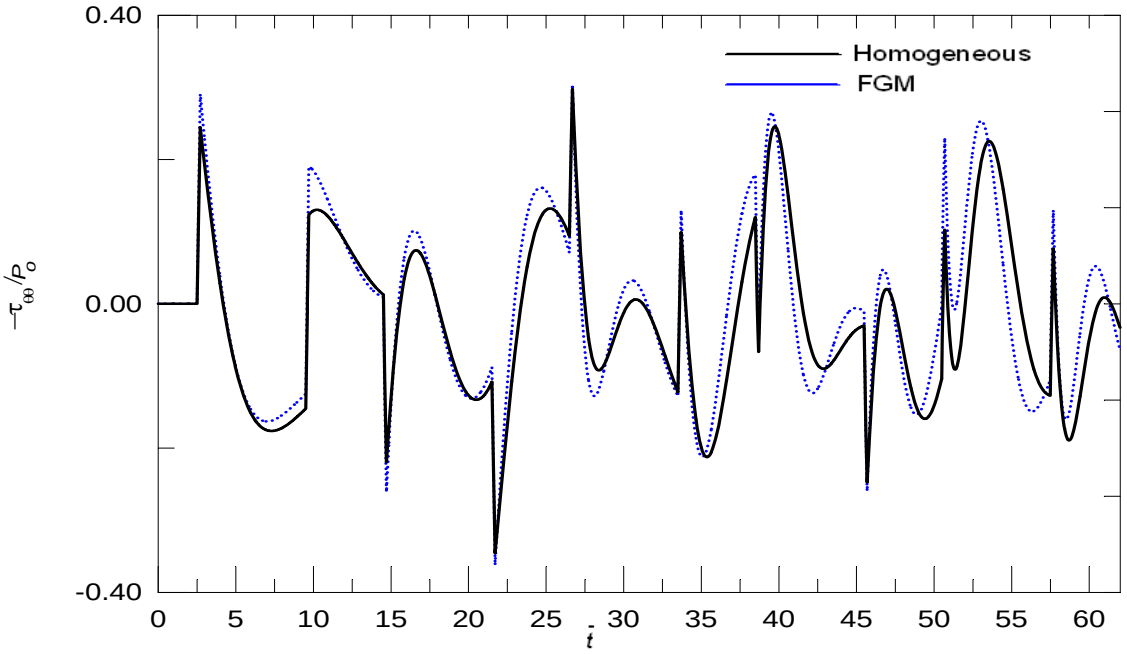

Fig. 3.13 Time variation of the normal stress $\frac{\tau_{\theta\theta}}{\rho_0}$ at $\bar{r} = 3.5$ for three pairs of layered cylindrical domain.

Example 4:

In this problem, we present some results for one-dimensional wave propagation in an FGM layer consists of nickel (*Ni*) and silicon (*Si*). On one surface of the layer is pure nickel and on the other surface pure silicon, and the material properties in-between these two surfaces vary smoothly in the radial direction. The material properties of the constituent materials are given in Table 1:

	$\mu(GPa)$	$\lambda(GPa)$	$\rho\left(Kg/m^3\right)$
Ni (Nickel)	79	129	8900
Si (Silicon)	90	46	3100

Table 3.1: Properties of materials used in example 4

Here we consider four different problems. These problems are: nickel-silicon (*Ni/Si*) or silicon-nickel (*Si/Ni*) FGM composites with free or fixed outer boundary conditions. The FGM cylindrical layers are assumed to be consisting of two different layers. Thus, in the use of the non-dimensionalization, the material properties for the two composites can be computed from Table 1 as:

for the *Ni/Si* FGM composite with $m = n + 2$, see Fig. 3.14a,

$$m=-0.58585,\quad n=-2.58585,\quad a=0.4964,\quad b=0.5036,$$
$$\bar{\rho}_0=1,\quad \bar{\mu}_0=0.27526,\quad \bar{\lambda}_0=0.44948,\quad \bar{c}_0=1, \tag{3.5}$$

and for the *Si/Ni* FGM composite with $m=n+2$, see Fig. 3.14b,

$$m=-0.58588,\quad n=-2.58588,\quad a=1.33492,\quad b=-0.33492,$$
$$\bar{\rho}_0=1,\quad \bar{\mu}_0=0.39823,\quad \bar{\lambda}_0=0.20354,\quad \bar{c}_0=1, \tag{3.6}$$

The variation of non-dimensional density ($\bar{\rho}$), stiffness ($\bar{c}$) and wave velocity ($\bar{c}_p$) with $\bar{r}$ for these composites, (3.5-3.6), are shown, respectively, in Fig. 3.14. In these examples In these examples, the inner surface ($\bar{r}=1$) is assumed to be subjected to uniform trapezoidal with an initial ramp with $\bar{P}_0=1$ as seen in the following figure

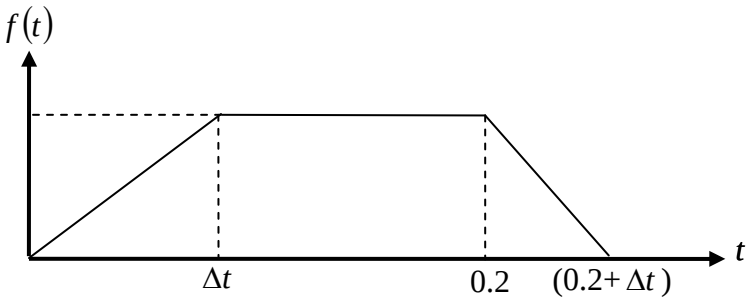

Time variation of the boundary conditions used in example 4, that is the normal stresses applied at the inner boundary ($\bar{r}=1$).

For various combination of boundary conditions and material compositions shown in Fig. 3.14, the variations of normalized normal stresses τ_{rr}/P_0 and $\tau_{\theta\theta}/P_0$ with non-dimensional time $\bar{t}$ at $\bar{r}=1.5$ are given in Figs. 3.15, 3.16, 3.19, 3.20, 3.23, 3.24, 3.27, and 3.28. The curves in Figs. 3.15, 3.16, 3.23, and 3.24, correspond to free outer boundary conditions, while the curves of Figs. 3.19, 3.20, 3.27, and 3.28 correspond to fixed outer boundary conditions. The variations of normalized normal stresses τ_{rr}/P_0 and $\tau_{\theta\theta}/P_0$ with non-dimensional time $\bar{t}$ at $\bar{r}=2.5$ are given in Figs. 3.17, 3.18, 3.21, 3.22, 3.25, 3.26, 3.29, and 3.30. The curves in Figs. 3.17, 3.18, 3.25, and 3.26, correspond to free outer boundary conditions, while the curves of Figs. 3.21, 3.22, 3.29, and 3.30 correspond to fixed outer boundary conditions. The dashed curves in these Figures, Figs. 3.15-3.30, correspond to FGM layers with material properties given in

Eq. (3.5) or Eq. (3.6), whereas the solid curves correspond to linear, homogeneous and isotropic material. The curves corresponding to the homogeneous layer are obtained as a special case by assigning *a*=1 and *b*=0 in Eqs. (3.5-3.6). The curves of Figs. 3.15-3.30 clearly show the effects of reflections at the inner and outer surfaces through the sudden changes in the stress levels. We note further that, reflections and refractions from the interfaces are also shown through the small sudden changes in the stress levels. Moreover, we note that the stress levels in the homogeneous layer are higher than those correspond to the *Ni/Si* FGM composite, Figs. 3.15-3.22, and they are less than those correspond to the *Si/Ni* FGM composite, Figs. 3.23-3.30. these deviations from the homogeneous material are due to the fact that the inner boundary $\bar{r}=1$ is the stiffer side in the *Ni/Si* FGM composite, Fig. 3.14a, and if $\bar{r}=1$ is the less stiff side then the stress levels will be higher than those correspond to the homogeneous layer. Because the wave velocity of the homogeneous layer ($\bar{c}_p=1$) is less than that of the *Ni/Si* FGM composite, Fig. 3.14a, the stress wave propagates faster in the *Ni/Si* FGM composite, Figs. 3.15-3.22. However, the stress wave in the homogeneous layer is traveling faster than that in the *Si/Ni* FGM layer, see Figs. 3.23-3.30, this is clearly pronounced as time increasing. We, further, note that if the outer boundary is free of surface traction than the compressive waves are reflected as tensile waves from that boundary, Figs. 3.15-3.18 and Figs. 3.23-3.26, and they are reflected as compressive waves if the outer boundary is fixed, Figs. 3.19-3.22 and Figs. 3.27-2.30.

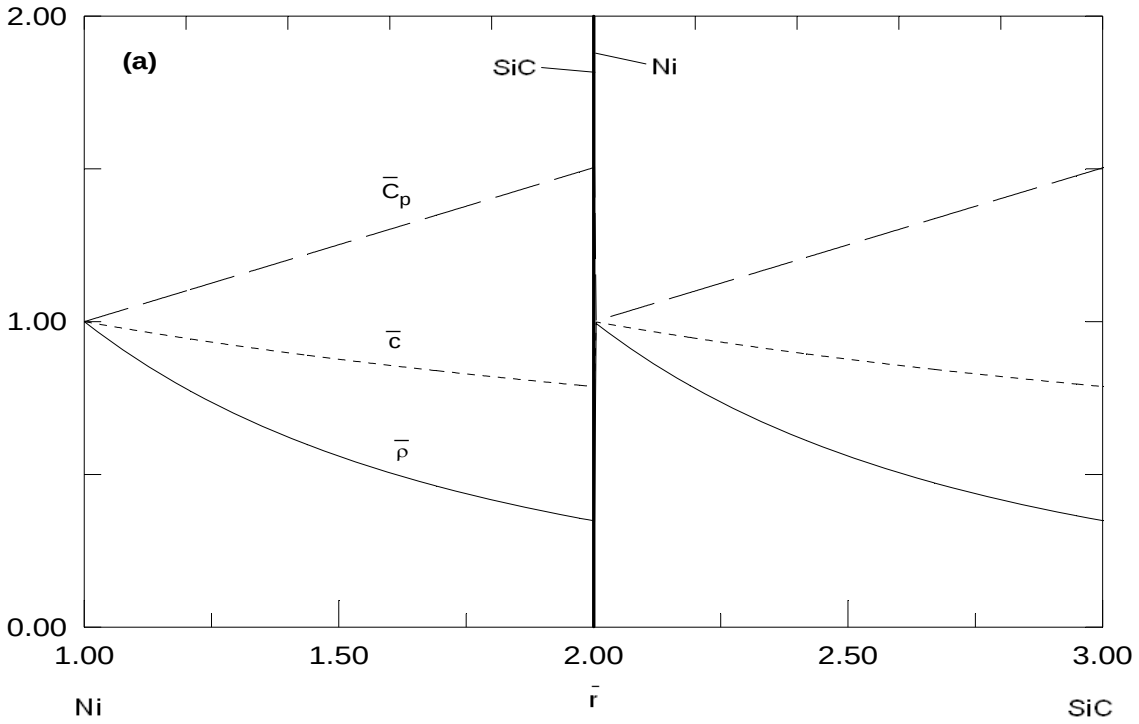

Fig. 3.14a Variation of non-dimensional density ($\bar{\rho}$), stiffness ($\bar{c}$) and wave velocity ($\bar{c}_p$) with $\bar{r}$ in Ni/Si FGM composite.

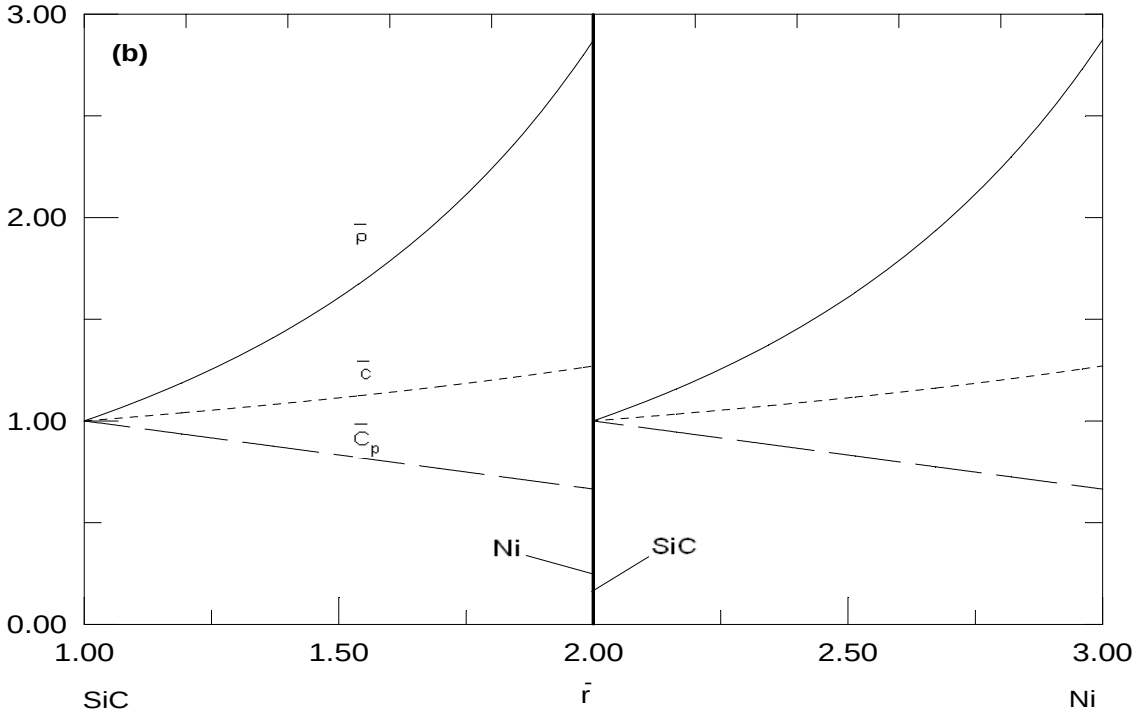

Fig. 3.14b Variation of non-dimensional density ($\bar{\rho}$), stiffness ($\bar{c}$) and wave velocity ($\bar{c}_p$) with $\bar{r}$ in Si/ Ni FGM composite.

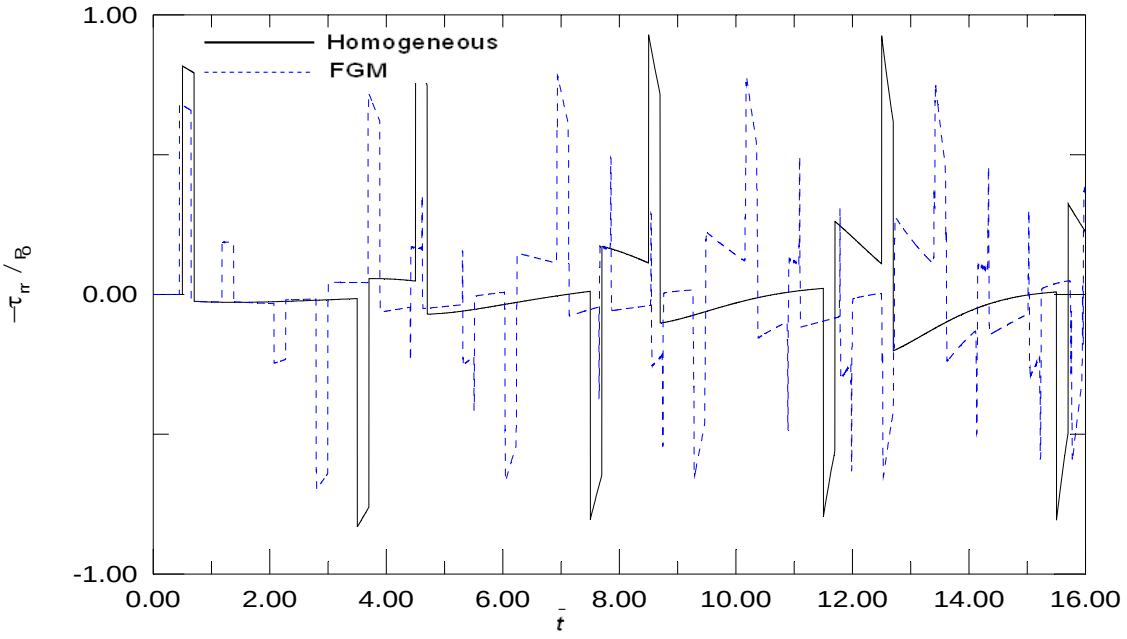

Fig. 3.15 Variation of (τ_{rr} / P_0) with $\bar{t}$ in Ni/Si FGM layer and in homogeneous layer at $\bar{r} = 1.5$ under free/free boundary conditions.

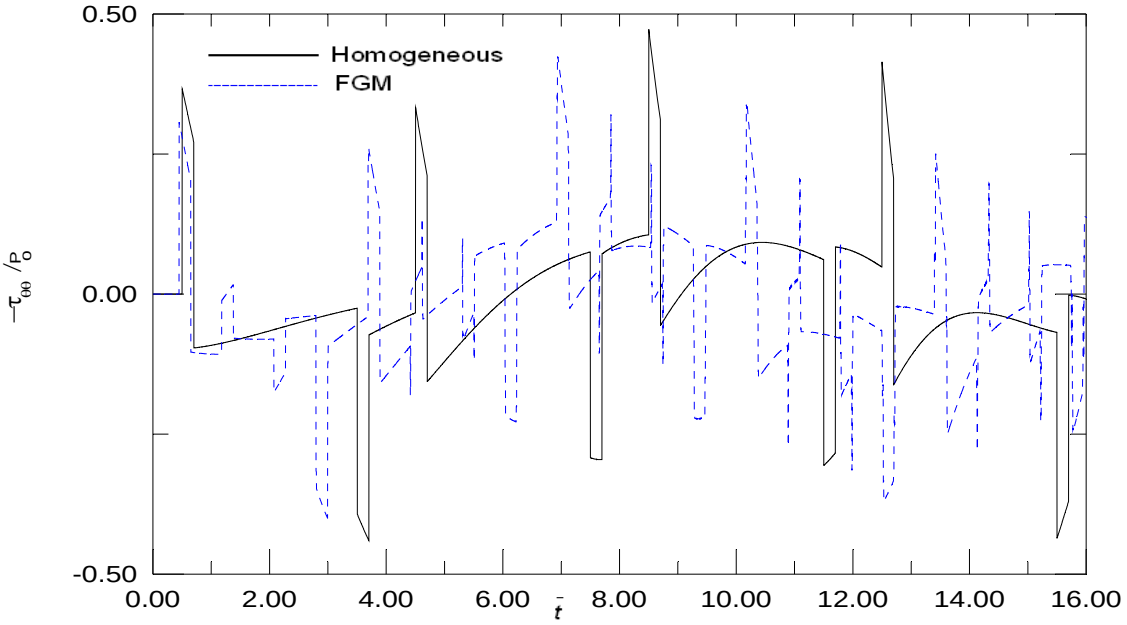

Fig. 3.16 Variation of ($\tau_{\theta\theta} / P_0$) with $\bar{t}$ in Ni/Si FGM layer and in homogeneous layer at $\bar{r} = 1.5$ under free/free boundary conditions.

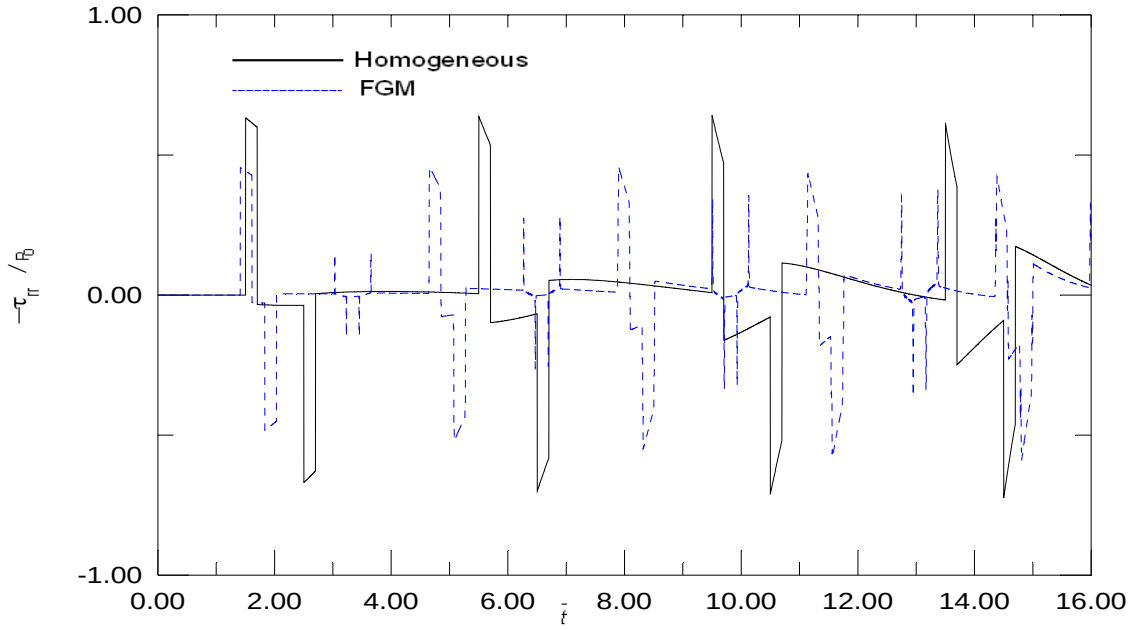

Fig. 3.17 Variation of (τ_{rr} / P_0) with $\bar{t}$ in Ni/Si FGM layer and in homogeneous layer at $\bar{r} = 2.5$ under free/free boundary conditions.

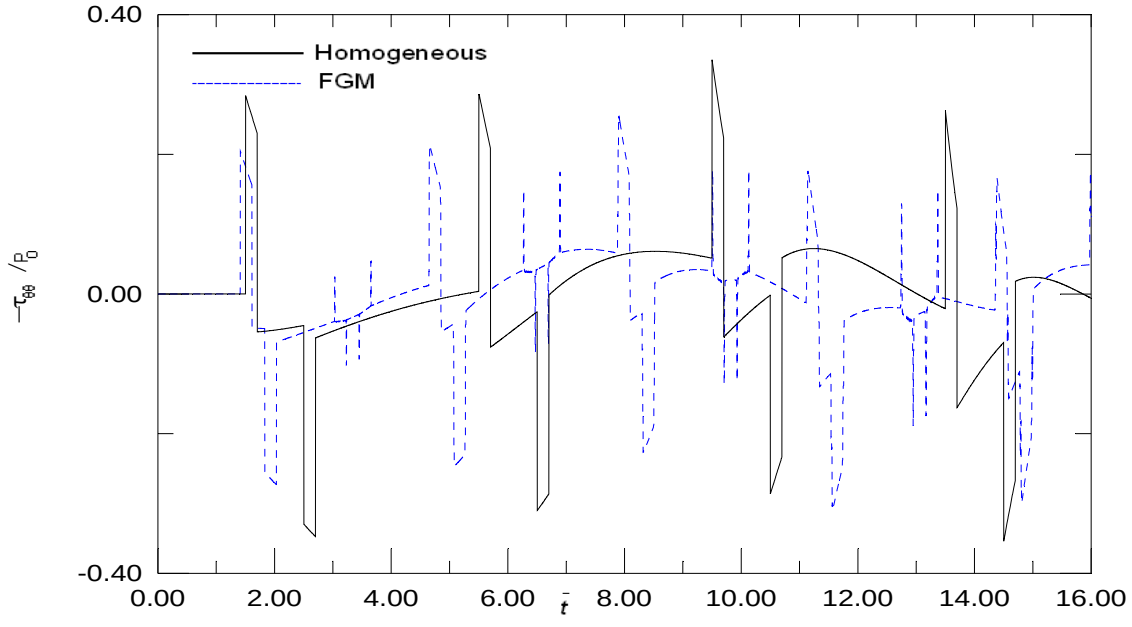

Fig. 3.18 Variation of ($\tau_{\theta\theta} / P_0$) with $\bar{t}$ in Ni/Si FGM layer and in homogeneous layer at $\bar{r} = 2.5$ under free/free boundary conditions.

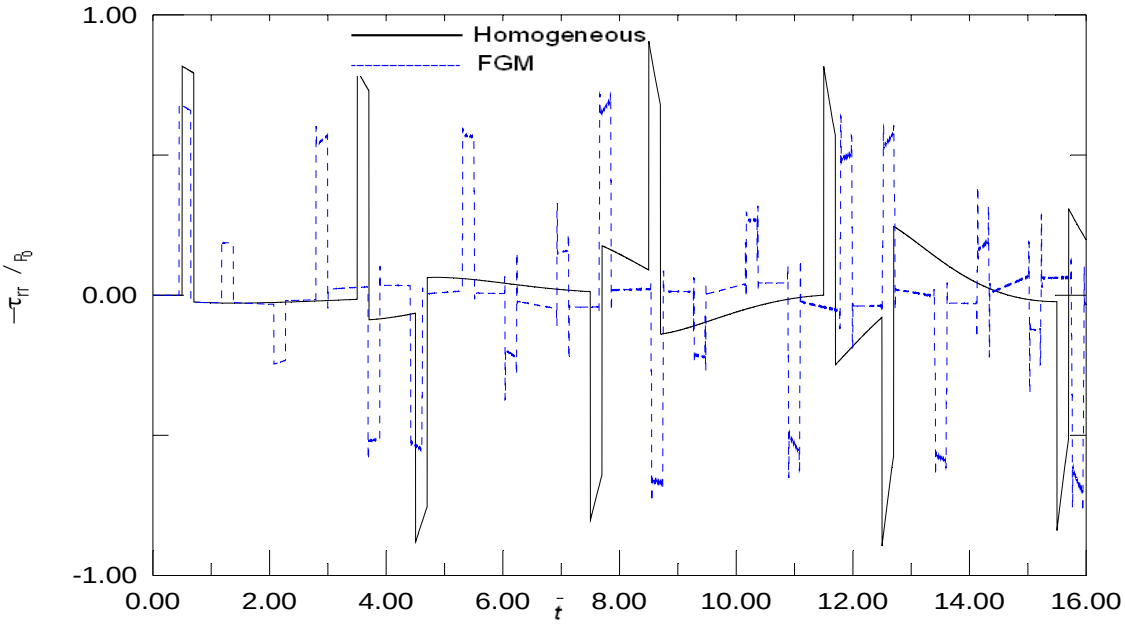

Fig. 3.19 Variation of (τ_{rr} / P_0) with $\bar{t}$ in Ni/Si FGM layer and in homogeneous layer at $\bar{r} = 1.5$ under free/fixed boundary conditions.

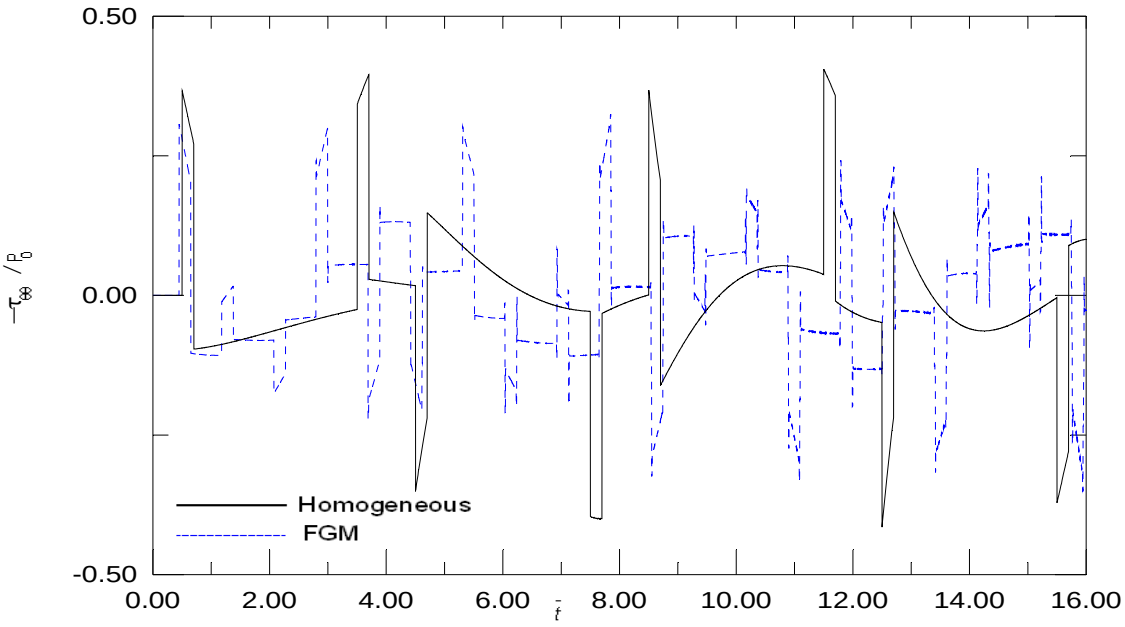

Fig. 3.20 Variation of ($\tau_{\theta\theta} / P_0$) with $\bar{t}$ in Ni/Si FGM layer and in homogeneous layer at $\bar{r} = 1.5$ under free/fixed boundary conditions.

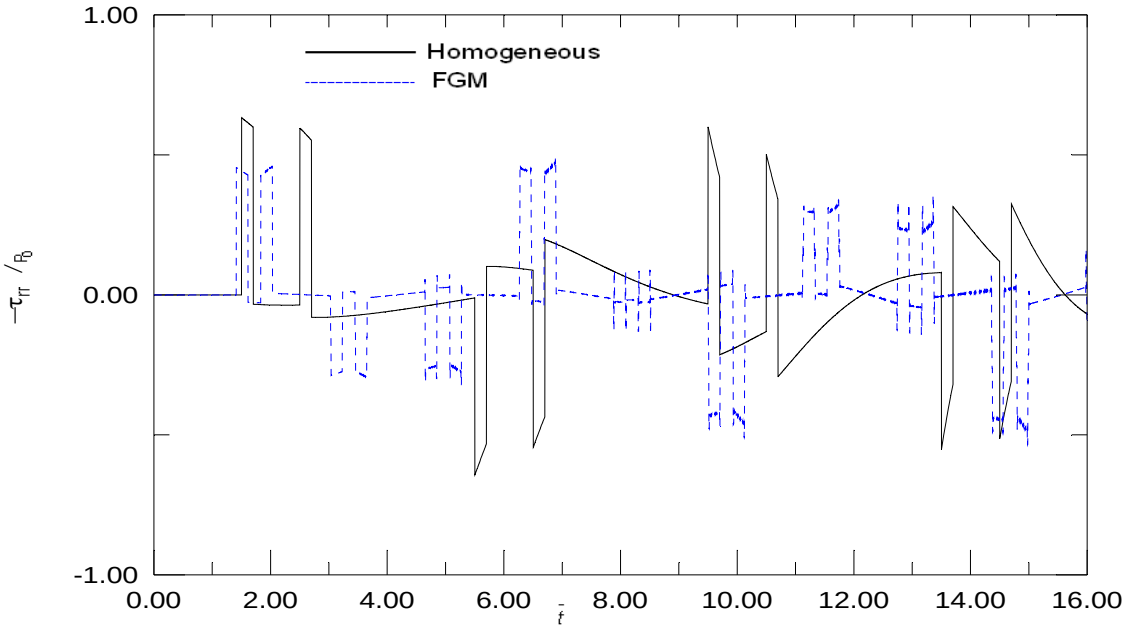

Fig. 3.21 Variation of (τ_{rr} / P_0) with $\bar{t}$ in Ni/Si FGM layer and in homogeneous layer at $\bar{r} = 2.5$ under free/fixed boundary conditions.

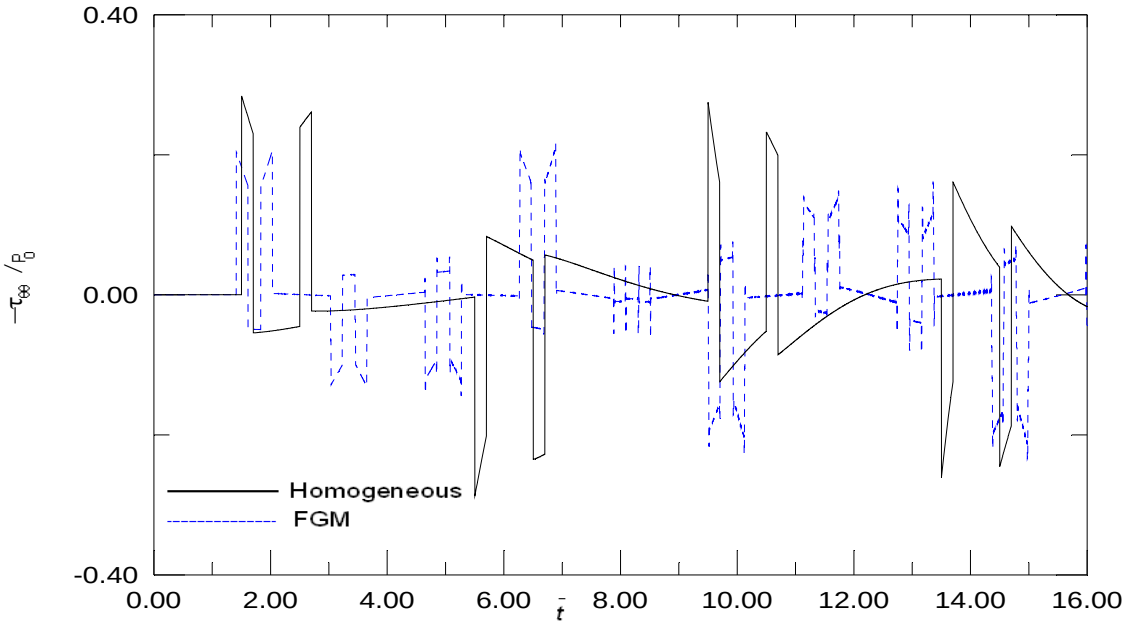

Fig. 3.22 Variation of ($\tau_{\theta\theta} / P_0$) with $\bar{t}$ in Ni/Si FGM layer and in homogeneous layer at $\bar{r} = 2.5$ under free/fixed boundary conditions.

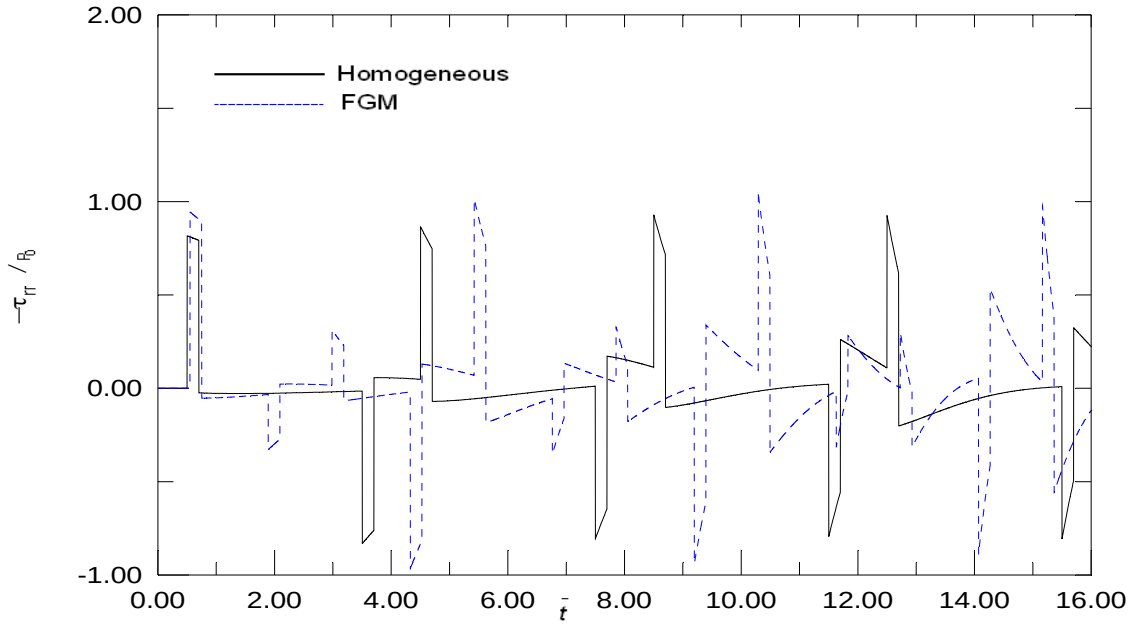

Fig. 3.23 Variation of (τ_{rr} / P_0) with $\bar{t}$ in Si/Ni FGM layer and in homogeneous layer at $\bar{r} = 1.5$ under free/free boundary conditions.

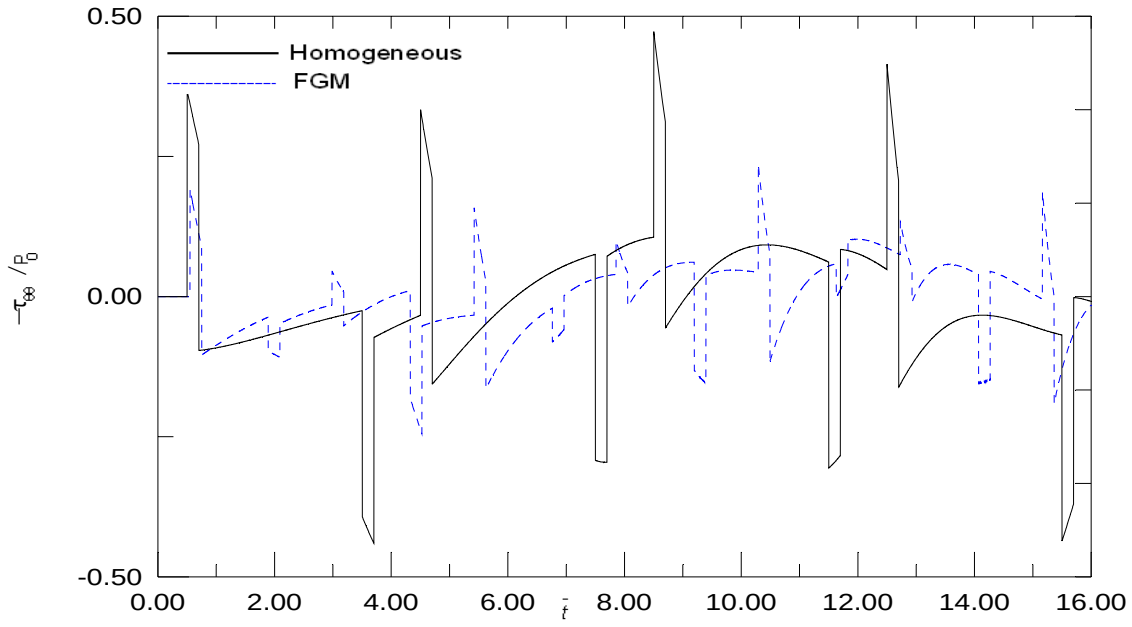

Fig. 3.24 Variation of ($\tau_{\theta\theta} / P_0$) with $\bar{t}$ in Si/Ni FGM layer and in homogeneous layer at $\bar{r} = 1.5$ under free/free boundary conditions.

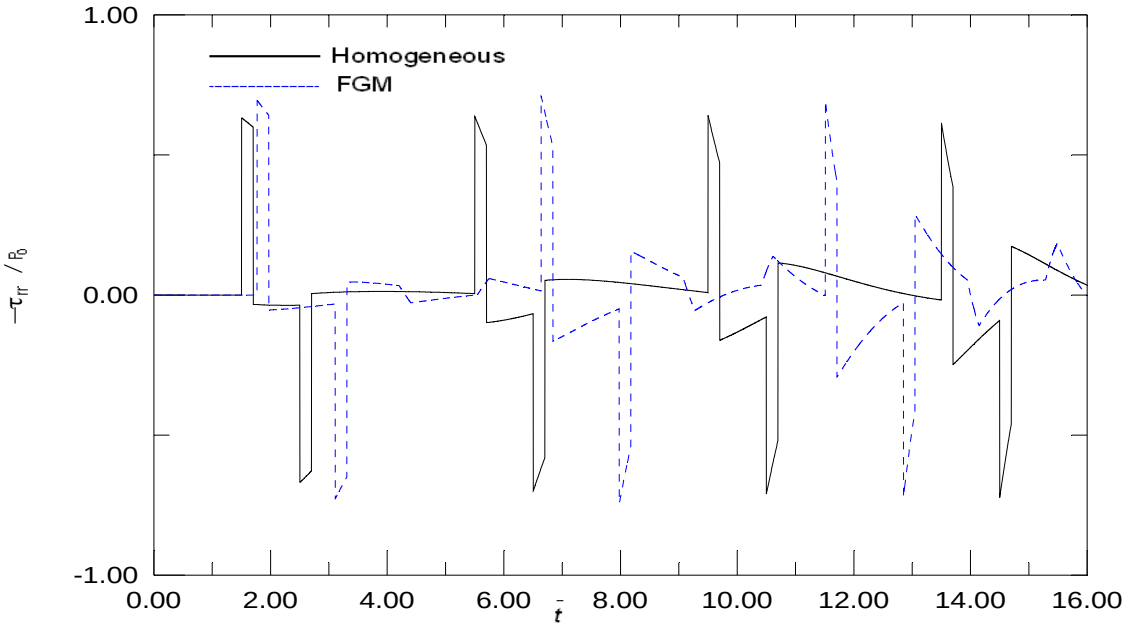

Fig. 3.25 Variation of (τ_{rr} / P_0) with $\bar{t}$ in Si/Ni FGM layer and in homogeneous layer at $\bar{r} = 2.5$ under free/free boundary conditions.

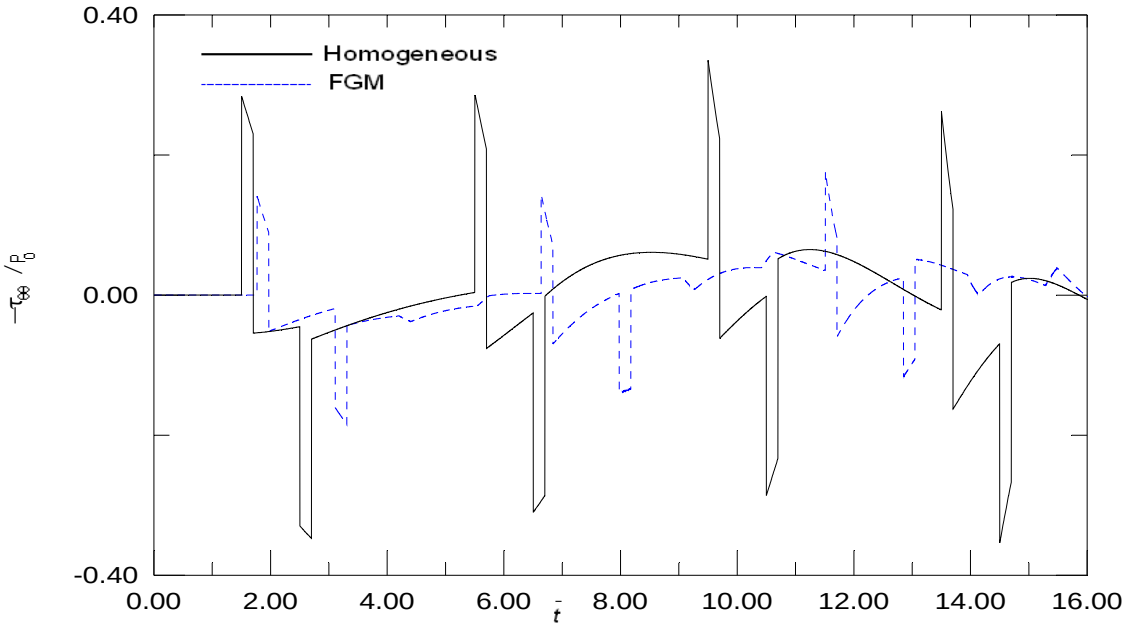

Fig. 3.26 Variation of ($\tau_{\theta\theta} / P_0$) with $\bar{t}$ in Si/Ni FGM layer and in homogeneous layer at $\bar{r} = 2.5$ under free/free boundary conditions.

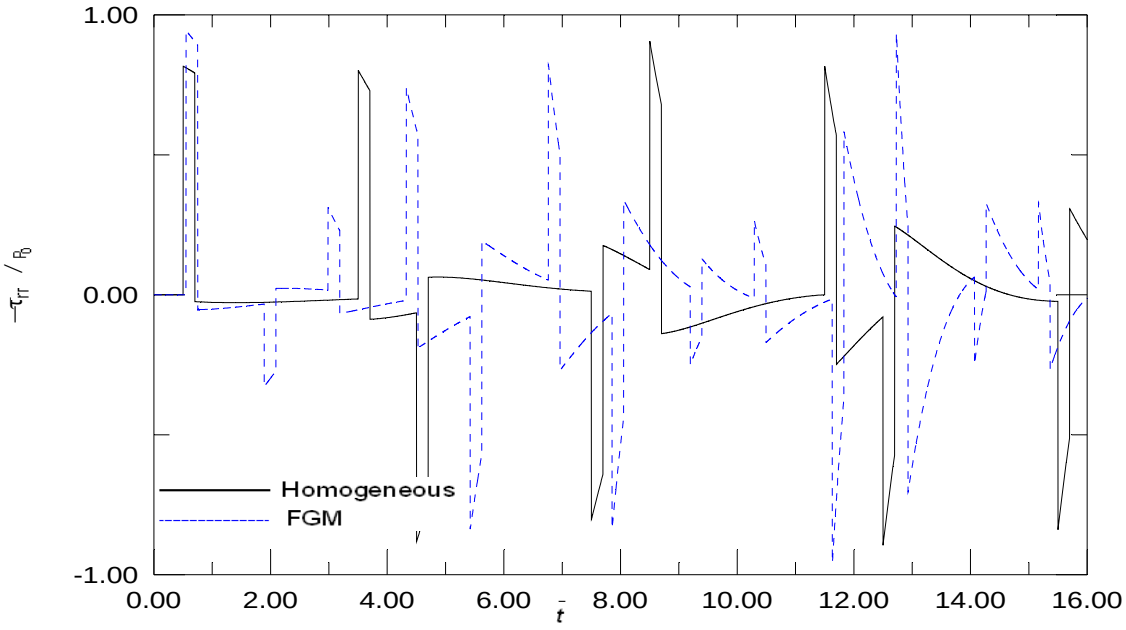

Fig. 3.27 Variation of (τ_{rr} / P_0) with $\bar{t}$ in Si/Ni FGM layer and in homogeneous layer at $\bar{r} = 1.5$ under free/fixed boundary conditions.

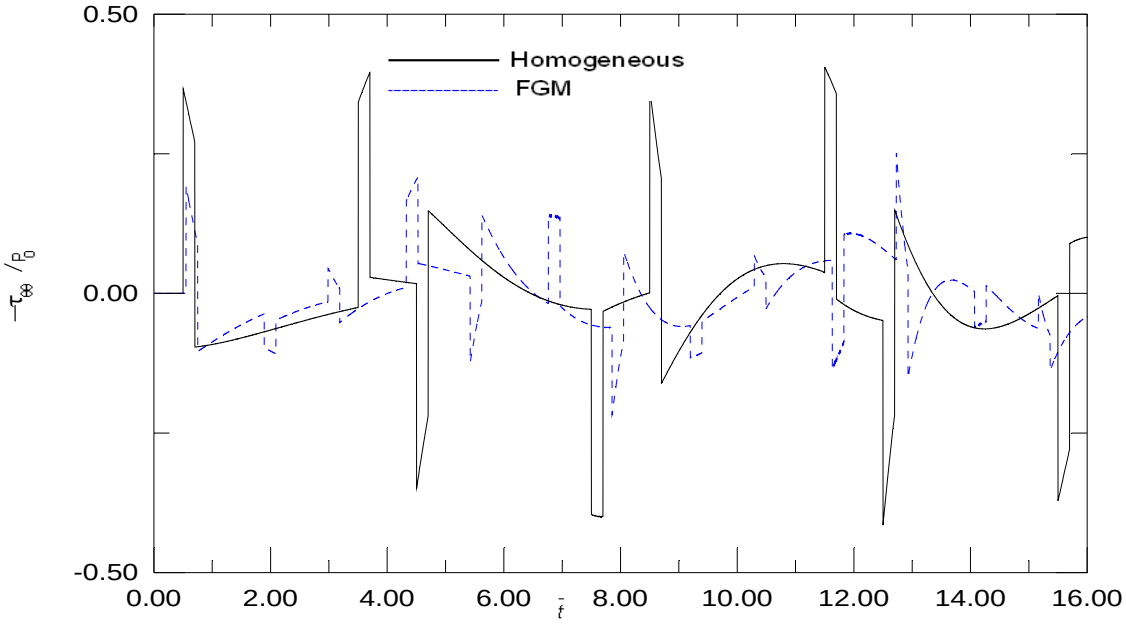

Fig. 3.28 Variation of ($\tau_{\theta\theta} / P_0$) with $\bar{t}$ in Si/Ni FGM layer and in homogeneous layer at $\bar{r} = 1.5$ under free/fixed boundary conditions.

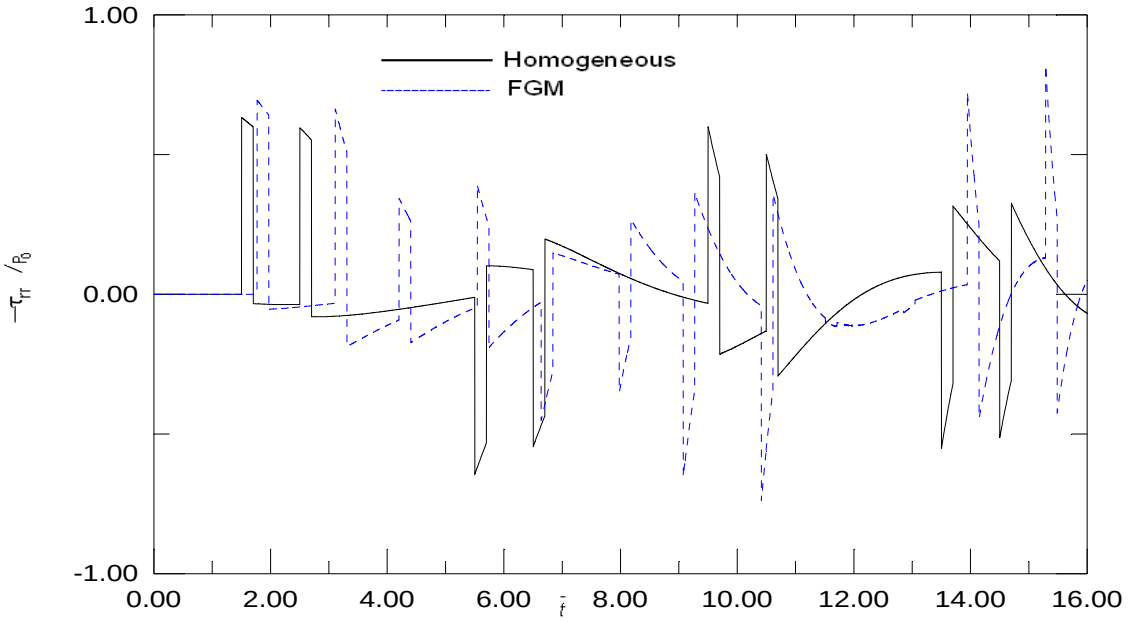

Fig. 3.29 Variation of (τ_{rr} / P_0) with $\bar{t}$ in Si/Ni FGM layer and in homogeneous layer at $\bar{r} = 2.5$ under free/fixed boundary conditions.

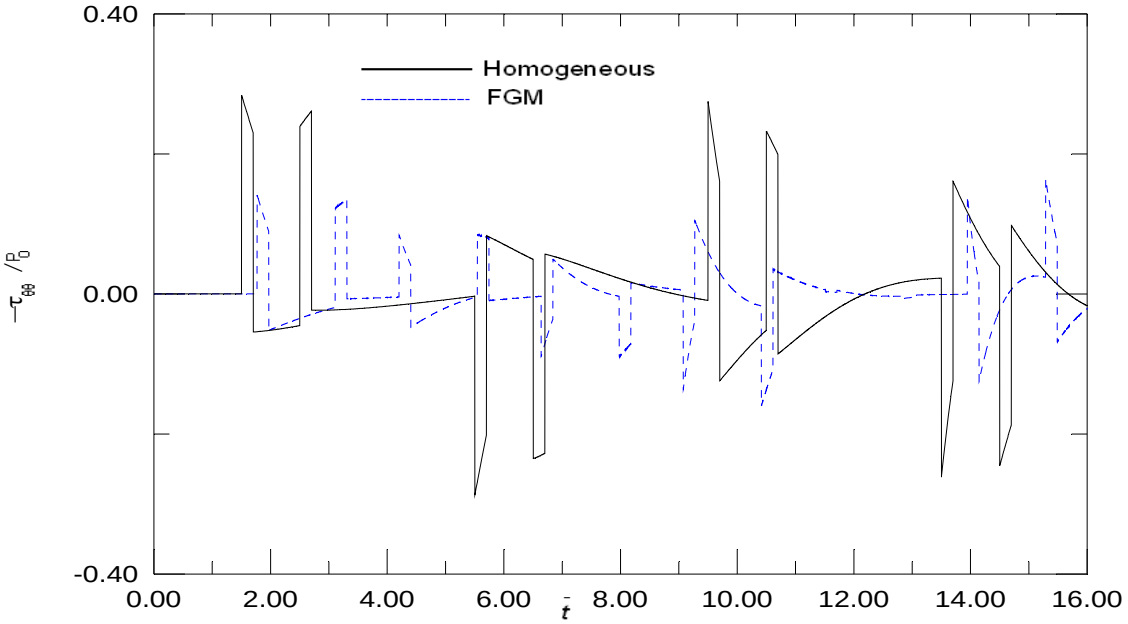

Fig. 3.30 Variation of ($\tau_{\theta\theta} / P_0$) with $\bar{t}$ in Si/Ni FGM layer and in homogeneous layer at $\bar{r} = 2.5$ under free/fixed boundary conditions.

CHAPTER 4

CONCLUSIONS

In this thesis, the one-dimensional transient stress-wave propagation in multilayered functionally graded media consisting of N different cylindrical layers has been investigated. The material properties are assumed to be varying smoothly in the thickness direction. By suitable adjusting the material properties, curves for homogeneous and linearly elastic multilayered cylindrical media have also been obtained. The method of characteristics is employed to obtain the numerical solutions of the considered initial-boundary-value problem. The results show that the applied numerical technique is capable of predicting the sharp variations at the wave fronts. Furthermore, this technique properly accounts for the effects caused by reflections and refractions of waves at the boundaries and interfaces between the layers and the homogeneity effects in the wave profiles.

Based on the results obtained, one may conclude that, depending on the material property grading, the location of the receiver point, boundary conditions and the amplitude of the input pulse, the resultant stress amplitudes may be greater or less than those applied at the inner boundary. It has been found that these amplitudes become less than those applied at the inner boundary, when the inner boundary ($r = 1$) is stiffer that the outer surface ($r = R_0$) and become greater when the outer surface of an FGM layer is stiffer than the inner surface.

Finally, the method of characteristics can be combined with Fourier or Laplace transform and used effectively in investigating two-dimensional transient dynamic response in multilayered FGM media.

REFERENCES

[1] M. Yamanouchi, M. Koizumi, M. Hirai and I. Shiota (Eds). Proceedings of the First International Symposium on Functionally Graded Materials, Sendai, Japan (1990).

[2] Y. Tanigawa, Some basic thermoelastic problems for non-homogeneous structural materials, Applied Mech. Rev. 48 (1995) 287--300.

[3] N. Noda, Thermal stresses in functionally graded material Journal of Thermal Stresses 22 (1999) 477--512.

[4] Y. Miyamoto, W.A. Kaysser, B.H. Rabin, A. Kawasaki and R.G. Ford, Functionally Graded Materials: design, processing and applications. Dordrecht: Kluwer Academic Publishers, (1999) 352pp.

[5] S. Suresh and A. Mortensen, Fundamentals of Functionally Graded Materials. London: Institute of Materials, IOM Communications Ltd, (1998) 176pp.

[6] L. Banks-Sills, R. Eliasi, Y. Berlin, Modeling of functionally graded materials in dynamic analyses. Composites Part B: Engineering 33 (2002) 7 --15.

[7] G.R. Liu and J. Tani, Surface waves in functionally gradient piezoelectric plates. Journal of Vibration and Acoustics 116 (1994) 440--448.

[8] T. Ohyoshi, Linearly inhomogeneous layer elements for reflectance evaluation of inhomogeneous layers. Dynamic Response and Behavior of Composites 46 (1995) 121--126.

[9] T. Ohyoshi, New stacking layer elements for analyses of reflection and transmission of elastic waves to inhomogeneous layers. Mechanics Research Communication 20 (1993) 353--359.

[10] X. Han, G. R. Liu, Effects of SH waves in functionally graded plate. Mechanics Research Communication 29 (2002) 327--338.

[11] G. R. Liu, X. Han, K. Y. Lam, Stress Waves in functionally gradient materials and its use for material characterization. Composites Part B: Engineering 30 (1999) 383--394.

[12] X. Han, G. R. Liu and K. Y. Lam, A quadratic layer element for analyzing stress waves in functionally gradient materials and its application in material characterization. Journal of Sound and Vibration 236 (2000) 307--321.

[13] T. C. Chiu and F. Erdogan, One-dimensional wave propagation in a functionally graded elastic medium. Journal of Sound and Vibration 222 (1999) 453--487.

[14] A. Berezovski, J. Engelbrecht and G. A. Maugin, Numerical simulation of two dimensional wave propagation in functionally graded materials. European Journal of Mechanics 22 (2003) 257--265.

[15] A. Berezovski, J. Engelbrecht and G. A. Maugin. Stress wave propagation in functionally graded materials. Paris:WCU 2003 (2003) 507--509.

[16] M. H. Santare, P. Thamburaj and G. A. Gazoans, The use of graded finite elements in the study of elastic wave propagation in continuously non-homogeneous materials. International Journal of Solids and Structures 40 (2003) 5621--5634.

[17] D. Turhan, Z. Celep, I. K. Zain-eddin, Transient wave propagation in layered media. Journal of Sound and Vibration 144 (1991) 247--261.

[18] Y. Mengi, A. K. Tanrikulu, A numerical technique for two- dimensional transient wave propagation analyses. Communication of Applied Numerical Methods 6 (1990) 623--632.

[19] J. L. Wegner, Propagation of waves from a spherical cavity in an unbounded linear viscoelastic solid. International Journal of Engineering Sciences 31 (1993) 493--508.

[20] I. Abu-Alshaikh, D. Turhan, Y. Mengi, Two-dimensional transient wave propagation in viscoelastic layered media. Journal of Sound and Vibration 244 (2001) 837--858.

[21] I. Abu-Alshaikh, D. Turhan and Y. Mengi, Transient waves in viscoelastic cylindrical layered media, European Journal Mechanics A/Solids 21 (2002) 811--830.

[22] X. Han, G. R. Liu, Z. C. Xi, K. Y. Lam, transient waves in functionally graded cylindir, International Journal of Solids and Structures 38 (2001) 3021--3037

[23] I. Abu-Alshaikh, B. Kokluce, One-dimensional transient dynamic response in functionally graded layered media. Kluwer Academic Publishers (2005).

[24] Y. C. FUNG, Foundations of Solid Mechanics. Englewood Cliffs, NJ: Prentice Hall (1965).

[25] A. Cemal Erimen, Mechanics of Continua. John Wiley & Sons, INC. New York, London, Sydney (1967).

[26] I. S. Sokolnikoff, Mathematical Theory of Elasticity. Krieger (1983).

[27] R. Courant and D. Hilbert, Methods of Mathematical Physics, vol. II. New York: Interscience Publishers, (1966).

[28] G. B. Whitham, Linear and Nonlinear Waves. New York: Wiley, (1974).

[29] F. G. Curtis and P. O. Wheatley, Applied Numerical Analysis. Addison-Wesley Publishing Company. Canada (1984).

[30] D. Turhan, Z. Celep, I. K. Zain-Edden, Transient wave propagation in layered media conducting heat, Journal of Sound and Vibration, (1991).

APPENDIX A

METHOD OF CHARACTERISTICS

In this appendix, the derivations of the basic equations used in the method of characteristics, namely, the characteristic equation and the canonical equations will be given. Let the system of governing 1-D partial differential equations be given in matrix form as

$$\underline{A}\,\underline{U}_{,t} + \underline{B}\,\underline{U}_{,x} + \underline{C} = \underline{0} \qquad \text{(A.1)}$$

where $\underline{A}$ and $\underline{B}$ are $(m \times m)$ square matrices, $\underline{C}$ is an m-dimensional vector and $\underline{U}$ is m-dimensional unknown vector

$$\underline{U} = (U_1, U_2, ..., U_m)^T. \qquad \text{(A.2)}$$

The unknown field variables $U_1, U_2, ..., U_m$ are functions of the space variable x and the time variable t. The system of governing equations, Eqs, (A.1), is assumed to be linear, i.e., $\underline{A}$ and $\underline{B}$ are function of x and t only and $\underline{C}$ is a linear function of $\underline{U}$,i.e.,

$$\underline{C} = \underline{D}\,\underline{U} + \underline{E} \qquad \text{(A.3)}$$

where $\underline{D}$ is an $(m \times m)$ square matrix and $\underline{E}$ is m-dimensional vector both of which are functions of x and t, only. Furthermore, comma denotes partial differentiation in Eq. (A.1), i.e., $\underline{U}_{,t} = \partial \underline{U} / \partial t$ and $\underline{U}_{,x} = \partial \underline{U} / \partial x$.

Let x=x(t) define the equation of the singular point (wave front) at which the field variables and/or their derivatives may suffer discontinuities. The plot of x(t) is given in Fig. A.1. If f denotes a function of x and t, the jump of f(x,t) at the singular point is defined and denoted as

$$[f] = f^+ - f^- \qquad \text{(A.4)}$$

where the superscripts + and – denote the values of the function on the disturbed and undisturbed sided of the singular point, respectively.

Now, assume that $\underline{U}$ is continuous and the first derivatives of $\underline{U}$ are discontinuous on the singular point x=x(t) , i.e., $[\underline{U}]=0$, $\lfloor \underline{U}_{,t} \rfloor \neq 0$ $\lfloor \underline{U}_{,x} \rfloor \neq 0$ on x=x(t).

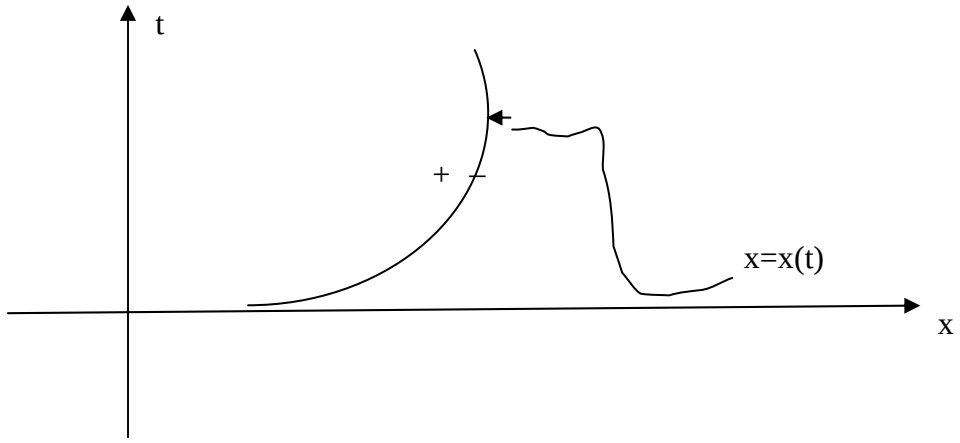

Figure A.1 Position of the singular point

Writing Eq. (A.1) on positive and negative sides of x=x(t), noting that $\underline{A}$, $\underline{B}$ and $\underline{C}$ are continuous on x=x(t), and taking the difference, we obtain on x=x(t)

$$\underline{A}\lfloor \underline{U}_{,t} \rfloor + \underline{B}\lfloor \underline{U}_{,x} \rfloor = 0 . \qquad \text{(A.5)}$$

The kinematical condition of compability given on x=x(t)

$$\left[\frac{\partial \underline{U}}{\partial t}\right] = -V\left[\frac{\partial \underline{U}}{\partial x}\right] \qquad \text{(A.6)}$$

where V denotes the propagation velocity of the singular point (wave front). Substituting Eq. (A.6) into Eq. (A.5), we get

$$(\underline{B} - V\,\underline{A})\underline{W} = \underline{0} \qquad \text{(A.7)}$$

where $\underline{W} = \lfloor \underline{U}_{,x} \rfloor$. This is an eigenvalue problem and $\underline{W}$ is the eigenvector and V is the eigenvalue. For non-trivial solution

$$\det(\underline{B} - V\,\underline{A}) = \underline{0} \qquad \text{(A.8)}$$

Equation (A.8) is called the characteristics equation. Solving this equation we find m roots (characteristics values), i.e, $V^{(i)} = (V^{(1)}, V^{(2)}, ..., V^{(m)})$. If the roots are real then the system is called hyperbolic and each $V^{(i)}$ corresponds to i^{th} family of characteristic curves $C^{(i)}$. This characteristic family can be determined by solving the following equation:

$$C^{(i)}: \frac{dx}{dt} = V^{(i)} \rightarrow x = x^{(i)}(\alpha^{(i)}, t) \text{ for } i = 1,2,.....,m \qquad (A.9)$$

where $\alpha^{(i)}$ are integrat.on constants. The family of the curves $C^{(1)}, C^{(2)}, ..., C^{(m)}$ constitutes the characteristic manifold.

Now we shall put Eq. (A.1) into canonical form. For this purpose, we define the left-hand eigenvector $\underline{\ell}^{(i)}$ corresponding to $V^{(i)}$ as

$$\underline{\ell}^{(i)T}\left(\underline{B} - V^{(i)}\ \underline{A}\right) = \underline{0} \quad (i = 1\text{-}m) \qquad (A.10)$$

or

$$\left(\underline{B}^{T} - V^{(i)}\ \underline{A}^{T}\right)\underline{\ell}^{(i)} = \underline{0} \quad (i = 1\text{-}m) \qquad (A.11)$$

Pre-multiplying Eq. (A.1) by $\underline{\ell}^{(i)T}$ (i=1-m) and substituting

$$\underline{\ell}^{(i)T}\underline{B} = V^{(i)}\,\underline{\ell}^{(i)T}\ \underline{A} \quad (i = 1\text{-}m) \qquad (A.12)$$

from Eq. (A.10), we can write

$$\underline{\ell}^{(i)T}\underline{A}\,(\underline{U}_{,t} + V^{(i)}\ \underline{U}_{,x}) + \underline{\ell}^{(i)T}\underline{C} = \underline{0} \qquad \text{on } C^{(i)}\ . \qquad (A.13)$$

Noting that $V^{(i)} = \frac{dx}{dt}$ and the quantity in parenthesis in Eq. (A.13) is equal to $\frac{d\underline{U}}{dt}$, we can write

$$\underline{\ell}^{(i)T}\underline{A}\,\frac{d\underline{U}}{dt} + \underline{\ell}^{(i)T}\underline{C} = \underline{0} \qquad (A.14)$$

which holds along $(dx/dt) = V^{(i)}$ $(i = 1 - m)$. Eqs. (A.14) are called the canonical equations. In these equations *d / dt* denotes the total time derivative along the characteristic lines. Thus, through the application of the method of the characteristics, the system of governing partial differential equations. Eqs. (A.1), is transformed into a system of ordinary differential equations, Eqs. (A.14), each of which is valid along a different family of characteristic lines.

APPENDIX B

PROGRAM MAIN

```
      IMPLICIT real*8 (a-h,o-z)
      PARAMETER(np=6,nl=8,jx=20001)
      COMPLEX*16 srxx(jx,np),sryy(jx,np),srzz(jx,np)
      COMMON dt,eps,nop,nol,zzz
      COMMON/arrays/hz(nl),mm(nl+1)/arry2/r0(nl),a(nl),b(nl),
     *pm(nl),pn(nl),yy(np),dz(10001),um0(nl),ul0(nl),
     *c(10001),co(10001),ro(10001)
       open(99,file='Inp333')
       open(88,file='OU333')
       open(80,file='OU333.dat')
       open(1,file='2LSNf1.dat')
       open(2,file='2LSNf2.dat')
       open(3,file='2LSNf3.dat')
       open(4,file='2LSNf4.dat')
       open(5,file='2LSNf5.dat')
       CALL INPUT(imax,jmax)
       CALL SOLVEE(imax,jmax,srxx,sryy,srzz)
       CALL OUT(jmax,srxx,sryy,srzz)
         close (99)
         close (88)
          STOP
          END
CCCCCCCCCCCCCCCCCCCCCCCCCCCCCCCCCCCCCCCCCCCCCCCCCCCCCCCCCCCCCCCCCCC
      SUBROUTINE INPUT(imax,jmax)
CCCCCCCCCCCCCCCCCCCCCCCCCCCCCCCCCCCCCCCCCCCCCCCCCCCCCCCCCCCCCCCCCCC
      IMPLICIT real*8 (a-h,o-z)
      PARAMETER(np=6,nl=8)
      COMMON dt,eps,nop,nol,zzz
            COMMON/arrays/hz(nl),mm(nl+1)/arry2/r0(nl),a(nl),b(nl),
            *pm(nl),pn(nl),yy(np),dz(10001),um0(nl),ul0(nl),
            *c(10001),co(10001),ro(10001)
```

```
      read(99,*)nop
      read(99,*)(yy(jj),jj=1,nop)
      read(99,*)jmax,nol
      read(99,*)zzz,dt,eps
      TH=0.0d0
      do jjj=1, nol
      read(99,*)hz(jjj)
      read(99,*)pm(jjj),pn(jjj)
      read(99,*)a(jjj),b(jjj)
      read(99,*)r0(jjj),um0(jjj), ul0(jjj)
      enddo
       z=zzz
       mm(1)=1
       lf=nol-1
       lm=nol+1
       m=0
       do 303   kk=1,nol
       z=z+dz1
       do    k=1,50001
       co(k+m)=(2.0d0*um0(kk)+ul0(kk))*((a(kk)+b(kk)*z)**pm(kk))
       ro(k+m)=r0(kk)*((a(kk)+b(kk)*z)**pn(kk))
       c(k+m)=dsqrt(co(k+m)/ro(k+m))
       dz(k+m)=c(k+m)*dt
      write(88,121) kk,k+m,z,ro(k+m),c(k+m)
121     Format(2(x,I6),3(x,e16.8),/)
      abb=z
      if(abb.ge.hz(kk)) then
      go to 304
      else
      endif
      z=z+dz(k+m)+0.000000000000001
      enddo
304   if(kk.LE.lf) then
      co1=(2.0d0*um0(kk+1)+ul0(kk+1))*((a(kk+1)+b(kk+1)*z)**pm(kk+1))
      ro1=r0(kk+1)*((a(kk+1)+b(kk+1)*z)**pn(kk+1))
      c1=dsqrt(co1/ro1)
      dz1=c1*dt
      mm(kk+1)=m+k
      m=m+k
      else
```

```
       mm(kk+1)=m+k
       endif
303  enddo
       imax=mm(lm)
       Do ii=1,lm
       write(88,*) 'mm(',ii,')=  ', mm(ii)
       enddo
       write(88,*)'Imax = ',imax,'    NOL = ', nol
      return
      End
CCCCCCCCCCCCCCCCCCCCCCCCCCCCCCCCCCCCCCCCCCCCCCCCCCCCCCCCCCCCCCCCCCCC
       SUBROUTINE INPFT(tt,pt,dt)
CCCCCCCCCCCCCCCCCCCCCCCCCCCCCCCCCCCCCCCCCCCCCCCCCCCCCCCCCCCCCCCCCCCC
     real*8 tt,pt,ddc,pi,dt
      pi=4.0d0*atan(1.0d0)
      ddc=dt
      if(tt.lt.dt) then
      pt=0.0d0
      else
     endif
     ddc=0.2d0
     if(tt.le.ddc) then
     pt=1.0d0
      else
      pt=0.0d0
      endif
     RETURN
     END
CCCCCCCCCCCCCCCCCCCCCCCCCCCCCCCCCCCCCCCCCCCCCCCCCCCCCCCCCCCCCCCCCCCC
     SUBROUTINE SOLL(N,NX,A,X)
CCCCCCCCCCCCCCCCCCCCCCCCCCCCCCCCCCCCCCCCCCCCCCCCCCCCCCCCCCCCCCCCCCCC
     COMPLEX*16 A(NX,NX), X(NX),TEMP,QUOT,SUM
      M=N+1
      DO 23 I=1,N
23     A(I,M)=X(I)
      L=N-1
      DO 12 K=1,L
      JJ=K
      BIG=CDABS(A(K,K))
      KP1=K+1
```

```
      DO 7 I=KP1,N
      AB=CDABS(A(I,K))
      IF((BIG-AB).GE.0.) GO TO 7
      BIG=AB
      JJ=I
 7    CONTINUE
      IF((JJ-K).EQ.0) GO TO 10
      DO 9 J=K,M
      TEMP=A(JJ,J)
      A(JJ,J)=A(K,J)
 9    A(K,J)=TEMP
10    DO 11 I=KP1,N
      QUOT=A(I,K)/A(K,K)
      DO 11 J=KP1,M
11    A(I,J)=A(I,J)-QUOT*A(K,J)
      DO 12 I=KP1,N
12    A(I,K)=0.
      X(N)=A(N,M)/A(N,N)
      DO 14 NN=1,L
      SUM=0.
      I=N-NN
      IP1=I+1
      DO 13 J=IP1,N
13    SUM=SUM+A(I,J)*X(J)
14    X(I)=(A(I,M)-SUM)/A(I,I)
      RETURN
      END
CCCCCCCCCCCCCCCCCCCCCCCCCCCCCCCCCCCCCCCCCCCCCCCCCCCCCCCCCCCCCCCCCCC
      SUBROUTINE SOLVEE(imax,jmax,srxx,sryy,srzz)
CCCCCCCCCCCCCCCCCCCCCCCCCCCCCCCCCCCCCCCCCCCCCCCCCCCCCCCCCCCCCCCCCCC
      IMPLICIT real*8 (a-h,o-z)
      parameter(np=6,nx=6,nl=8)
      COMPLEX*16 sryy(jmax,np),srxx(jmax,np),
     *srzz(jmax,np),uf(nl,imax,nx),uff(nl,imax,nx),zz(2*nx-1),
     *af(nx,nx),z(nx),ad(nx,nx),z2(nx),gg(2*nx-1,2*nx-1)
      COMMON dt,eps,nop,nol,zzz
      COMMON/arrays/hz(nl),mm(nl+1)/arry2/r0(nl),a(nl),b(nl),
      *pm(nl),pn(nl),yy(np),dz(10001),um0(nl),ul0(nl),
      *c(10001),co(10001),ro(10001)
      ns=nx-1
```

```
      nns=2*(nx-1)
      nnx=2*nx-1
      do  70  kl=1,nol
      do  70  ij=mm(kl),mm(kl+1)
      do  70  kf=1,ns
70    uf(kl,ij,kf)=0.0d0
       do  90  j=2,jmax
      write(*,*) j
      tt=(j-1)*dt
      xx=zzz
      xx=xx+dz(1)
      do   100  nm=1,nol
      if(nm.eq.1) then
      xx=xx-dz(1)
      kk=mm(1)
      else
      kk=mm(nm)+1
      endif
      do   100  iq=kk,mm(nm+1)
      if(j.eq.2) then
      write(80,122) xx,ro(iq),co(iq),c(iq)
122   Format(4(x,e20.10),/)
      else
      endif
      CALL VECTOR(iq,nm,xx,uf,nx,z,imax)
      CALL MATRIX(nm,nx,af,xx)
      do ikl=1,ns
      Write(88,*)z(ikl)
      write(88,*)(af(ikl,jjj),jjj=1,ns)
      write(88,*) iq,ikl
      enddo
      if(iq.eq.1) go to 200
      if(iq.eq.imax) go to 300
      if(iq.eq.mm(nm+1)) go to 500
      go to 600
 200  do jj=1,ns
      af(1,jj)=cmplx(0.0d0,0.0d0)
      enddo
      af(1,1)=1.0d0
      CALL INPFT(tt,pt,dt)
```

```
      z(1)=1.0d0*pt
      CALL SOLL(ns,nx,af,z)
      go to 400
300 do jj=1,ns
      af(2,jj)=cmplx(0.0d0,0.0d0)
      enddo
 EITHER:
 FOR FREE OUTER BOUNDARY CONDITIONS USE af(2,1)
     af(2,1)=1.0d0
 OR:
FOR FIXED OUTER BOUNDARY CONDITIONS USE af(2,4)
      af(2,4)=1.0d0
      CALL INPFT(tt,pt)
      z(2)=0.0d0
     CALL SOLL(ns,nx,af,z)
      go to 400
500 nnm=nm+1
    CALL VECTOR(iq,nnm,xx,uf,nx,z2,imax)
    CALL MATRIX(nnm,nx,ad,xx)
  do 510 ll=1,nns
  do 510 jj=1,nns
  zz(ll)=cmplx(0.0d0,0.0d0)
  gg(ll,jj)=cmplx(0.0d0,0.0d0)
510     continue
    do 515  kn=3,ns
    do 517  jj=1,ns
    gg(kn,jj)=af(kn,jj)
    gg(1,jj)=af(1,jj)
    gg(kn+ns,jj+ns)=ad(kn,jj)
    gg(7,jj+ns)=ad(2,jj)
51 continue
    zz(kn)=z(kn)
    zz(kn+ns)=z2(kn)
51 continue
    zz(1)=z(1)
    zz(7)=z2(2)
    gg(2,1)=1.0d0
    gg(2,6)=-1.0d0
    gg(6,4)=1.0d0
    gg(6,9)=-1.0d0
```

```
   CALL  SOLL(nns,nnx,gg,zz)
   do  577  jn=1,ns
   z(jn)=zz(jn)
57  uff(nnm,iq,jn)=zz(jn+ns)
    go to 400
60 CALL SOLL(ns,nx,af,z)
400 do  ikj=1,nop
   if(abs(yy(ikj)-xx).lt.eps) then
   srxx(j,ikj)=z(1)
   sryy(j,ikj)=z(2)
   srzz(j,ikj)=z(4)
   else
   endif
   enddo
   do  710  k=1,ns
710 uff(nm,iq,k)=z(k)
   xx=xx+dz(iq)+0.000000000000001
100 continue
  do    720  ml=1,nol
  do    720  is=mm(ml),mm(ml+1)
  do    720  k=1,ns
 uf(ml,is,k)=uff(ml,is,k)
720 continue
90   continue
 RETURN
 END
CCCCCCCCCCCCCCCCCCCCCCCCCCCCCCCCCCCCCCCCCCCCCCCCCCCCCCCCCCCCCCCCCCCC
     SUBROUTINE MATRIX(nm,nx,ai,xx)
CCCCCCCCCCCCCCCCCCCCCCCCCCCCCCCCCCCCCCCCCCCCCCCCCCCCCCCCCCCCCCCCCCCC
 IMPLICIT real*8 (a-h,o-z)
 PARAMETER(np=6,nl=8)
 COMPLEX*16 ai(nx,nx)
 COMMON dt,eps,nop,nol,zzz
COMMON/arrays/hz(nl),mm(nl+1)/arry2/r0(nl),a(nl),b(nl),
* pm(nl),pn(nl),yy(np),dz(10001),um0(nl),ul0(nl),
* c(10001),co(10001),ro(10001)
do  79  kf=1,nx
do  79  kr=1,nx
79  ai(kf,kr)=cmplx(0.0d0,0.0d0)
cp=dsqrt((2.0d0*um0(nm)+ul0(nm))*((a(nm)+b(nm)*xx)**pm(nm))/
```

```
* (r0(nm)*((a(nm)+b(nm)*xx)**pn(nm))))
RO=r0(nm)*((a(nm)+b(nm)*xx)**pn(nm))
TML=(2.0d0*um0(nm)+ul0(nm))*((a(nm)+b(nm)*xx)**pm(nm))
Lamd=ul0(nm)*((a(nm)+b(nm)*xx)**pm(nm))
Dlamd=ul0(nm)*b(nm)*pm(nm)*((a(nm)+b(nm)*xx)**(pm(nm)-1.0d0))
DTML=b(nm)*pm(nm)*(2.0d0*um0(nm)+ul0(nm))*
* ((a(nm)+b(nm)*xx)**(pm(nm)-1.0d0))
ai(1,1)=(-dt/2.0d0/xx/(r0(nm)*((a(nm)+b(nm)*xx)**pn(nm))))
ai(1,2)=(dt/2.0d0/xx/(r0(nm)*((a(nm)+b(nm)*xx)**pn(nm))))
ai(1,3)=(-dsqrt((2.0d0*um0(nm)+ul0(nm))*
* ((a(nm)+b(nm)*xx)**pm(nm))/
* (r0(nm)*((a(nm)+b(nm)*xx)**pn(nm)))))-
* (dt/2.0d0/(r0(nm)*((a(nm)+b(nm)*xx)**pn(nm))))*
* (b(nm)*pm(nm)*(2.0d0*um0(nm)+ul0(nm))*
* ((a(nm)+b(nm)*xx)**(pm(nm)-1.0d0)))
  ai(1,4)=((-ul0(nm)*((a(nm)+b(nm)*xx)**pm(nm)))/
* (r0(nm)*((a(nm)+b(nm)*xx)**pn(nm)))/
* (dsqrt((2.0d0*um0(nm)+ul0(nm))*((a(nm)+b(nm)*xx)**pm(nm))/
* (r0(nm)*((a(nm)+b(nm)*xx)**pn(nm)))))/xx)+
* (dt/2.0d0/(r0(nm)*((a(nm)+b(nm)*xx)**pn(nm)))/(xx))*
* (((ul0(nm)*((a(nm)+b(nm)*xx)**pm(nm)))/xx)-
* (ul0(nm)*b(nm)*pm(nm)*((a(nm)+b(nm)*xx)**(pm(nm)-1.0d0))))
ai(1,5)=1.0d0+(dt/2.0d0/xx/(r0(nm)*
* ((a(nm)+b(nm)*xx)**pn(nm))))*
* ((ul0(nm)*((a(nm)+b(nm)*xx)**pm(nm)))/
* (dsqrt((2.0d0*um0(nm)+ul0(nm))*((a(nm)+b(nm)*xx)**pm(nm))/
* (r0(nm)*((a(nm)+b(nm)*xx)**pn(nm))))))
ai(2,1)=(-dt/2.0d0/xx/(r0(nm)*((a(nm)+b(nm)*xx)**pn(nm))))
ai(2,2)=(dt/2.0d0/xx/(r0(nm)*((a(nm)+b(nm)*xx)**pn(nm))))
ai(2,3)=(dsqrt((2.0d0*um0(nm)+ul0(nm))*
* ((a(nm)+b(nm)*xx)**pm(nm))/
* (r0(nm)*((a(nm)+b(nm)*xx)**pn(nm)))))-
* (dt/2.0d0/(r0(nm)*((a(nm)+b(nm)*xx)**pn(nm))))*
* (b(nm)*pm(nm)*(2.0d0*um0(nm)+ul0(nm))*
* ((a(nm)+b(nm)*xx)**(pm(nm)-1.0d0)))
ai(2,4)=((ul0(nm)*((a(nm)+b(nm)*xx)**pm(nm)))/
* (r0(nm)*((a(nm)+b(nm)*xx)**pn(nm)))/
 * (dsqrt((2.0d0*um0(nm)+ul0(nm))*((a(nm)+b(nm)*xx)**pm(nm))/
 * (r0(nm)*((a(nm)+b(nm)*xx)**pn(nm)))))/xx)+
 * (dt/2.0d0/(r0(nm)*((a(nm)+b(nm)*xx)**pn(nm)))/(xx))*
```

```
 * (((ul0(nm)*((a(nm)+b(nm)*xx)**pm(nm)))/xx)-
 * (ul0(nm)*b(nm)*pm(nm)*((a(nm)+b(nm)*xx)**(pm(nm)-1.0d0))))
 ai(2,5)=1.0d0-(dt/2.0d0/xx/(r0(nm)*
 * ((a(nm)+b(nm)*xx)**pn(nm))))*
* ((ul0(nm)*((a(nm)+b(nm)*xx)**pm(nm)))/
* (dsqrt((2.0d0*um0(nm)+ul0(nm))*((a(nm)+b(nm)*xx)**pm(nm))/
* (r0(nm)*((a(nm)+b(nm)*xx)**pn(nm))))))
ai(3,1)=1.0d0
ai(3,2)=-(((2.0d0*um0(nm)+ul0(nm))*
* ((a(nm)+b(nm)*xx)**pm(nm)))/
* (ul0(nm)*((a(nm)+b(nm)*xx)**pm(nm))))
ai(3,5)=(dt/2.0d0/xx)*(((((2.0d0*um0(nm)+ul0(nm))*
* ((a(nm)+b(nm)*xx)**pm(nm)))**2.0d0)/
* (ul0(nm)*((a(nm)+b(nm)*xx)**pm(nm))))-
* (ul0(nm)*((a(nm)+b(nm)*xx)**pm(nm))))
ai(4,1)=1.0d0
ai(4,3)=(-(2.0d0*um0(nm)+ul0(nm))*
* ((a(nm)+b(nm)*xx)**pm(nm)))
ai(4,5)=(-dt/2.0d0/xx)*(ul0(nm)*((a(nm)+b(nm)*xx)**pm(nm)))
ai(5,4)=1.0d0
ai(5,5)=-dt/2.0d0
RETURN
END
CCCCCCCCCCCCCCCCCCCCCCCCCCCCCCCCCCCCCCCCCCCCCCCCCCCCCCCCCCCCCCCCCC
     SUBROUTINE VECTOR(i,nm,xx,uf,nx,z,imax)
CCCCCCCCCCCCCCCCCCCCCCCCCCCCCCCCCCCCCCCCCCCCCCCCCCCCCCCCCCCCCCCCCC
IMPLICIT real*8 (a-h,o-z)
PARAMETER(np=6,nl=8)
complex*16 z(nx),uf(nl,imax,nx)
COMMON dt,eps,nop,nol,zzz
COMMON/arrays/hz(nl),mm(nl+1)/arry2/r0(nl),a(nl),b(nl),
*pm(nl),pn(nl),yy(np),dz(10001),um0(nl),ul0(nl),
*c(10001),co(10001),ro(10001)
 do  jjj=1,nx
z(jjj)=cmplx(0.0d0,0.0d0)
 enddo
xx1=xx
xx2=xx
if (i.eq.1) then
go to 700
```

```
else
z(1)=uf(nm,i-1,1)*((dt/2.0d0/xx1/
* (r0(nm)*((a(nm)+b(nm)*xx1)**pn(nm)))))-
* uf(nm,i-1,2)*((dt/2.0d0/xx1/
* (r0(nm)*((a(nm)+b(nm)*xx1)**pn(nm)))))+
* uf(nm,i-1,3)*((-dsqrt((2.0d0*um0(nm)+ul0(nm))*
* ((a(nm)+b(nm)*xx)**pm(nm))/
* (r0(nm)*((a(nm)+b(nm)*xx)**pn(nm)))))+
* (dt/2.0d0/(r0(nm)*((a(nm)+b(nm)*xx1)**pn(nm))))*
* (b(nm)*pm(nm)*(2.0d0*um0(nm)+ul0(nm))*
* ((a(nm)+b(nm)*xx1)**(pm(nm)-1.0d0))))+
* uf(nm,i-1,4)*(((-ul0(nm)*((a(nm)+b(nm)*xx1)**pm(nm)))/
* (r0(nm)*((a(nm)+b(nm)*xx1)**pn(nm)))/
* (dsqrt((2.0d0*um0(nm)+ul0(nm))*((a(nm)+b(nm)*xx)**pm(nm))/
* (r0(nm)*((a(nm)+b(nm)*xx)**pn(nm)))))/xx1)-
* (dt/2.0d0/(r0(nm)*((a(nm)+b(nm)*xx1)**pn(nm)))/(xx1))*
* (((ul0(nm)*((a(nm)+b(nm)*xx1)**pm(nm)))/xx1)-
* (ul0(nm)*b(nm)*pm(nm)*((a(nm)+b(nm)*xx1)**(pm(nm)-1.0d0)))))+
* uf(nm,i-1,5)*(1.0d0-(dt/2.0d0/xx1/(r0(nm)*
* ((a(nm)+b(nm)*xx1)**pn(nm))))*
* ((ul0(nm)*((a(nm)+b(nm)*xx1)**pm(nm)))/
* (dsqrt((2.0d0*um0(nm)+ul0(nm))*((a(nm)+b(nm)*xx)**pm(nm))/
* (r0(nm)*((a(nm)+b(nm)*xx)**pn(nm)))))))
endif
700     if(i.eq.imax) then
go to 800
else
z(2)=uf(nm,i+1,1)*((dt/2.0d0/xx2/
* (r0(nm)*((a(nm)+b(nm)*xx2)**pn(nm)))))-
* uf(nm,i+1,2)*((dt/2.0d0/xx2/(r0(nm)*
* ((a(nm)+b(nm)*xx2)**pn(nm)))))+
* uf(nm,i+1,3)*((dsqrt((2.0d0*um0(nm)+ul0(nm))*
 * ((a(nm)+b(nm)*xx)**pm(nm))/
 * (r0(nm)*((a(nm)+b(nm)*xx)**pn(nm)))))+
* (dt/2.0d0/(r0(nm)*((a(nm)+b(nm)*xx2)**pn(nm))))*
* (b(nm)*pm(nm)*(2.0d0*um0(nm)+ul0(nm))*
* ((a(nm)+b(nm)*xx2)**(pm(nm)-1.0d0))))+
* uf(nm,i+1,4)*(((ul0(nm)*((a(nm)+b(nm)*xx2)**pm(nm)))/
* (r0(nm)*((a(nm)+b(nm)*xx2)**pn(nm)))/
* (dsqrt((2.0d0*um0(nm)+ul0(nm))*((a(nm)+b(nm)*xx)**pm(nm))/
```

```
* (r0(nm)*((a(nm)+b(nm)*xx)**pn(nm)))))/xx2)-
* (dt/2.0d0/(r0(nm)*((a(nm)+b(nm)*xx2)**pn(nm)))/(xx2))*
* (((ul0(nm)*((a(nm)+b(nm)*xx2)**pm(nm)))/xx2)-
* (ul0(nm)*b(nm)*pm(nm)*((a(nm)+b(nm)*xx2)**(pm(nm)-1.0d0)))))+
* uf(nm,i+1,5)*(1.0d0+(dt/2.0d0/xx2/(r0(nm)*
* ((a(nm)+b(nm)*xx2)**pn(nm))))*
* ((ul0(nm)*((a(nm)+b(nm)*xx2)**pm(nm)))/
* (dsqrt((2.0d0*um0(nm)+ul0(nm))*((a(nm)+b(nm)*xx)**pm(nm))/
* (r0(nm)*((a(nm)+b(nm)*xx)**pn(nm)))))))
  endif
800     continue
z(3)=uf(nm,i,1)-
*  uf(nm,i,2)*((((2.0d0*um0(nm)+ul0(nm))*
 * ((a(nm)+b(nm)*xx)**pm(nm)))/
* (ul0(nm)*((a(nm)+b(nm)*xx)**pm(nm)))))-
* uf(nm,i,5)*((dt/2.0d0/xx)*(((((2.0d0*um0(nm)+ul0(nm))*
* ((a(nm)+b(nm)*xx)**pm(nm)))**2.0d0)/
* (ul0(nm)*((a(nm)+b(nm)*xx)**pm(nm))))-
* (ul0(nm)*((a(nm)+b(nm)*xx)**pm(nm)))))
z(4)=uf(nm,i,1)-
* uf(nm,i,3)*(((2.0d0*um0(nm)+ul0(nm))*
* ((a(nm)+b(nm)*xx)**pm(nm))))+
* uf(nm,i,5)*((dt/2.0d0/xx)*
* (ul0(nm)*((a(nm)+b(nm)*xx)**pm(nm))))
z(5)=uf(nm,i,4)+uf(nm,i,5)*(dt/2.0d0)
RETURN
END
CCCCCCCCCCCCCCCCCCCCCCCCCCCCCCCCCCCCCCCCCCCCCCCCCCCCCCCCCCCCCCCCCC
      SUBROUTINE OUT(jmax,srxx,sryy,srzz)
CCCCCCCCCCCCCCCCCCCCCCCCCCCCCCCCCCCCCCCCCCCCCCCCCCCCCCCCCCCCCCCCCC
IMPLICIT real*8 (a-h,o-z)
parameter(np=6,nl=8)
complex*16 srxx(jmax,np),sryy(jmax,np),srzz(jmax,np)
COMMON dt,eps,nop,nol,zzz
COMMON/arrays/hz(nl),mm(nl+1)/arry2/r0(nl),a(nl),b(nl),
* pm(nl),pn(nl),yy(np),dz(10001),um0(nl),ul0(nl),
* c(10001),co(10001),ro(10001)
do ii=1,nop
do jj=2,jmax
ttt=(jj-1)*dt
```

```
sssrxx=dreal(srxx(jj,ii))
sssryy=dreal(sryy(jj,ii))
sssrzz=dreal(srzz(jj,ii))
write(ii,101) ttt,sssrxx,sssryy,sssrzz
101    format(f14.8,1x,3(1x,f20.10))
enddo
enddo
return
end
```

APPENDIX C

EXAMPLE OF INPUT FILE "inp333":

The following input file is included to the results presented in Figs. 3.22 – 3.29 for the Si/Ni FGM composite.

```
5
1.00  1.50080412  2.000438265  2.500499031  3.000059837
8001     2
1.0d0    0.0020d0    0.000001d0

2.0d0
-0.5858690d0   -2.5858690d0
1.3349220150d0    -0.3349220150d0
1.0d0    0.398230d0     0.203540d0

3.0d0
-0.5858690d0   -2.5858690d0
1.66984403d0    -0.3349220150d0
1.0d0    0.398230d0     0.203540d0
```

The first line: (5), shows the number of pointd where solutions are required.

The second line: (1.00 1.50080412 2.000438265 2.500499031 3.000059837), shows the location of points where solutions are required in (r – direction).

The third line: (8001 2), $J_{\max} = 8001$ and number of layers are 4.

The fourth line: (1.0d0 0.0020d0 0.000001d0), the first entry is the location of the top surface $r = 1.0\text{d}0$ of the layered media. The second entry is $\Delta t = 0.0020\text{d}0$, the third entry is $\varepsilon = 0.000001\text{d}0$ which is a stopping criterion.

Under the fourth line we have four sets, each set pertains to the geometric and material properties of the four layers, for example, the first entry in each set gives the location of the outer boundary of that layer. The other three lines give:

m n

a b

ρ_0 μ_0 λ_0

, respectively.